QUANTITATION OF ANTI-INFECTIOUS DISEASE MOLECULES UTILIZING PAPER SPRAY MASS SPECTROMETRY

by

Christine Lynn Skaggs

A Dissertation

Submitted to the Faculty of Purdue University

In Partial Fulfillment of the Requirements for the degree of

Doctor of Philosophy

Department of Chemistry and Chemical Biology at IUPUI

Indianapolis, Indiana

August 2021

THE PURDUE UNIVERSITY GRADUATE SCHOOL
STATEMENT OF COMMITTEE APPROVAL

Dr. Nicholas Manicke, Chair

Department of Chemistry and Chemical Biology

Dr. John Goodpaster

Department of Chemistry and Chemical Biology

Dr. Rajesh Sardar

Department of Chemistry and Chemical Biology

Dr. Christoph Naumann

Department of Chemistry and Chemical Biology

Approved by:

Dr. Eric C. Long

To the person whose confidence in me has never wavered. Thank you, Papaw, may you rest in peace.

ACKNOWLEDGMENTS

A wise man once told me that to be a successful chemist, you didn't have to be a well-renowned scientist. You just had to be able to do one thing and you had to work hard to be an expert in that singular topic. Thank you, Dr. Carl Lecher, for pushing me in the right direction and for giving me a light of hope to guide me even in my bleakest days.

To the friends that spent late nights and weekends studying, performing experiments, and supporting me. It is true when they say education is a team effort. I also would have never succeeded without the support of my fellow lab-mates and friends. You all are so much more to me than just the people that I work with. Thank you to Dr. Frédérique Deiss for supporting me through my numerous blunders and for helping me to stand tall in the face of adversity. Thank you to Dr. Lindsey Kirkpatrick for allowing me to find myself as a researcher and guide me towards my passions. I would also like to thank my father, grandparents, and sister for their endless support through the long hours and incessant talk of research.

I would be remiss without profusely thanking my mother, my mentor, my best friend. Without you, none of my successes would have been possible. You know me better than anyone, and you've put me before yourself to ensure that I will always succeed. Thank you for being tough on me and showing me what it means to be a dedicated researcher and, more importantly, a kind and thoughtful person.

Finally, I would like to thank my Principal Investigator, Dr. Nicholas Manicke. You provide our lab with so much more than a boss-like figure or baking contest tie breaker. You allow us to grow not only as researchers but also as individuals. You inspire me to do my best – to be my best – every day. Being the boss is often a thankless job, and words cannot begin to portray how much the effort you give is appreciated, but I am going to try. Thank you for the sacrifices you made to teach me. Thank you for your endless patience, which allowed me to grow at my own pace. Most importantly, thank you for believing in me when nobody else did.

Christine Lynn Skaggs

TABLE OF CONTENTS

LIST OF TABLES

LIST OF FIGURES

ABSTRACT

Suboptimal dosing of anti-microbial agents increases the likelihood of therapeutic failure and resistance. Dosing optimization, while an attractive approach to combat these issues, is difficult to implement due to the different pharmacokinetics of each individual. These limitations highlight the inadequacies of a "standardized" dosing strategy. Therapeutic drug monitoring (TDM) provides a tailored treatment for individuals while avoiding adverse side effects from compounds with a narrow therapeutic window where elevated concentrations of a drug cause organ toxicity. This strategy involves accurately measuring the concentration of the analyte and interpreting the results based on pharmacokinetic parameters. Clinicians then draw conclusions regarding dose adjustment for their patient. However, TDM is expensive and difficult to perform because measurements occur in biofluids. Rapid and robust methods are necessary to quantify antimicrobial agents at the institutional level to guide patient care toward improved outcomes in serious infection. Paper spray ionization (PS), an emerging ambient ionization technique for clinical settings, demonstrations a wide versatility both in analyte variety and applications. This technique offers a rapid, accurate method to analyze these compounds with low rates of false positives even when multiplexing.

The work herein explains the method development of assays for TDM of various antimicrobial agents. Chapters two and three describe ways to improve the quantitative capability of paper spray through substrate pre-treatment, modification, and manipulation of key factors. Chapter four describes real-world applications for paper spray utility in clinical settings with the cross-validation of antifungal agents against a "gold standard" method. The final chapter, while not clinical based, describes the method development process for a LC-MS/MS assay to detect urobilinoids in fly guts.

CHAPTER 1. AMBIENT IONIZATION FOR CLINICAL APPLICATIONS

1.1 Overview

The need for rapid, cost-effective medical tests has resulted in the development of new technologies for clinical applications. Mass spectrometry (MS) is a technique capable of analyzing a diverse array of molecules in different matrices. Mass spectrometry is suitable for a wide variety of applications due to its multiplexing capabilities, and ability to deliver both sensitive and specific results.[1] These instruments are composed of an ion source, a mass analyzer, and an ion detector (**Figure 1.1**).

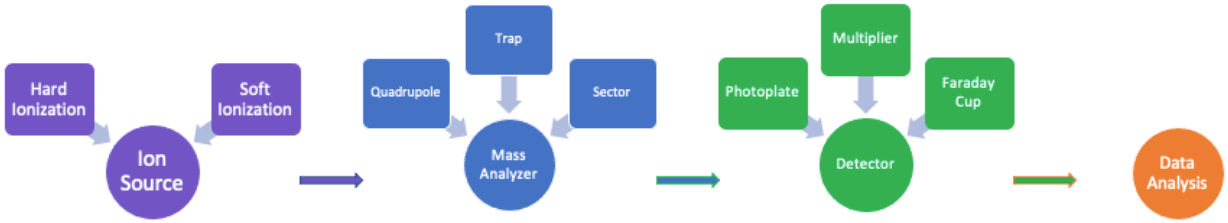

Figure 1.1 Anatomy of a mass spectrometer with examples depicting specific types of ion sources, mass analyzers, and detectors.

Because mass spectrometers operate under vacuum and utilize magnetic or electric fields, molecules must enter both a gaseous and charged state.[2] In some cases, the ion source generates molecules by vaporizing the analyte then inducing a charge resulting from the input of energy during ionization. The amount of energy required to produce charged species depends on the type of ionization mechanism utilized.[3] This energy originates in various forms. Techniques such as electron ionization (EI), one of the earliest developed techniques for mass spectrometry, employ electrons.[2] Here, neutral analyte molecules enter the mass spectrometer and are subsequently accelerated towards an electron beam generated by a heated filament.[4] Alternatively, techniques such as matrix-assisted laser desorption/ionization (MALDI) and atmospheric pressure photoionization (APPI) utilize photon beams to produce charged species.[2] Ion beams can also be applied for ionization as depicted in secondary fast atom bombardment (FAB) and secondary-ion mass spectrometry (SIMS). Reagent gases, such as those required for chemical ionization (CI), offer another mechanism employed for ion formation. Finally, a widespread ionization agent

involves electric fields. Electrospray ionization (ESI), direct analysis in real time (DART) and atmospheric pressure chemical ionization (APCI) represent examples of ionization techniques utilizing electric fields.[1]

Ion sources create many types of charged species. These include intact molecular ion adducts, generated in soft ionization techniques, or mostly fragment ions such as those produced with hard ionization methods.[2] Hard ionization techniques include electron ionization (EI), secondary ion mass spectrometry (SIMS), and field ionization (FI).[1] Soft ionization techniques include methodologies such as, soft laser desorption ionization (SLD), fast atom bombardment (FAB), matrix-assisted laser desorption ionization (MALDI), and electrospray ionization (ESI).[2] The method of choice depends on the sample introduction mechanism, the mass range of the analytes, the sample matrix, and the desired information gleaned from the analysis.[1] For example, hard ionization methods are employed for the introduction of small, volatile analytes into the mass spectrometer via gas chromatography. These methods are reproducible and compatible with library databases.[4] Softer ionization techniques are applicable for both small and large molecules and operate with liquid chromatography or other ambient ionization techniques.[1] A more comprehensive list of ionization sources and their unique parameters can be found in **Table 1.1**.

Table 1.1 List of common ion sources with their unique parameters as well as advantages and disadvantages of each.

Ion Source					
Ionization Method	**Typical Analytes**	**Mass Range (Da)**	**Agent for Ionization**	**Advantages**	**Disadvantages**
Electron Impact (EI)	Small organic volatile	50 to 800	Electrons	Extensive fragmentation is helpful for structure elucidation and identification; cheap	May not see molecular ion due to extensive fragmentation Limited mass range Probes result in contamination or vacuum failure
Chemical Ionization (CI)	Small organic volatile	50 to 800	Ion Beam	Produces ions with little excess energy Less fragmentation so parent more present	Not reproducible from lab to lab (no libraries) Traditional methods need high vacuum to ionize

Table 1. 1 continued

Electrospray (ESI)	Small and large polar Peptides/ Proteins (nonvolatile)	5k to 200k	Electric Field	Production of molecular ions directly from samples in solution Can produce multiply charged ions	Sample must be soluble, stable, and clean Not tolerant of non-volatile salts
Fast Atom Bombardment (FAB)	Polar ionic Carbohydrates Organometallics Peptides (nonvolatile)	100 to 4k	Ion Beam	No heating required so good for nonvolatile molecules	Prone to suppression effects by impurities from matrix Difficult to find correct matrix
Matrix Assisted Laser Desorption (MALDI)	Peptides Proteins Nucleotides small polymers (nonvolatile)	5k to 300k	Photons	Low sample volume needed Insensitive to contaminants High mass range	Reproducibility issues
Atmospheric Pressure Chemical Ionization (APCI)	Small neutral sort of nonpolar nonvolatile	1k	Electric Field	Can handle mobile phase with buffering agents Can handle high flow rates Less carryover between samples	Need MS/MS for structural info Sample must be in solution
Atmospheric Pressure Photo-ionization (APPI)	Nonpolar neutral nonvolatile	1k	Photons	Can analyze molecules with high ionization energies	More sensitive to experimental conditions Broad methods expose samples to harsher conditions
Direct Analysis in Real Time (DART)	Large variety	Wide	Electric Field	No sample prep needed Ambient ionization	Need large power supply Dependent on angle on gun
Desorption Electrospray Ionization (DESI)	Small nonpolar to large polar	60k	Electric Field	No sample prep needed Sample can be freely moved during experiment Any sample holder can be used Sample not in solution	Performance is dependent on experimental parameters

After ionization, mass analyzers will separate these charged species based on their mass-to-charge ratios. Common mass analyzers comprise of quadrupoles (Q), ion traps (IT), time-of-flight (TOF), magnetic sector, Fourier-transform ion cyclotron resonance (FTICR), and orbitrap[2]. As with the ion source, the selection of mass analyzer depends on the application and molecules of interest as well as practical concerns like cost and size. Four fundamental principles define all

mass analyzers: 1) they delineate the mass of an ion, 2) determine the mass-to-charge ratio, 3) measure gas-phase ions, and 4) operate at low pressures ($< 10^{-4}$ Torr).[5] These mass analyzers vary drastically in their resolution, analysis speeds, transmission, mass accuracy, mass range limits, and overall costs.[5, 6] In particular, more affordable instruments, such as ion traps and triple quadrupoles, utilize smaller mass ranges and have lower resolving power than expensive, high resolution, high mass accuracy instrumentation such as orbitraps and FTICR mass analyzers.[2] **Table 1.2** summarizes fundamental information regarding common mass analyzers.[5] Resolution describes the ability of the mass analyzer to separate ions with similar masses. Mass accuracy describes the ability of the mass analyzer to determine the mass of an ion in relation to its true mass. Mass range describes the upper and lower m/z values perceived by the mass analyzer. The scan speed defines the rate at which a mass spectrum can be generated relative to time. Sensitivity describes the ability of the mass analyzer to detect an analyte.[5]

Table 1.2 List of common mass analyzers and their defining parameters as well as major advantages and disadvantages.

Mass Analyzers						
Transmission	**Quadrupole**	**Ion Trap**	**TOF**	**Magnetic Sector**	**Orbitrap**	**FT-ICR**
Resolution	Low (1,000)	Low (1,000-10,000)	High (10k -60k)	Moderate	High (100,000)	High (1,000,000)
Cost	$	$	$$$	$$$$	$$$$	$$$$$$
m/z Range When Coupled to ESI (u)	5-2,000	50-2,000	up to 40,000	10-10,000	50-6,000	50-2,000
Scan Speed	4,000 u/s max	4,000 u/s	1-50 u/s	500 u/s	10 u/s	1 u/s
Kinetic Energy (eV)	5	5	20,000	8,000	High	High
Vacuum (torr)	10^{-4}-10^{-5}	10^{-3}	10^{-7} or higher	10^{-7}	High	10^{-10}
LC/MS Interface	APCI, ESI	ESI, APCI	MALDI	ESI, APCI	ESI, APCI	MALDI
Mass Accuracy (ppm)	100	50	2	<5	sub	sub
Ion Production	Continuous	Pulsed	Pulsed	Continuous	Pulsed	Pulsed
Ion Separation	Band Pass Filter	Voltage	Flight Time	Magnetic Field	Frequency	Frequency
Mass Equations	$m/z = [k'/\Omega^2 r^2]V$	$m/z = [k'/\Omega^2 r^2]V$	$m/z = [kV/D^2]t^2$	$m/z = [kr^2/V]B^2$	$m/z = k/\omega_z^2$	$m/z = [Be]/\Omega$
How It Works	Uses oscillating electric fields between charged rods to separate ions according to m/z	Uses quadrupolar field trapping ions in two or three dimensions	Separates ions after initial acceleration according to their velocities when they drift through the flight tube	Select ions according to their momentum after acceleration through a flight tube	Ions are injected and an electrostatic voltage is applied causing the ions to oscillate in the trap Fourier transform applied	Ions in magnetic field move in circular orbits until ions absorb energy enabling them to be detected

Table 1. 2 continued

Advantages	Tolerant of high pressure Good at tracking single ions over time Robust	High stability Simple design Robust	Theoretically unlimited mass range High duty cycle	High sensitivity Reliable	Larger trapping capacity Increased space-charge capacity at higher masses	Highest recorded mass resolution, nondestructive
Disadvantages	Variable peak heights Not good for pulsed ionization methods Limited mass range	Limited mass range	Difficult coupling to ESI Space requirements Low scan rate	Large instrument Higher cost Not tolerant of high pressure	Expensive Not robust	Large instrument Space charge effects Expensive Hard to maintain

Detectors amplify the current produced from ions and transform it into a usable signal, where the current intensity is directly proportional to the abundance of the ions.[7] Although the mechanisms of action for each detectors may differ, all detectors separate ions based on mass, charge, or velocity.[1] **Table 1.3** summarizes properties of common detectors. The marks of a good detector include high count rates (> 10^6 counts/s), good sensitivity, fast response times, large dynamic range, long lifetime, high collection efficiency, high accuracy, and low noise.[4, 8] Count rates define the quantity of a particular m/z measured over time. Sensitivity describes the minimum amount of an analyte required to receive a measurable signal. Response times represent the time discrepancy between the electronic input and the output of the signal. Dynamic range portrays the capability of the detector to scan a specified m/z window without significant loss of signal intensity. The lifetime of a detector quantifies the lifespan of a detector before it must be replaced. Collection efficiency explains how capably the input response is converted into a usable signal. Accuracy describes how close the measured value is to the true value. Nosie depicts the inherent electronic signal produced by the detector. The ion detector interacts with the separated ions to produce mass spectra that can be stored and compared to databases.[2] Databases offer a quick tool for identification of an unknown. This match process is highly reproducible due to the match criteria established resulting in probability scores for the compound of interest.[2]

Table 1.3 List of common detectors and their defining parameters as well as major advantages and disadvantages.

Detectors							
Detector Type	**Sensitivity**	**Analysis Speed**	**Mass Accuracy**	**Instruments Found In**	**Advantages**	**Disadvantages**	**Function**
Faraday Cup	low	slow	high	TIMS, IRMS	simple, inexpensive, rugged, reliable, high accuracy, constant sensitivity, low electronic noise	long time constant resulting in slow measurements, can have secondary electrons resulting in errors if not suppressed, positive ions only, low dynamic range	Ions making contact with detector are neutralized after passing through resistor; the drop in voltage measured and amplified in form of ion current which is proportional to the number of ions and number of charges per ion
Electron Multiplier	high	fast	low	GC/MS, QMS, ITMS, ICPMS, TOFMS	High efficiency, can detect + and - ions, wide linear dynamic range, high amplification, fast response times, can detect high mass ions	No electrometer detector, gain is variable, mass discrimination, saturation effects, variation when in presence of magnets, electronic noise, shorter lifetime	Ion beam from mass analyzer focuses on conversion dynode; dynode emits e^- proportional to number of ions; secondary e^- are focused onto second dynode creating a cascading effect for amplification
Daly	medium	medium	high	TIMS, ICPMS	can detect + and – ions, longer lifetime, quick response times, improved detection limits, wide linear dynamic range	Complex design, large footprint, large dead time	Combines ion and photo detection; ions hit dynode resulting in secondary e^-; these e^- accelerate to a phosphorescent screen emits photons detected by a photomultiplier; this results in a conversion into current that is amplified and measured
Fourier Transform	low	fast	high	FI-ICR MS, Orbitrap	High resolution, can detect + and – ions	Can only be used in FT instruments, finite ion storage capacity	Ions are trapped by a strong electric or magnetic field and are excited into an orbit where ions oscillate at different frequencies and separate based on mass-to-charge; Fourier transform used to turn frequencies into m/z measurement

n

1.2 Ambient Ionization for Mass Spectrometry

Recent advancements in mass spectrometry and sample introduction procedures aim to eliminate the lengthy sample handling and long analysis times associated with traditional techniques, such as chromatography. As mentioned prior, ions generate under a variety of conditions. Modern developments in ambient ionization reduce the reliance on labor intensive sample introduction methods. Ambient ionization techniques, such as paper spray, differ from their in vacuo counterparts because ion formation no longer transpires under vacuum inside the mass spectrometer.[9] This encompasses a multitude of techniques where ions are produced outside of the mass spectrometer in atmospheric conditions.[4] Based on the ambient technique utilized, ion formation occurs in a variety of ways. This permits an assortment of molecules, particularly those relevant for clinical analysis, to be analyzed via this methodology. For instance, desorption electrospray ionization (DESI), one of the earliest ambient ionization methods[10], currently has uses in tissue analysis, bacterial cultures, and biological fluids analysis.[11]

Ambient ionization is beneficial due to the simplistic sample handling. Because of this, ambient techniques have spread in their versatility to comprise of applications in forensics[12, 13] clinical[14-17], environmental[18, 19], and national security.[20] Complex biofluid matrices are common in clinical analysis, and the lack of sample preparation aims to simplify the methods enough for untrained operators to run equipment and handle samples. Ambient ionization is actively commissioned for the analysis of tissue[21, 22], proteins[23], lipids[24, 25], polysaccharides[26, 27], microorganisms[28, 29], and biological fluids[30] to name a few.[31] **Table 1.4** depicts many of the current ambient ionization techniques and describes the mechanism of action: extraction, plasma based, two-step non-laser, two-step laser, acoustic, and other as well as some current applications. Extraction techniques describe methods utilizing solvents or other mediums to extract/desorb molecules from the sample. Plasma based desorption explains techniques generating plasma discharge to desorb/ionize molecules. The two-step ionization sources are coupled to two ionization source mechanisms. Two-step laser ablation methods utilize an IR or UV laser source to promote sample desorption whereas two-step non-laser methods do not. Acoustic methods exploit ultrasonic or vibrational processes to induce ionization. Samples classified as other do not fall into any of these categories.[10, 32-35]

Table 1.4 Common ambient ionization techniques, their mechanism of action, and application (T = Toxicology, F = Forensics, D = Diagnostic Medicine, E = Environmental, TDM = Therapeutic Drug Monitoring, B = Biological, OM = Organic Molecules, M = Microsampling, N = National Security, P = Pharmacology, FB = Food and Beverage, PS = Polymer Science, EA = Environmental Analysis, M = Material Science, C = Cosmetic Science, O = Organometallics).

Ionization Method	Acronym	Mechanism of Action	Use
Wooden-tip ESI		Extraction	P
Air flow-assisted desorption electrospray ionization	AFADESI	Extraction	B, D, F
Air flow-assisted ionization	AFAI	Extraction	B, D, P
Ambient Flame Ionization	AFI	Other	FB, E
Atmospheric pressure glow discharge desorption ionization	APGDDI	Plasma	E
Ambient pressure pyroelectric ion source	APPIS	Other	N
Atmospheric pressure thermal desorption chemical ionization	APTDCI	Two-step	B, DM
Atmospheric pressure thermal desorption/ionization	APTDI	Plasma	O
Atmospheric pressure solids analysis probe	ASAP	Plasma	B, D, E, FB, PS, T
Beta electron-assisted direct chemical ionization	BADCI	Two step	P
Brush-Spray Ionization	BS	Two-step	Paint
Coated Blade Spray	CBD	Extraction	B, E, P, T
Carbon fiber Ionization	CFI	Extraction	B, E, P
Desorption atmospheric pressure chemical ionization	DAPCI	Plasma	B, E, F, FB, N, P
Desorption atmospheric pressure photoionization	DAPPI	Extraction	B, D, E, F, FB, N, P, T
Direct analysis in real time	DART	Plasma	B, D, E, F, FB, N, T, TDM
Dielectric barrier discharge ionization	DBDI	Plasma	B, D, E, F, FB, T
Desorption corona beam ionization	DCBI	Plasma	B, E, F, FB, P
Desorption chemical ionization	DCI	Plasma	B, F, OM, P
Desorption electro-flow focusing ionization	DEFFI	Extraction	F, T
Desorption electrospray/metastable-induced ionization	DEMI	Multimode	T
Desorption electrospray ionization	DESI	Extraction	D, E, P, T
Desorption ionization by charge exchange	DICE	Extraction	E, O
Direct inlet probe–atmospheric-pressure chemical ionization	DIP-APCI	Two-step	PS
Electrode-assisted desorption electrospray ionization	EADESI	Extraction	B
Easy ambient sonic-spray ionization	EASI	Extraction	E, FB, T
Extractive electrospray ionization	EESI	Two step	B, C, E, FB, T
Electrospray laser desorption ionization	ELDI	Laser	B, D, F
Electrospray-assisted pyrolysis ionization	ESA-Py	Spray	B, E, PS
Electrostatic spray ionization	ESTASI	Extraction	C, D, FB
Flowing atmospheric pressure afterglow	FAPA	Plasma	E, O
Field-induced droplet ionization	FIDI	Other	OM
Fiber-Spray Ionization	FS	Extraction	E, F, T
High-voltage-assisted laser desorption ionization	HALDI	Laser	B
Hydrogen flame desorption ionization	HFDI	Other	B
Infrared laser ablation metastable-induced chemical ionization	IR-LAMICI	Laser	E, F, P
Laser ablation inductively coupled plasma	LA-ICP	Laser	EA, M
Laser assisted desorption electrospray ionization	LADESI	Laser	B, D
Laser ablation direct analysis in real time	LADI	Laser	D, F

Table 1. 4 continued

Laser ablation electrospray ionization	LAESI	Laser	D
Laser desorption atmospheric pressure chemical ionization	LD-APCI	Laser	B
Laser desorption electrospray ionization	LDESI	Laser	B, D, P
Laser desorption spray post-ionization	LDSPI	Laser	B, FB
Laser diode thermal desorption	LDTD	Laser	B, E, F, FB, P, T, TDM
Laser electrospray mass spectrometry	LEMS	Laser	B, E, F
Liquid extraction surface analysis	LESA	Extraction	B, D, FB, P
Laser-induced acoustic desorption-electrospray ionization	LIAD-ESI	Acoustic	B
Liquid microjunction-surface sampling probe	LMJ-SSP	Extraction	B, E, P
Leidenfrost phenomenon-assisted thermal desorption	LPTD	Two-step	T
Leaf spray ionization	LS	Extraction	E
Liquid sampling-atmospheric pressure glow discharge	LS-APGD	Plasma	EA, OM
Laser spray ionization	LSI	Other	B, P
Low temperature plasma	LTP	Plasma	E, T
Matrix-assisted inlet ionization	MAII	Other	B
Microfabricated glow discharge plasma	MFGDP	Plasma	E, FB, D
Microwave induced plasma desorption ionization	MIPDI	Plasma	C
Nanospray desorption electrospray ionization	nano-DESI	Extraction	B, OM
Neutral desorption extractive electrospray ionization	ND-EESI	Two step	C
Plasma-assisted desorption ionization	PADI	Plasma	E, FB
Paint spray	Paint Spray	Extraction	OM, PS
Plasma-assisted laser desorption ionization	PALDI	Laser	D, PS
Plasma-based ambient sampling/ionization/transmission	PASIT	Extraction	B, E, P
Paper assisted ultrasonic spray ionization	PAUSI	Other	B
Probe electrospray ionization	PESI	Two step	B, D, E, F, P, PS, T
Paper spray	PS	Extraction	D, N, T, TDM
Pipette tip column electrospray ionization	PTC-ESI	Extraction	OM
Rapid Evaporative ionization	REI	Other	B, D, FB
Robotic plasma probe ionization	RoPPI	Two-step	D
Surface activated chemical ionization	SACI	Other	B, P, T
Solvent-assisted electrospray ionization	SAESI	Other	B, FB
Solvent-assisted inlet ionization	SAII	Other	B
Surface acoustic wave nebulization	SAWN	Acoustic	B, D, F, FB
Surface-enhanced laser desorption ionization	SELDI	Other	B, D, T
Secondary electrospray ionization	SESI	Vapor-ion, charge transfer	B, D, E, F, T
Slug flow microextraction nanoESI	SFME	Other	B, T, TDM
Solid probe assisted nanoelectrospray ionization	SPA-nanoESI	Two-step	D
Single-particle aerosol mass spectrometry	SPAMS	Other	E, F, FB, N, OM
Sponge-Spray Ionization	SSI	Extraction	M
Switched ferroelectric plasma ionizer	SwiFerr	Other	P
Transmission mode desorption electrospray ionization	TM-DESI	Extraction	F
Touch spray	TS	Two-step	D, T
Ultrasonication-assisted spray ionization	UASI	Acoustic	B, OM
Venturi easy ambient sonic-spray ionization	V-EASI	Extraction	B, E

1.2.1 Paper Spray Mass Spectrometry

Paper spray mass spectrometry is an ionization technique developed to further simplify the sample handling process and to reduce analysis times.[36] Early accounts of this technique were reported in 2010 under the direction of Dr. Cooks for the application of direct analysis in complex mixtures.[37] Briefly, this technique requires a small, triangular shaped piece of chromatography paper. The sample of interest is directly spotted onto the substrate (3 µL – 100 µL) without the sample clean up procedures used in chromatographic assays, such as solid-phase extraction (SPE) or liquid-liquid extraction (LLE). A solvent volume ranging from 30 µL – 200 µL is applied to the triangular paper with subsequent voltage application ranging from 2500 kV – 5000 kV. This induces a Taylor cone formation of charged droplets at the tip of the paper, similar to those in ESI.[36] As the solvent travels through the paper via capillary action, the analyte of interest is extracted from the paper abandoning the complex matrix. Typical analysis times range from 30 seconds to 2 minutes (**Figure 1.2**).[38] Since its development, paper spray has drastically increased its versatility and use to incorporate both small and large molecules with varying hydrophilicities and polarities.[16, 39, 40] Despite these major advancements, detection limits, especially for hydrophilic molecules, are subpar in biofluid matrices. Unfortunately, clinical assays utilizing paper spray have been hindered due to the hydrophilicity of many clinical drugs. This dissertation evaluates various options to improve the sensitivity and quantitative capability of paper spray for this application

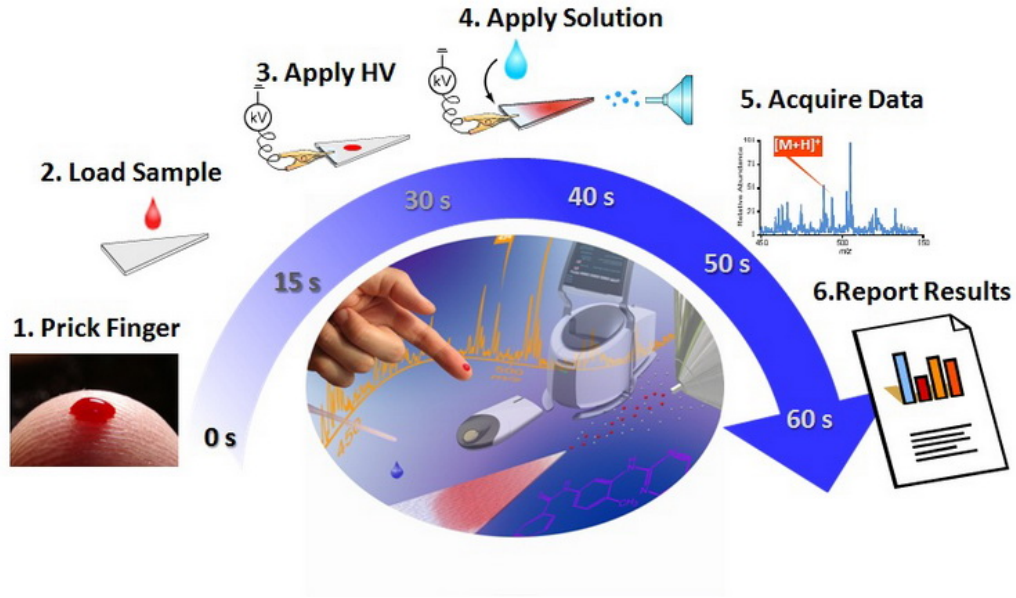

Figure 1.2 Figure of the paper spray process created by the Ouyang group.[38]

1.3 Design of Experiment

The work herein utilizes the design principles of DOEs. The second and third chapters describe how various paper spray factors were manipulated for screening experiments. These results underwent confirmation experiments as well as subsequent optimization phases as described above. Although most of the work performed in this dissertation centers around factorial designs, other models were employed to fully characterize the data. The complexity and restrictions imposed by clinical applications require advanced experimental design for successful quantitation.

To assess the various paper spray parameters capable of enhancing sensitivity, complex experimental design tools were employed to efficiently optimize the desired response variables while conserving on resources. This involved lengthy evaluation of the paper spray process with subsequent identification of meaningful variables. One of the most important, and often overlooked, part of research involves experimental design. Typical scientific experiments comprise manipulation of a single variable by setting it at various levels, termed one-factor-at-a-time (OFAT) experiments.[41, 42] While a common way to run experiments, interactions between terms are overlooked resulting in suboptimal signal. Because of this, an entire field of statistical design was developed to analyze multiple variables simultaneously to assess their combined impact on a designated response variable. This field, Design of Experiments (DOE), encompasses a branch of applied statistics where multiple input factors affect a single output.[41-43] This type of planning and statistical analysis detects interactions between input variables. It can also be commissioned as a confirmatory and predictive analysis tool.[43, 44] A well-designed DOE incorporates a planning, screening, optimization, and a verification phase. The planning phase is the most important step in creating an effective experiment. Here, resources are assessed, major input factors are identified, and potential interactions are evaluated. The screening phase involves analyzing large amounts of factors while minimizing analytical runs. A worthwhile experiment contains sufficient randomization, replication, and appropriate factor level settings.[42, 45] The optimization phase improves the desired outcome and develops successive experiments to assess the response variable within the design space defined by the screening phase. Finally, the verification phase appears intermittently between each of the specified phases to confirm the results.

Many design models exist to perform the multivariate experiments found in DOEs. Examples of common statistical models are screening, factorial, and response surface designs.[42, 43, 45] Screening designs cast a wide net to determine significant factors when relevant input variables remain uncharacterized. The goal is to analyze many factors with as few experimental runs as possible. This ensues through some type of factorial analysis with succeeding confirmation experiments to determine the validity of the assessment from the screening phase. These optimization runs occur via response surface designs. Factorial designs estimate the significance of an input variable, termed main effect, and any interaction effects occurring between terms.[43, 45] This can be performed as a full factorial, fractional factorial, or Plackett-Burman design. Factorial designs will be discussed in later sections. Response surface designs are used after characterizing a design space.[44, 46] This progressive design tool better ascertains the input variables' impact on the response. Whereas screening experiments set many factors (4+) at high and low values, response surface designs set only a few factors (2-3) at multiple levels (3+) within an established inference space. This assesses curvature to determine the optimal signal response.[44, 46] The critical part of constructing a competent experimental design is ensuring the DOE is orthogonal and balanced. Orthogonality, in this context, is synonymous with uncorrelated; all factors can be considered independently. Balanced defines an equal number of observations at each factor level for each factor pairs ensuring the weight of each term is identical.

1.3.1 Full Factorial Design

Full factorial designs involve the study of all combinations of factor levels. Factorial designs are typically described by 2^k number of runs where k represents the total number of factors explored at a high and low level.[41-43] Although more levels could be added, this increases the complexity of the experiment and increases the total number of runs required. One of the advantages of a factorial design over an OFAT is the efficiency and ability to evaluate the entire data set to compute interaction effects on a response variable. This is described by **Equation 1.1** where y is the response, β_0 is constant, β_i is the coefficient for factor A, x_i represents the level of factor A effects, β_j is the coefficient for factor B, x_j represents the level of factor B effects, β_{ij} is the coefficient of the interaction between factors A and B, and ε indicates the experimental errors. It is important to note more terms are added with an increasing amount of factors.[42]

$$y = \beta_0 + \sum_{i=1}^{k} \beta_i x_i + \sum_{j=1}^{k} \beta_j x_j + \Sigma\sum_{i<j} \beta_{ij} x_i x_j + \ldots + \varepsilon \qquad \text{Equation 1.1}$$

In the case of a 2 factor 2 level design, 4 total runs (2 x 2) are required to have a complete design. This means factor A will be run at a high and low level as will factor B (**Figure 1.3**). For a three-factor design, 8 runs (2 x 2 x 2) are necessary to have a complete design.

Two-factor Two-Level (2^2) Design

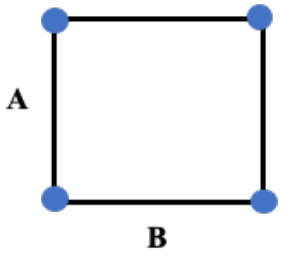

Run	Factor A	Factor B	AB
1	-	-	+
2	+	-	-
3	-	+	-
4	+	+	+

Three-factor Two-Level (2^3) Design

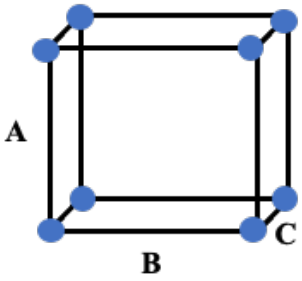

Run	Factor A	Factor B	AB	Factor C	AC	BC	ABC
1	-	-	+	-	+	+	-
2	+	-	-	-	-	+	+
3	-	+	-	-	+	-	+
4	+	+	+	-	-	-	-
5	-	-	+	+	+	-	+
6	+	-	-	+	-	+	-
7	-	+	-	+	+	+	-
8	+	+	+	+	-	-	+

Figure 1.3 Visual representation of full factorial experiments for 2^2 and 2^3 designs including the experimental design tables for each.

1.3.2 Fractional Factorial Design

As explained in the previous section, the more factors evaluated, the more runs required for the design to conserve all combinations. This can become unwieldy when more than four factors are evaluated simultaneously assuming adequate replication ensues. Additionally, higher order interactions also increase. To reduce the number of runs while still retaining many terms, a fractional factorial design can be performed.[42, 43] This type of design uses the highest order interactions as the identity term, defined as the subset of data that is fractionated. This causes the remaining interactions and main effects to be aliased, also termed confounded. Depending on the resolution of the design and the number of factors present, high-order interactions are indistinguishable from certain low-order interactions and main effects because not all the runs are

performed.[43] Resolution describes how much aliasing occurs within a given design. In a Resolution III design, no main effects are aliased with each other, but they are aliased with the remaining interactions. In a Resolution IV design, no main effects are aliased with each other or two-factor interactions; however, they are aliased with the remaining interactions. This same trend continues with the higher resolution designs. In higher resolution designs, the risk associated with the fractionated model is reduced because of the sparsity-of-effects principle, which assumes high-order interactions are unlikely.[42] For example, in the case of a 2^3 factorial experiment, for a full factorial design 8 runs must occur. In a Res III ½ fraction design, only 4 runs are performed (**Figure 1.4**). In this type of experiment, all two-way interactions will be aliased with main effects (I = ABC).

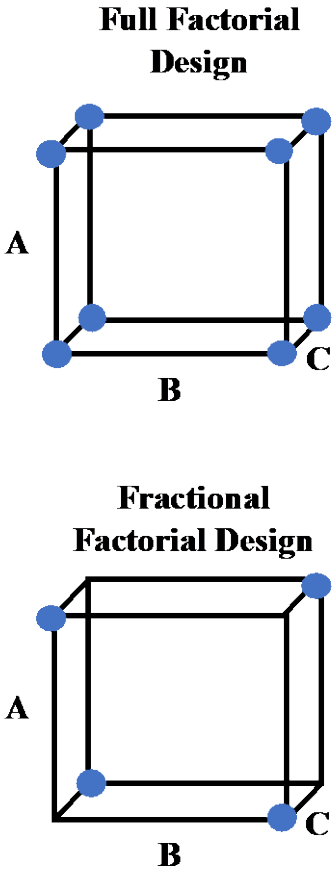

Alias	
I	ABC
A	BC
B	AC
C	AB

Figure 1.4 Visual representation of a full factorial 23 design versus a Resolution III ½ fractional factorial design with the aliasing table. This table shows that main effects are confounded with two-way interactions and the three-way interaction is the identity.

1.3.3 Central Composite Design

Central composite design (CCD) is one of the major types of response surface model. This type of design differs from a factorial experiment in that the equation describing the model contains a squared (quadratic) term to account for curvature in the response variable.[42] These designs contain not only the standard high, low and center point values, but also contain a designed number of axial points to assess curvature. This type of model is described by **Equation 1.2** where y is the response, β_0 is constant, β_k is the coefficient for each factor and the interactions between factors, x_k represents the level of each factor effects and the interaction terms, and ε indicates the experimental errors.[42]

$$y = \beta_0 + \sum_{i=1}^{k} \beta_i x_i + \sum_{i=1}^{k} \beta_{ii} {x_i}^2 + \Sigma\sum_{i<j} \beta_{ij} x_i\, x_j + \ldots + \varepsilon \qquad \text{Equation 1.2}$$

These answer specific questions about the effects of listed factors. When properly utilized, they will answer questions about the weight each factor has on a response and which settings these terms should be set at to meet process specifications.[42] Additionally, the design curvature allows for the determination of which settings produce optimal response for the factors. Similarly to factorial designs, CCD should also retain orthogonality to accurately interpret results.

CHAPTER 2. A STATISTICAL APPROACH TO OPTIMIZING PAPER SPRAY MASS SPECTROMETRY PARAMETERS

2.1 Abstract

Paper spray mass spectrometry (PS-MS) was used to analyze and quantify ampicillin, a hydrophilic compound and frequently utilized antibiotic. Hydrophilic molecules are difficult to analyze via PS-MS due to their strong binding affinity to paper substrates and low ionization efficiency, among other reasons. Solvent and paper parameters were optimized to increase the extraction of ampicillin from the paper substrate. After optimizing these key parameters, a Resolution IV 1/16 fractional factorial design with two center points was employed to screen eight different design parameters simultaneously. Pore size, sample volume, and solvent volume were the most significant factors affecting average peak area under the curve (AUC) and the signal-to-blank (S/B) ratio for the 1μg/mL ampicillin calibrant. After optimizing the key parameters, a linear calibration curve with a range of 0.2 μg/mL to 100 μg/mL was generated ($R^2 = 0.98$) and the limit of detection (LOD) and lower limit of quantification (LLOQ) were calculated to be 0.07 μg/mL and 0.25 μg/mL, respectively. The statistical optimization procedure undertaken here increased the mass spectral intensity by more than a factor of 40. This statistical method of screening followed by optimization experiments proved faster and more efficient and produced more drastic improvements than typical one-factor-at-a-time experiments.

2.2 Introduction

Desorption electrospray ionization (DESI)[47] and direct analysis in real time (DART)[48] paved the way for a variety of ambient ionization techniques for mass spectrometry, which are utilized for the direct analysis of samples without extensive sample preparation or separations.[48-50] Paper spray mass spectrometry (PS-MS) is one such example as it provides a rapid and cost-effective method for the analysis of small organic molecules, complex mixtures, peptides, and intact proteins in a variety of environmental and biological matrices with little to no sample preparation.[13, 20, 37, 51] Samples can be preloaded onto triangular-shaped paper spray substrates, or the substrates themselves can be used to wipe the sample off of various surfaces.[13, 20, 37, 51, 52] Pre-loading analyte onto the paper substrates allows for potential long-term storage of the sample prior to analysis, which is beneficial when sample collection occurs in the field.[53] Dried sample can be directly

analyzed from the paper substrates by simply wetting the paper substrate with an organic spray solvent and applying a high voltage while in close proximity to the mass spectrometer inlet (1–4 mm). Analysis times typically range from 30 s to 1 min.[54] This methodology is particularly beneficial in clinical and forensic applications for the analysis of crude biofluids (i.e. whole blood, plasma, and urine) or when access to miniature mass spectrometers is practical.[13, 55-59] When analyzing biofluids, the applied spray solvent allows the analyte of interest to be quickly extracted while leaving the bulk of the biofluid behind due to the affinity of the analyte and spray solvent, as well as mobility of the molecules in the sample.[37, 53, 54] Other benefits of PS-MS include low sample and solvent consumption, improved detection limits, and inexpensive substrates.[13, 20, 37, 51]

There is a need to improve analytical approaches for therapeutic drug monitoring (TDM). Mass spectrometry (MS)-based methods for TDM tend to be technically complex. Patient care can be further delayed when samples must be sent to an outside reference laboratory for analysis. Paper spray MS assays have been reported for a number of different therapeutic drugs.[60-62] Nearly all the PS- MS literature on therapeutic or abused drugs concerns the analysis of hydrophobic molecules.[54] While most drugs are hydrophobic molecules, there are still a significant number of hydrophilic drugs, including beta-lactam antibiotics such as ampicillin. Detection and quantification limits for hydrophilic compounds are generally significantly higher than for hydrophobic molecules, however, making water-soluble drugs a challenging class for PS-MS. The relatively poor detection limits are caused by a combination of the strong binding affinity of these molecules to the paper substrate, poor recovery in organic solvents, co-extraction of matrix components in polar spray solvents leading to greater ion suppression, and lower intrinsic electrospray ionization efficiency of hydrophilic molecules. To overcome this, optimizing solvent and substrate properties is imperative to obtain adequate sensitivity, accuracy, and reproducibility.

This work presents a fractional factorial statistical design approach where eight different paper spray experimental factors were screened simultaneously to improve quantitation of ampicillin. This optimization procedure significantly improved detection limits and reproducibility, which enabled quantitative analysis of ampicillin in dried plasma with a detection limit of 0.07 μg/mL. This paper represents the first report of the analysis of a beta-lactam antibiotic by PS-MS, and offers a comprehensive, statistical, and systematic approach to method optimization.

2.3 Experimental

2.3.1 Safety

Flammable solvents are used throughout the method. Special care, including the use of personal protective equipment, should be taken when analyzing biofluids.

2.3.2 Chemicals and reagents

Whatman paper (31ET, Filter 5, Filter 1575 and Filter 4) (Sanford, ME, USA), polyethylene paper (Fisher Scientific, Pittsburg, PA, USA), graphene paper (Sigma Aldrich, St. Louis, MO, USA), 3 M Durapore paper (Fisher Scientific), Whatman silica-coated paper and pre-made laser cut cartridges (Prosolia, Inc, Indianapolis, IN, USA) were all tested as paper substrates in the paper screening study. Analytical grade acetonitrile, N,N-dimethylformamide, ethyl acetate, chloroform, dichloromethane, methanol, ethanol, isopropanol, acetone, and water were purchased from Fisher Scientific. A 90:10 acetonitrile:water solution was used for the spray solvent in all paper substrate screening experiments. Formic acid (FA) at a concentration of 0.1% was added to all spray solvents to aid in ionization. Ampicillin and ampicillin-D5 were purchased from Sigma Aldrich and Toronto Research Chemicals, Inc. (North York, ON, Canada), respectively.

2.3.3 Modifying of paper substrates

The Whatman chromatography paper (31ET, Filter 5, Filter 1575, and Filter 4) was coated using a silanization reagent reported by Damon et al.[63] Carbon-nanotube coatings were prepared as described by Zhang et al.[64] Polyethylene, 31ET, Filter 5, and Filter 1575 were coated in a layer of carbon exceeding 100 nm in thickness using a Vacuum Desk V sputtering system (Denton, Moorestown, NJ, USA) as previously described by Wichert et al.[65] Briefly, paper substrates were cut to fit within the sputter chamber, approximately 20 cm . Carbon rods were sharpened and held in contact via a spring-loaded mount, and a current (~15 A) was applied to slowly deposit the carbon, which yielded a uniform layer on the paper substrates.

2.3.4 Sample preparation

Because ampicillin can be methanolized or hydrolyzed in methanol or water, respectively, it was dissolved in N,N-dimethylformamide (1 mg/ mL). The 1 mg/mL ampicillin solution was further diluted to 10 μg/mL and 1 μg/mL solutions in acetonitrile. Paper tips for the thirteen

substrate types were cut for manual paper spray. A volume of 8 µL of neat solution was spotted onto each of the paper substrates at three concentrations: 10 µg/mL, 1 µg/mL, and a blank. All experiments were run in triplicate, and samples were allowed to dry for 1 h after spotting. For studies that took place in crude biofluid media, this same procedure was followed; however, only 3 µL of each concentration was spotted to avoid overloading the paper substrate with biofluid.

2.3.5 Paper spray setup

The samples were analyzed on a LTQ XL linear ion trap mass spectrometer (Thermo Fisher Scientific, San Jose, CA, USA). The mass spectrometry parameters were optimized during tuning and utilized as follows: 250°C capillary temperature, 43 V capillary voltage, 90 V tube lens voltage, 4000 V spray voltage, 1 microscan, and 15 eV collision energy. All spectra were acquired in positive ion mode and tandem mass spectrometry (MS/MS) with collision- induced dissociation was utilized for analyte identification. Xcalibur software (Xcalibur Software, Inc., Arlington, VA, USA) was used for collecting and processing. The transitions used were the $[M + H]^+$ m/z 350 ➔ 160 for ampicillin and the $[M+H]^+$ m/z 355 ➔ 160 for ampicillin-D5.

2.3.6 Statistical analysis

The two concentrations (10 µg/mL and 1 µg/mL) and blanks for the thirteen different paper substrate and coating combinations were compared statistically at each level. A one factor analysis of variance (ANOVA) test compared the peak AUCs for the fragmented m/z 350 data followed by a post-hoc Fisher Least Significant Difference (LSD) test. Statistical analyses were performed using SPSS (IBM, Armonk, NY, USA) and Minitab (Minitab, Inc., State College, PA, USA). After optimizing the paper substrate, spray solvent solutions containing tetrahydrofuran (THF), ethyl acetate, dichloromethane, chloroform, acetonitrile, acetone, methanol, isopropyl alcohol, or ethanol were mixed in a 90:10 ratio with water and were analyzed for optimal peak AUC, S/B ratio, blank signal, and blank standard deviation. In this study, signal-to-blank is defined as the AUC of the m/z 160 ion in the extracted ion chromatogram for the 1µg/mL ampicillin calibrant versus the AUC of the m/z 160 ion in the extracted ion chromatogram for the blank.

2.3.7 Optimization of ampicillin

Optimization of experimental conditions was carried out to maximize the S/B ratio and average AUC for the 1 μg/mL ampicillin calibrant after selecting a paper substrate and solvent composition. A screening Design of Experiment (DOE) tool was used after the factors were properly identified. This experiment is classified as a screening DOE due to the highly fractionated design used. From this screening, solvent volume (40 μL and 100 μL), sample volume (1 μL and 3 μL), paper pore size (2 μm and 16 μm), PS mounting type (alligator clip and pre-made plastic paper spray cartridges from Prosolia), paper that was washed (sonicated in THF for 10 min and allowed to air dry) or unwashed paper, the cut quality of the paper (bad with frayed or dulled edges and good cut quality with no fraying and sharp tips), and the location of the solvent when applied to the dried biofluid spot (back half of the dried biofluid spot and front half of the dried biofluid spot) were identified as the most likely causes of changes seen in intensity, S/B ratio, blank signal, and variation. A randomized Resolution IV 1/16 fractional factorial design with two center points was employed to identify main effects with low order interactions between factors more efficiently (**Table 2.1**). A center point, represented as 0 in the design table, was run to assess curvature within the design matrix. A factorial design uses a statistical technique to analyze which variable(s) affect the specified response. This design is ideal when interactions between factors can occur as the conditions of one factor will require a specific condition of another factor to have the appropriate response. Factorial designs fit a regression model:

$$y = \beta_0 + \sum_{i=1}^{k} \beta_i x_i + \sum_{j=1}^{k} \beta_j x_j + \Sigma\sum_{i<j} \beta_{ij} x_i x_j + \ldots + \varepsilon \qquad \text{Equation 2.1}$$

where y is the response, β0 is constant, βi is the coefficient for factor A, xi represents the level of factor A effects, βj is the coefficient for factor B, xj represents the level of factor B effects, βij is the coefficient of the interaction between factors A and B, and ε indicates the experimental errors[42]. More terms can be added with an increasing amount of factors[42].

Table 2.1 Eight-factor DOE on untreated 31ET paper using THF in dried plasma spots. The units −1, 0, and 1 represent low, center, and high values, respectively.

Run Order	Pore Size	Sample Volume	Solvent Volume	Paper Spray Mount	Solvent Mixture	Washing Paper	Cut Paper	Solvent Location
1	0	0	0	0	0	0	0	0
2	1	1	1	-1	-1	-1	1	-1
3	-1	-1	-1	-1	-1	-1	-1	-1
4	-1	1	1	-1	-1	1	-1	1
5	1	-1	1	1	-1	1	-1	-1
6	-1	1	1	1	1	-1	-1	-1
7	-1	1	-1	1	-1	1	1	-1
8	0	0	0	0	0	0	0	0
9	1	1	-1	-1	1	1	-1	-1
10	1	1	1	1	1	1	1	1
11	-1	-1	1	1	-1	-1	1	1
12	1	-1	1	-1	1	-1	-1	1
13	1	-1	-1	-1	-1	1	1	1
14	-1	-1	1	-1	1	1	1	-1
15	-1	-1	-1	1	1	1	-1	1
16	1	1	-1	1	-1	-1	-1	1
17	-1	1	-1	-1	1	-1	1	1
18	1	-1	-1	1	1	-1	1	-1

These variable terms are coded −1, 0, and 1 to represent low, center, and high points, respectively. The physical values for the factors are specified above. It is important to note that due to the high fractionality of the design, some factors and interactions will be indistinguishable. A Resolution IV design was used instead of a full factorial to minimize the amount of experimental trials without losing the lower order interactions, which better classifies this design as a screening experiment.

2.3.8 Calibration curve preparation

A calibration curve ranging from 0.20 μg/mL to 100 μg/mL was generated from ampicillin spiked into pooled human plasma. To reduce carryover and blank signal, the plastic pieces from the paper spray cartridges were pre-rinsed by sonicating the cartridges for 60 min in water twice while rinsing with methanol between steps and allowing them to air-dry prior to reassembly. Whatman 31ET paper was razor cut to fit in pre-made plastic paper spray cartridges. Ampicillin was spiked into plasma, and 8 μL of the ampicillin or blank plasma was spotted onto the respective cartridge. The sample was allowed to dry for 1 h. The cartridge was secured in close proximity to the mass spectrometer inlet using a manual paper spray set-up, and 60 μL of the spray solvent containing 60:30:10 ACN:THF:H2O with 0.1% FA and high voltage (4 kV) were applied. The

data was fitted using a weighted least-squares regression analysis with a weighting of $1/x^2$. The limit of detection (LOD) was defined as three times the standard deviation of the AUC in drug-free plasma divided by the slope of the calibration curve ($3* s_b/m$).[66] The lower limit of quantitation (LLOQ) was calculated as $10* s_b/m$.

2.4 Results and discussion

2.4.1 Selection of paper substrates and spray solvent

An initial screening of neat ampicillin standards was performed using Whatman 31ET laser-cut paper, carbon-sputtered polyethylene paper, hydrophobic Filter 5 paper, hydrophobic Filter 4 paper, porous polyethylene paper, carbon-nanotubes coated paper, carbon- sputtered 31ET paper, 3 M Durapore paper, silica-coated paper, and graphene paper. Upon initial analysis, the laser-cut 31ET paper had the highest AUC for a neat sample. However, the carbon-sputtered polyethylene had the highest S/B (data not shown). Neither the silica-coated nor the graphene paper substrates could be analyzed due to difficulties with spray stabilization and corona discharge. The substrates with the highest AUC and S/B ratio were used in further studies containing dried biofluids. This eliminated the various polyethylene papers, 3M Durapore paper, and carbon-nanotubes coated paper. When comparing the peak AUC and S/B ratio of the 1µg/mL ampicillin calibrant in dried plasma spots among various coatings and paper types, the untreated Filter 1575 paper had the highest peak AUC (**Figure 2.1A**) while the carbon-sputtered 31ET paper had the highest S/B ratio (**Figure 2.1B**). Both carbon-sputtered Filter 1575 paper and untreated Filter 1575 paper were also quantifiable, meaning that the S/B ratio was calculated to be 10 or greater. No clear determination could be made as to whether it was the paper type or the coating type that improved the AUC and S/B ratio. Due to the lack of preparation required for the untreated paper substrate, the carbon sputtered substrate was not further investigated. Additionally, carbon sputtered substrates have an optimal thickness to where too much or too little coating results in decreased S/B (data not shown). This is difficult to control with sputtering techniques which was not ideal for this quantitative assay.

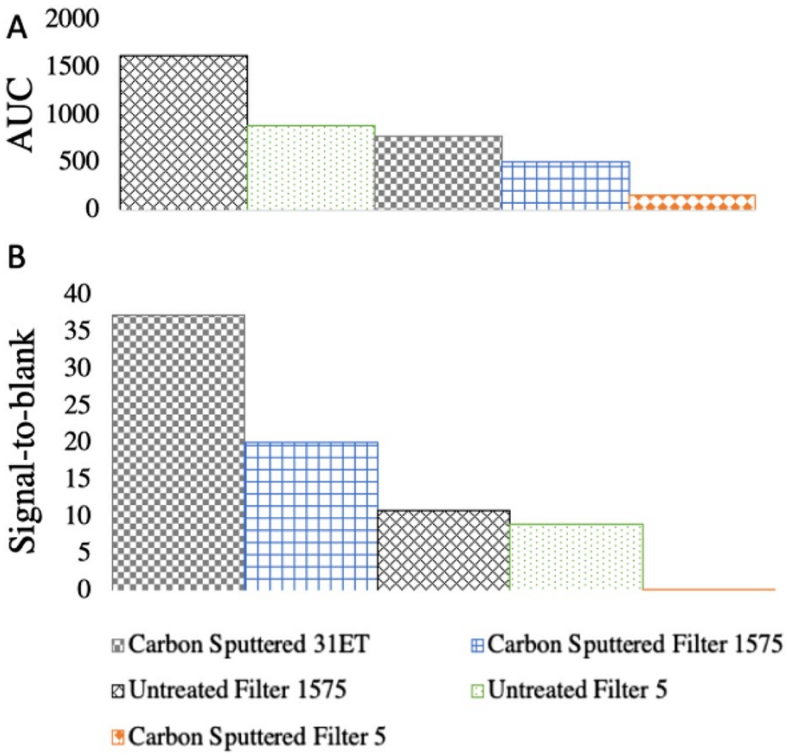

Figure 2.1 A) Area under the curve and B) S/B ratio for ampicillin (1 µg/mL) in dry plasma spots on various paper types.

As previously reported, the spray solvent composition affects both the recovery of the analyte and ion suppression.[67-69] To evaluate the spray solvent, a screening experiment using the middle pore size paper (Filter 5; 2.5 µm) and a medium solvent composition, 90:10 organic solvent:water with 0.1% FA, was performed for nine different solvents on four different paper coating types (hydrophobic, carbon-sputtered, untreated razor-cut Filter 5 paper, and laser-cut Whatman 31ET). The results showed an interaction between paper type and solvent type; the same solvent behaved differently depending on the paper coating type (**Figure 2.2**). The highest AUC for the 1 µg/mL ampicillin calibrant in dried plasma was obtained with the carbon-sputtered Filter 5 paper using 90:10 ethyl acetate:water with 0.1% FA ($P = 0.002$) and untreated razor-cut Filter 5 paper with 90:10 THF:water with 0.1% FA ($P = 0.005$). The THF solvent showed poor signal stability despite having the highest average AUC. Methanol and acetonitrile were added to this solvent to attempt to maintain the favorable extraction properties of THF while stabilizing the spray. Both acetonitrile and methanol stabilized the signal, but the S/B ratio was close to 1 when methanol was used. Addition of acetonitrile, on the other hand, did not have a deleterious effect

on the ampicillin signal. A 60/30/10 mixture of ACN/THF/water with 0.1% FA was therefore selected for further optimization in the screening DOE described below.

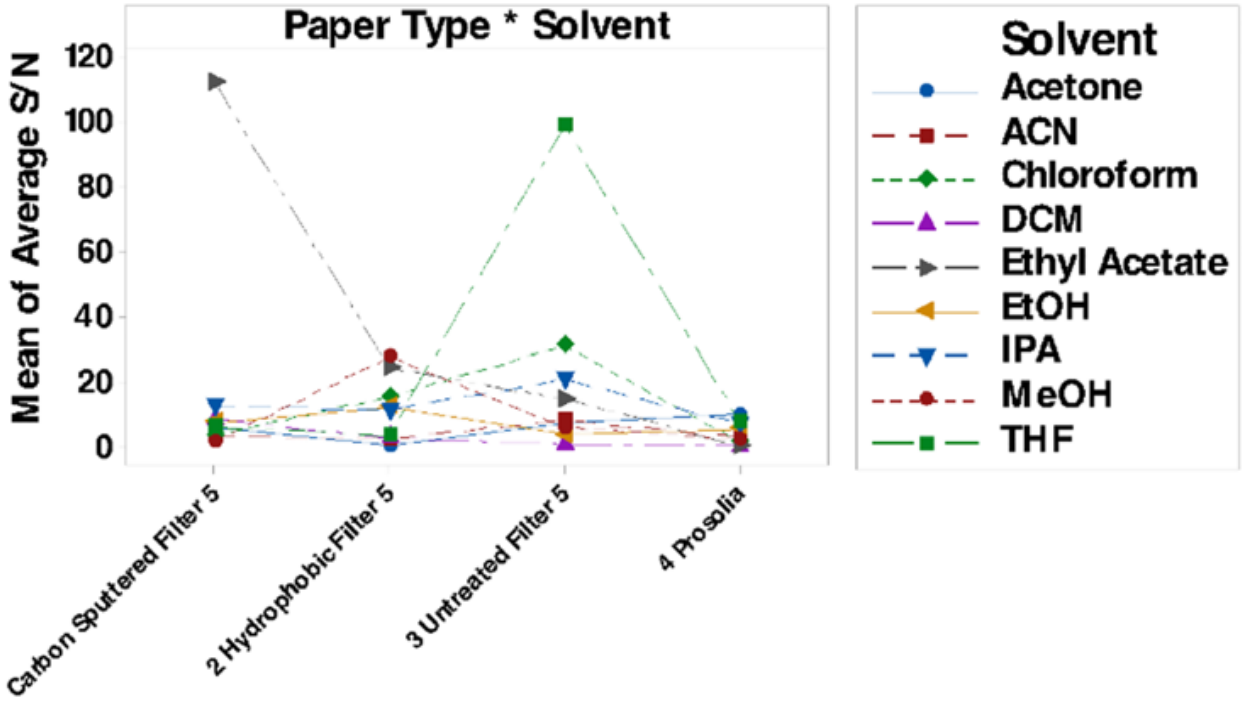

Figure 2.2 Interaction plot of coating and solvent type for the average S/B ratio of ampicillin (1 µg/mL) in dried plasma spots.

2.4.2 Optimization of experimental conditions

A screening DOE was conducted to test the effects of paper pore size, sample volume, solvent volume, the paper spray mount, paper wash, quality of tip cut, solvent mixture, and solvent location on ampicillin detection from dried plasma. Solvent volume, sample volume, and pore size significantly affected the peak AUC of the 1 µg/mL ampicillin calibrant (**Figure 2.3A**). There was an observable two-way interaction between pore size and solvent volume, meaning that one factor was directly affected by the other factor. There was also one three-way interaction between pore size, sample volume, and solvent volume. Similar results were observed for the S/B ratio (**Figure 2.3B**). A cube plot was used to show interactions between the three factors and the predicted response of each of the factor combinations. The predicted value was at its highest point when the sample volume (3 µL), solvent volume (100 µL), and pore size (31ET paper) were at their high levels (**Figure 2.4**), meaning that these factors should be set at high values to obtain the highest

signal. This finding implied that these factors could be further optimized to increase the signal of the 1μg/mL ampicillin calibrant. The pre-made plastic cartridge holder with razor-cut 31ET paper was chosen for ease of use and the 60:30:10 ACN:THF:water with 0.1% FA solvent mixture was chosen due to the improved reproducibility as discussed previously. The remaining three factors (paper washing, quality of tip cut, and solvent location) were confirmed as not statistically significant. The high and low values of the three-way interaction were run to confirm these results. Pore size of the paper was not investigated further as the Whatman 31ET paper is a widely used paper in dried blood cards and for paper spray MS. Sample volume and solvent volume were investigated further to see if increasing these volumes would increase the AUC and S/B ratio. It was found that sample volume was the only factor that was statistically significant, indicating that higher sample volume produces higher analyte signal (data not shown). Our model indicated that a larger sample volume could be used but, due to the physical limitations of the paper substrate, the sample volume was not increased past 8 μL. Too much solvent can "overload' the paper and cause leaking which will cause high variability in the AUC of the analyte. To prevent solvent leakage from the cartridge, 10 μL of solvent was added onto the dry plasma spot followed by adding 60 μL to the back of the cartridge rather than utilizing the maximized solvent volume from the model. This "prewetting" step of adding solvent in the front of the cartridge was to reconstitute the analyte in solvent to allow capillary action to still be effective even with the reduced solvent volume. This decrease in signal did not affect the ability to detect the 1 μg/mL ampicillin calibrant. None of the eight factors reduced the signal for the blank or reduced the standard deviation of the blank.

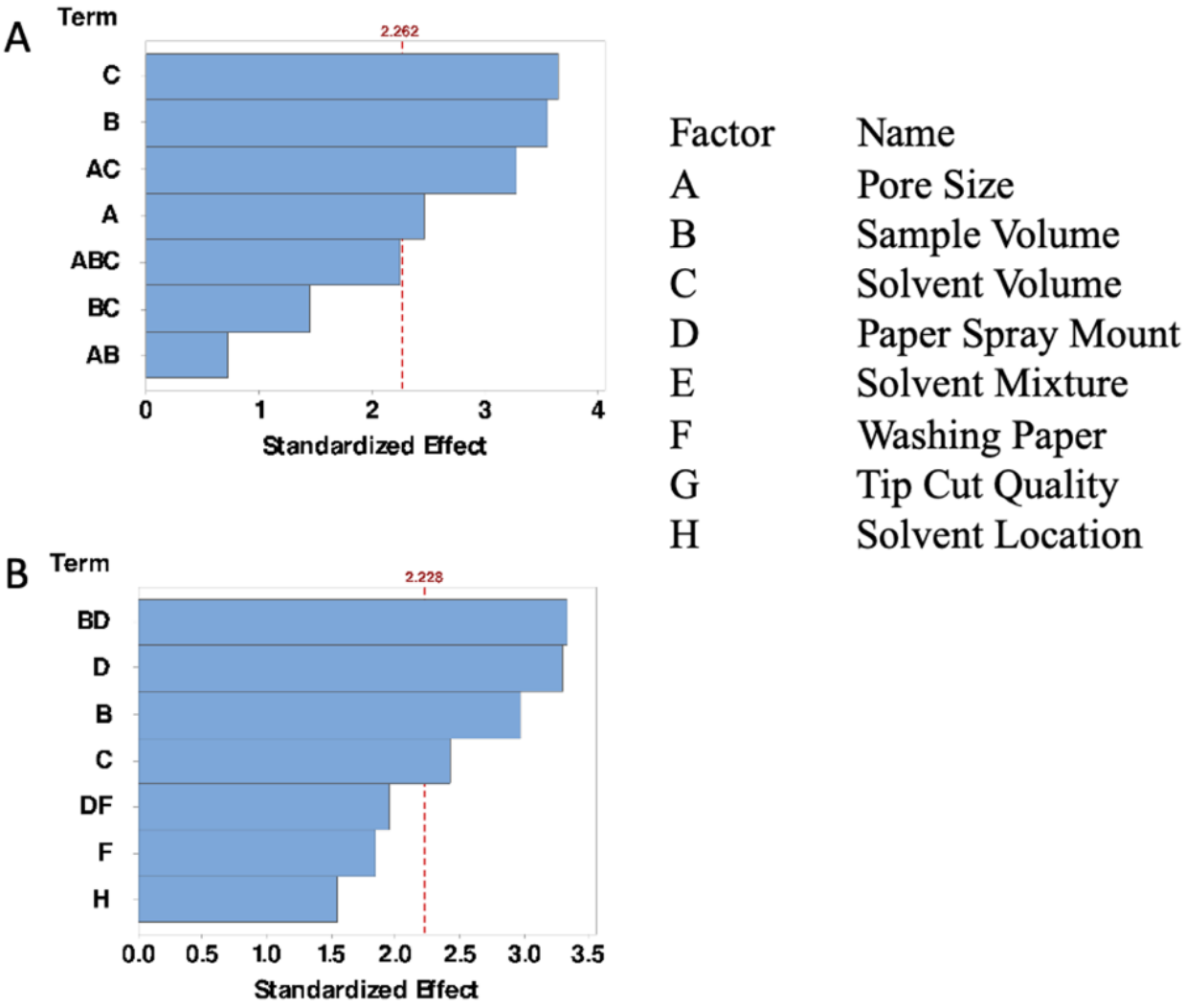

Figure 2.3 Pareto chart of the standardized effects for A, average AUC and B, average S/B ratio of the 1 µg/mL ampicillin calibrant in dried plasma. Standardized effect refers to the T-statistics gathered for each factor when testing if the factor will have no effect (effect = 0) on the average AUC or S/B ratio. Effects below the red dashed line indicate this null hypothesis being rejected with an alpha ≥0.05 (i.e. no significant effect). The standardized effect is an absolute value and therefore only the magnitude of the response can be determined, not the direction (see cube plot for direction).

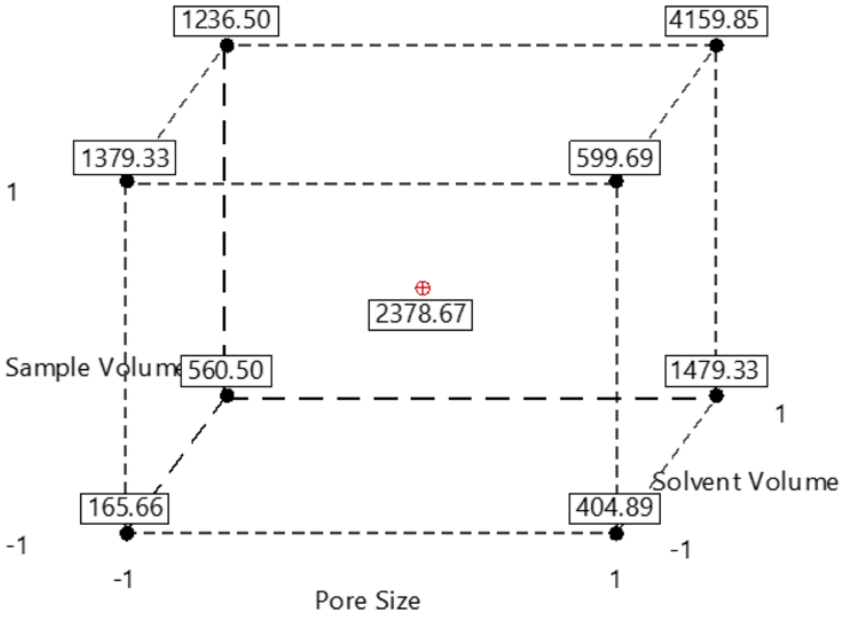

Figure 2.4 Cube plot of three-way interaction between pore size (x), solvent volume (z), and sample volume (y) for average AUC of 1 µg/mL ampicillin. The boxes on each vector depict the AUC of the 1 µg/mL ampicillin for each factor combination run at the high (1) and low (−1) factor parameter.

2.4.3 Analysis of dried plasma samples

To confirm the parameter optimization model, a calibration curve was generated (**Figure 2.5**). The data was linear for the range of 0.2–100 µg/mL (R^2 = 0.98) with a LOD of 0.07 µg/mL and a LLOQ of 0.25 µg/mL. The range of this calibration curve is consistent with other methods in the literature for monitoring ampicillin plasma concentrations for TDM.[70] The average AUC for the 1 µg/mL ampicillin plasma calibrant increased from 500 to 21,000 with the optimized conditions compared with the original method. Likewise, the S/B ratio at the 1 µg/mL level increased from 2 to 58.

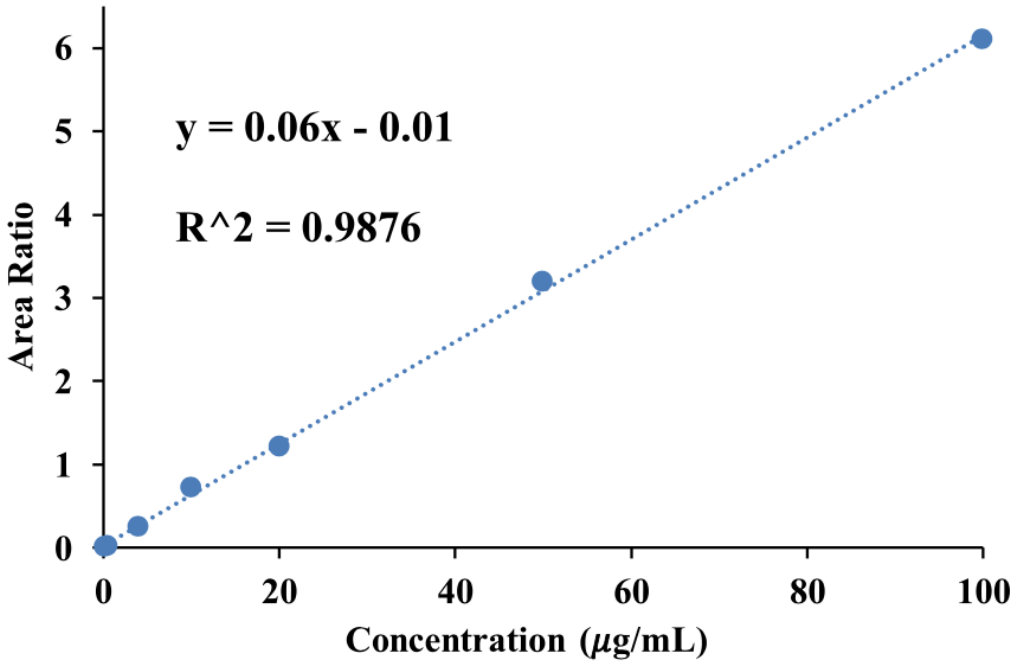

Figure 2. 5 Calibration curve of ampicillin in a dry plasma spot using PSI-MS. Each data point is the average of two analytical replicates.

2.5 Conclusions

A fractional factorial design was employed for the analysis of the hydrophilic compound, ampicillin, in a dried plasma spot using PS- MS. Pore size, sample volume, solvent volume, paper spray mount, and solvent mixture were all optimized to improve the average peak AUC of the 1μg/mL ampicillin calibrant and the S/B ratio compared with a blank signal. The cut of the paper, paper wash, and the solvent location were not statistically significant factors, indicating that they would not contribute greatly to changes in signal. This finding highlights the robustness of the process. A seven-point calibration curve was performed and showed linear values (R^2 = 0.98). An LOD of 0.07 μg/mL and a LLOQ of 0.25 μg/ mL were calculated, well below the minimum inhibitory concentration (MIC) reported for all pathogens sensitive to this antibiotic. The AUC of ampicillin increased by a factor of 42, and the S/B ratio increased by a factor of 29 using our optimized conditions. This statistical method of screening followed by optimization experiments is faster, and more efficient, and produces more drastic improvements than typical one-factor-at-a- time (OFAT) experiments.

CHAPTER 3. SIMULTANEOUS OPTIMIZATION OF PAPER SUBSTRATES AND SOLVENTS FOR HYDROPHILIC AND HYDROPHOBIC MOLECULES

3.1 Abstract

Paper spray mass spectrometry is an ambient ionization technique capable of the direct ionization of analyte from a bio-fluid spot on a paper substrate. Different solvents and types of paper can have different interactions with the analytes of interest; therefore, they can significantly impact the analyte signal and the assay as a whole. In this study, we examined the effects of substrate-solvent composition on signal intensity, blank signal intensity, and signal-to-blank ratio for a variety of pharmaceutical drugs, illicit drugs, chemical warfare agent (CWA) simulants, and CWA hydrolysis products. The analytes were prepared either neat or spiked into human plasma and deposited on a variety of modified paper substrates. Extraction occurred with a range of different solvents. Optimizing the substrate-solvent combination improved the signal-to-blank ratio for all compounds ranging from 1 to 7,964 factor improvement, with the substrate providing a more impactful improvement. Aprotic solvents, such as tetrahydrofuran and ethyl acetate, tended to produce optimal signal-to-blank ratios, while carbon sputtered and glass fiber substrates were the top paper substrates. The research presented herein illustrates the need for systematic optimization of substrate and spray solvent combinations to achieve the best detection limits for paper spray analysis.

3.2 Introduction

Ambient ionization in tandem with mass spectrometry has garnered considerable interest for the detection of small to medium sized compounds at trace concentrations in a variety of complex matrices. These methods are advantageous because they do not require chromatography or significant sample preparation.[14] As a result, the development of ambient ionization techniques has exploded over the past two decades with the conception of such techniques as desorption electrospray ionization (DESI)[71, 72] direct analysis in real time (DART)[48], dielectric barrier discharge ionization (DBDI)[73], ionization by low temperature plasma (LTP)[74], extractive electrospray ionization (EESI)[75], secondary electrospray ionization (SESI)[76], as well as a number of atmospheric pressure-based desorption/post-ionization combinations.[77-81] These methods were

ground-breaking as they allowed for the direct detection of chemicals from solid surfaces or complex liquid matrices. However, the sensitivity of most methods did not translate to the analysis of blood or crude biofluid matrices. To overcome this obstacle, other techniques, like paper spray (PS), were developed to help fill this void.[51]

Paper spray-mass spectrometry (PS-MS) was unique at its inception in its ability to achieve low detection limits (ng/mL to pg/mL, depending on the analyte) from the direct analysis of dried blood, plasma, and urine spots without the need for sample preparation.[40, 51, 60, 82-86] Paper spray has been used in clinical[60, 82, 83, 85, 87, 88], environmental[18, 19, 89], national security[20, 90, 91], and forensics analyses.[13, 84, 88, 92] This technique is useful in a variety of mediums, including biological fluids[20, 60, 82-88, 93], insect gut[94], and environmental samples.[18, 19, 65, 89] Briefly, PS-MS is performed by depositing a small amount of crude bio-fluid (i.e. whole blood, urine, plasma) onto a porous, triangular shaped paper substrate, which is secured directly in front of the inlet to a mass spectrometer. A spray solvent is applied to the rear of the paper where it diffuses through the paper substrate via capillary action and extracts the soluble analyte from the matrix as it wicks through the dried spot. A high voltage (3 - 5 kV) is applied inducing the formation of an electrospray-like Taylor cone at the sharp tip of the paper. Positively- or negatively-charged gas-phase ions of the desired analyte are produced, fragmented, and then detected inside the mass spectrometer. Total extraction and analysis time is approximately one minute.[51]

As the applications for paper spray expand, the properties of this ionization technique are being further investigated. Optimization studies have been performed to identify major factors influencing the signal response of analytes, including sample and solvent volume, paper substrate type, and solvent type.[51, 67, 95, 96] Additionally, solvent flow rates and applied voltages can alter the spray stability, thereby affecting the signal intensity.[97, 98] Most drugs are hydrophobic; therefore, traditional paper spray substrates produce relatively low detection limits for these analyte classes. The analysis of hydrophilic analytes, however, has been an ongoing struggle due to poor detection limits. This is due in part to the low ionization efficiency of hydrophilic molecules by electrospray ionization owing to low surface activity. Strong binding affinity between the paper substrate and the analyte is also a contributing factor. Finally, hydrophilic molecules tend to be less soluble in organic solvents, which results in poor recovery in the spray solvent. Paper substrate modification utilizing coatings has been explored to mitigate these bonds and increase analyte signal response.[63, 69, 99-107] Moreover, the solvent should be chosen based on its dielectric properties, viscosity, and

polarity to increase spray stability and recovery of the analyte. A wide variety of solvents have been used from highly nonpolar, like hexane, to polar protic, like methanol.

In this study, we systematically studied the effect of different paper substrate-solvent combinations on signal-to-blank ratio and repeatability. The molecules investigated encompass compounds with a wide range of hydrophilicities (logP ranging from -2.5 to 7.5) and molecular weights (from 124 to 1,202). Optimizing the substrate-solvent conditions for each analyte resulted in improved signal-to-blank ratios up to 7,964x. This paper offers a practical approach to optimizing the substrate and solvent for various analytes in different media.

3.3 Methods

3.3.1 Chemicals and Reagents

Polyethylene (Fisher Scientific, Pittsburg, PA, USA), 31ET Whatman chromatography paper (Sanford, USA), and silicon-coated paper (Whatman, Sanford, USA) were all used as paper substrates in the paper screening study. Analytical grade acetonitrile (ACN), N,N-Dimethylformamide (DMF), tetrahydrofuran (THF), ethyl acetate (EA), methanol (MeOH), isopropanol (IPA), acetone, and water were purchased from Fisher Scientific (Pittsburg, PA, USA). Formic acid, dimethyl sulfoxide (DMSO), and carbon tetrachloride (CCl_4) were all purchased from Sigma Aldrich (St. Louis, MO, USA). For the substrate-solvent optimization experiments, a solvent mixture in a ratio of 90:10 organic:CCl_4 acted as the spray solvent for the chemical warfare agents in the paper substrate screening experiments. An 80:10:10 organic:water:CCl_4 acted as the spray solvent for the antifungals, antibiotics, antivirals, immunosuppressants, and fentanyl analogs. Adding formic acid to these mixtures at a concentration of 0.1% aided in ionization. It is important to note that long-term exposure of the mass spectrometer to carbon tetrachloride mixed with aprotic solvents can cause corrosion of steel. If carbon tetrachloride is a necessary addition, the system should immediately be flushed with a polar protic solvent mixture to minimize these corrosion effects.

Acetyl fentanyl, carfentanil, cyclopropyl fentanyl, fentanyl, furanyl fentanyl, remifentanil, hydromorphone, hydrocodone, oxycodone, and oxymorphone were acquired from Cerilliant (Round Rock, TX, USA). Fluoroisobutyryl fentanyl (FIBF), everolimus, cyclosporin A, tacrolimus, acyclovir, ampicillin, piperacillin, meropenem, ceftriaxone, cefepime, and linezolid were purchased from Cayman Chemicals (Ann Arbor, MI, USA). Chemical warfare simulants: dimethyl

methylphosphonate (DMMP), diethyl phosphoramidate (DEPA) and diisopropyl methylphosphonate (DIMP), hydrolysis products: ethyl methylphosphonate (EMPA), isopropyl methylphosphonate (IMPA), and pinacolyl methylphosphonate (PinMPA), and organophosphorus pesticides: dichlorvos and malathion were obtained from Sigma Aldrich (St. Louis, MO, USA), as well as itraconazole, posaconazole, fluconazole, voriconazole, valganciclovir, oseltamivir, and ganciclovir. Hydroxy-itraconazole was purchased from Fitzgerald Industries International (Acton, MA, USA). Remdesivir was purchased from Asta Tech (Bristol, PA, USA) while baloxavir was purchased from BioVision (Milpitas, CA, USA).

3.3.2 Sample Preparation

Fentanyl Analog Stock and Working Solutions

A stock solution for carfentanil was diluted to 10 µg/mL in methanol. The concentration of cyclopropyl fentanyl, fentanyl, and FIBF were 1 mg/mL, while the concentrations of furanyl fentanyl and remifentanil were 100 µg/mL. From these individual stock solutions, a working solution containing all the analytes was prepared at 0.2 µg/mL in acetonitrile with 0.1% (v/v) formic acid. All stock and working solutions were stored at -20°C until use. Neat and plasma samples were prepared volumetrically by diluting the working solution in acetonitrile or pooled human plasma, respectively, to achieve a final concentration of 50 ng/mL. Finally, 8 µL of blank, neat, or spiked plasma was spotted onto pretreated Verispray cassettes (ThermoFisher Scientific, San Jose, CA, USA) and allowed to dry for one hour.

Antifungal Stock and Working Solutions

Stock solutions were prepared in DMF at the following concentrations: fluconazole (6 mg/mL), voriconazole (1 mg/mL), hydroxyitraconazole (1 mg/mL), posaconazole (2 mg/mL), and itraconazole (2 mg/mL). These were stored at -20°C until use. A 20 µg/mL spiking solution was made in 95:5 methanol/water with 0.01% acetic acid. Pooled human plasma was spiked to achieve a final concentration of 0.67 µg/mL for voriconazole, itraconazole, hydroxyitraconazole, and posaconazole. Fluconazole was at a final concentration of 10 ppm. Finally, 8 µL of blank or spiked plasma was spotted onto pre-treated Verispray cassettes and allowed to dry for one hour.

Antiviral Stock and Working Solutions

Stock solutions were prepared in DMSO at the following concentrations: remdesivir (1 mg/mL), acyclovir (1.24 mg/mL), ribavirin (1.63 mg/mL), valganciclovir (1.25 mg/mL), oseltamivir (1.17 mg/mL), and baloxavir (3.21 mg/mL). A 200 µg/mL spiking solution was made in methanol and stored at -20°C until use. Ganciclovir and foscarnet were made in water at 1.67 mg/mL and 1.64 mg/mL respectively. This was diluted to 50 µg/mL in water and stored at -20°C until use. These were spiked into a single pooled human plasma sample to achieve a final concentration of 25 µg/mL. Finally, 8 µL of blank or spiked plasma was spotted onto pre-treated Verispray cassette and allowed to dry for one hour.

Immunosuppressant Stock and Working Solutions

Stock solutions were prepared in DMSO at the following concentrations: tacrolimus (5 mg/mL), everolimus (1.51 mg/mL), and cyclosporin A (1.62 mg/mL) and stored at -20°C until use. A 200 µg/mL spiking solution was made in methanol. These were spiked into a single pooled human plasma sample to achieve a final concentration of 1 µg/mL. Finally, 8 µL of blank or spiked plasma was spotted onto pre-treated Verispray cassette and allowed to dry for one hour.

Chemical Warfare Agent Hydrolysis Products (CWA) Stock and Working Solutions

A working solution was prepared at 1 mg/mL in methanol for the CWA simulants and pesticides. The hydrolysis products were prepared at 1 mg/mL in water. A 2 µg/mL solution of all analytes in water was prepared from the working solutions and stored at -20°C until use. A 8 µL sample volume of neat solution was spotted onto the VeriSpray cassette and dried for one hour.

Antibiotic Stock and Working Solutions

Stock solutions were prepared in DMF at 20 mg/mL for ampicillin, linezolid, meropenem, and piperacillin. Cefepime and ceftriaxone stock solutions were prepared in water at 20 mg/mL. All stock solutions were stored at -20°C until use. A 2 mg/mL spiking solution containing ampicillin, linezolid, and piperacillin was prepared in acetonitrile and a 2 mg/mL spiking solution containing meropenem, ceftriaxone, and cefepime were prepared in water. These were spiked into a single

pooled human plasma sample to achieve a final concentration of 50 µg/mL. Finally, 8 µL of blank or spiked plasma was spotted onto pre-treated Verispray cassette and allowed to dry for one hour.

Opiate Stock and Working Solutions

Stock solutions were purchased at 1 mg/mL for oxycodone, oxymorphone, hydrocodone, and hydromorphone. All stock solutions were stored at -20°C until use. A 10 µg/mL spiking solution containing oxycodone, oxymorphone, hydrocodone, and hydromorphone was prepared in methanol. These were spiked into a single pooled human plasma sample to achieve a final concentration of 500 ng/mL. Finally, 8 µL of blank or spiked plasma was spotted onto pre-treated Verispray cassette and allowed to dry for one hour.

3.3.3 Paper Substrate Preparation and MS Parameters

The Whatman 31ET chromatography paper and silicon-coated paper were laser cut using a Trotec laser engraver (Plymouth, MI, USA). The paper substrate template was made using Adobe Illustrator (San Jose, CA, USA). A standard process mode with 1000 dpi resolution was used for the paper substrate cut file. The paper was cut using 55% laser power and 12% velocity. After cutting, paper was coated using either a silanization reagent reported by Damon et al[63], carbon sputtered as reported by Wichert, et al[65], or used as is for untreated paper. Glass fiber paper was laser cut using the same conditions and then treated with an ammonium sulfate solution as reported by Dhummakupt et al.[108] Briefly, the silanization occurred by adding 0.5 mL of tri-chloro(3,3,3-trifluoropropyl) silane under vacuum for one hour. Polyethylene paper was razor cut because the laser cuts were not clean. Samples were run on a Thermo Fisher TSQ Altis (San Jose, CA, USA). The MS parameters were optimized for each compound class. SRM transitions and instrument parameters can be seen in **Table 3.1**. The collision gas pressure was set at 2 mTorr. A total volume of 10 µL prewet and 110 µL of solvent B was dispensed using the Verispray system at the following dispense speed (in seconds): 1, 1, 1, 1, 3, 3, 3, 5, 5, 7, 7. Data was collected for 1.2 minutes in positive ion mode for all compounds except for the CWA. A segmented method was used to acquire data for 30 sec in each ionization mode.

Table 3.1 Analyte and MS SRM parameters. LogP values were obtained via Pubchem.[109]

Chemical Warfare Agent Hydrolysis Products							
Analyte Name	**logP**	**Precursor (m/z)**	**Fragment (m/z)**	**CE (eV)**	**RF (V)**	**Voltage (V)**	**Temperature (°C)**
DMMP [M+H]	-0.7	125	97	11	46	4800	350
DEPA [M+H]	-0.5	154	98	14	45		
Dichlorvos [M+H]	1.4	221	109	21	55		
DIMP [M+H]	0.6	181	97	15	53		
Malathion [M+H]	2.4	331	127	13	60		
EMPA [M-H]	-0.7	123	95	14	30	3500	
IMPA [M-H]	-0.3	137	95	15	41		
PinMPA [M-H]	1.1	179	95	17	46		
Fentanyl Analogs							
Analyte Name	**logP**	**Precursor (m/z)**	**Fragment (m/z)**	**CE (eV)**	**RF (V)**	**Voltage (V)**	**Temperature (°C)**
Cyclopropyl Fentanyl [M+H]	4.0	348	188	20	80	4800	350
Fentanyl [M+H]	4.0	337	188	22	76		
FIBF [M+H]	4.7	369	188	23	81		
Furanyl Fentanyl [M+H]	4.6	375	188	21	80		
Remifentanil [M+H]	1.9	377	345	12	73		
Carfentanil [M-H]	3.8	395	363	12	77		
Antifungals							
Analyte Name	**logP**	**Precursor (m/z)**	**Fragment (m/z)**	**CE (eV)**	**RF (V)**	**Voltage (V)**	**Temperature (°C)**
Fluconazole [M+H]	0.4	307	220	18	66	4200	350
Itraconazole [M+H]	5.7	705	392	36	125		
Hydroxyitraconazole [M+H]	4.5	721	408	36	148		
Posaconazole [M+H]	4.6	701	344	44	134		
Voriconazole [M+H]	1.5	350	281	16	65		
Antivirals							
Analyte Name	**logP**	**Precursor (m/z)**	**Fragment (m/z)**	**CE (eV)**	**RF (V)**	**Voltage (V)**	**Temperature (°C)**
Acyclovir [M+H]	-1.9	226	167	13	48	4300	270
Baloxavir [M+H]	3.6	572	247	26	112		
Ganciclovir [M+H]	-2.5	256	152	14	69		
Oseltamivir [M+H]	1.1	313	225	11	43		
Remdesivir [M+H]	1.9	603	200	38	91		
Valganciclovir [M+H]	-1.5	355	152	19	53		

Table 3. 1 continued

Immunosuppressants							
Analyte Name	**logP**	**Precursor (m/z)**	**Fragment (m/z)**	**CE (eV)**	**RF (V)**	**Voltage (V)**	**Temperature (°C)**
Cyclosporin A [M+H]	7.5	1202	224	55	229	4500	270
Everolimus [M+Na]	5.9	980	389	55	249		
Tacrolimus [M+Na]	2.7	826	616	36	206		
Antibiotics							
Analyte Name	**logP**	**Precursor (m/z)**	**Fragment (m/z)**	**CE (eV)**	**RF (V)**	**Voltage (V)**	**Temperature (°C)**
Ampicillin [M+H]	-1.1	350	106	19	60	4100	250
Cefepime [M+H]	-0.1	481	396	12	70		
Ceftriaxone [M+H]	-1.3	555	396	13	73		
Meropenem [M+H]	-2.4	384	141	16	65		
Piperacillin [M+H]	-0.5	518	143	21	80		
Linezolid [M+H]	0.7	338	296	18	98		
Opiates							
Analyte Name	**logP**	**Precursor (m/z)**	**Fragment (m/z)**	**CE (eV)**	**RF (V)**	**Voltage (kV)**	**Temperature (°C)**
Hydromorphone [M+H]	1.0	316	230	35	61	4000	300
Oxycodone [M+H]	0.7	302	216	35	63		
Oxymorphone [M+H]	0.8	300	242	35	76		
Hydrocodone [M+H]	-2.2	286	222	35	82		

3.3.4 Statistical Analysis

Xcalibur (Xcalibur Software, Inc, Arlington, VA) was used for data collection. Data analysis was performed utilizing Tracefinder 3.3 (Thermo Fisher Scientific Inc., San Jose, CA, USA). All statistics were performed utilizing Minitab (Minitab Inc., State College, PA, USA) or Excel (Microsoft Corp., Redmond, WA, USA).

3.4 Results

3.4.1 Substrate-Solvent Optimization Conditions

Either neat or plasma samples were prepared and analyzed using four paper substrate types (glass fiber, untreated, carbon sputtered, and silanized) and six different solvent conditions (acetone, acetonitrile, isopropyl alcohol, methanol, tetrahydrofuran, or ethyl acetate). Silica and polyethylene substrates were omitted due to difficulty of use and high variability in spray stability. The CWA simulants are not commonly found in biofluids and so they were only prepared neat for

these studies. The fentanyl analogs and opiates were analyzed both neat and in plasma due to their importance in toxicology and environmental detection. All other compounds were analyzed in plasma only. As an initial screen, each sample condition was analyzed in duplicate, and an average ratio of signal-to-blank was calculated to determine optimal substrate-solvent conditions for each analyte (**Figure 3.1**). Once the optimal substrate-solvent combination was identified for each analyte, six replicates of both spiked and blank samples were run for each condition in a confirmation experiment to assess repeatability and reliability of the screening experiment. To evaluate the optimal solvent-substrate combination, samples were evaluated for high analyte signal, low blank response, and chronogram stability. If the results from the confirmation run revealed irreproducible signal-to-blank ratios or poor chronogram stability, the substrate-spray solvent combination giving the second or even third highest S/B was subjected to additional confirmation. This was the case for IMPA, EMPA, and PinMPA.

Figure 3.1 Heat map depicting S/B value for every combination neat (A) and in plasma (B). Conditional formatting was used to indicate the lowest S/B (white), 50% percentile (light green), and highest S/B (dark green). Changing the solvent or paper type produced drastically different results across all analyte classes.

The screening experiment (**Figure 3.1**) showed that the optimal substrate-solvent combination was dependent not only on the individual analyte but also on the analyte matrix. For example, the fentanyl analogs in neat samples had optimal S/B using carbon sputtered paper with ethyl acetate as a solvent. In plasma, however, the optimal solvent-substrate combination was the silanized paper with THF. This was different for the opiates where glass fiber paper and acetonitrile produced optimal S/B overall for neat samples and carbon sputtered paper with ethyl acetate produced optimal S/B overall for plasma samples. Analyte classes with similar chemical properties often produced similar optimal conditions. The CWA simulants and hydrolysis products are a good example of this tendency. The positive ion molecules DMMP, DEPA, and dichlorvos all had optimal S/B using carbon-sputtered paper with methanol as a solvent. Negative ion mode phosphonic acids (IMPA, EMPA, and PinMPA) were optimal when analyzed using glass fiber paper with methanol as a solvent. When the chemical structure and masses varied, as was the case with the immunosuppressant drugs, optimal S/B occurred with different solvent-substrate combinations for each drug. The immunosuppressants showed varying optimal paper conditions (glass fiber, carbon sputtered, and silanized) with solvents ranging from aprotic to polar aprotic. Despite this, compromises can often be made if multiplexing is desired. In the case of the immunosuppressants, although each analyte had different optimal conditions, they all produced high S/B using glass fiber paper with acetonitrile as a solvent. The same follows for the other analyte classes. The antifungals were optimal, as a whole, using carbon sputtered paper-THF solvent while both the antibiotics and antivirals could be simultaneously quantitated using glass fiber paper with IPA as a solvent.

Across all analyte classes, ethyl acetate was the most versatile solvent while carbon sputtered and glass fiber papers were the most useful substrates. This is depicted in **Figure 3.2** using a rank one evaluation for the various solvents and substrates. The rank one evaluation was executed by summing all analyte/matrix combinations (48 total) with optimal S/B for each solvent or substrate. Signal-to-blank improved for each analyte/matrix combination after optimization. For 41 combinations (85%), coating the paper resulted in a decrease in blank signal. However, 24 combinations (50%) saw a reduction in analyte signal due to the substrate coating. The overall S/B still improved in these cases due to the larger decrease in blank signal. For 24 combinations (50%), the optimization procedure resulted in an increase in analyte signal with 35% of those combinations (17 analytes) also having reduced blank signal. Finally, 15% (7 analyte/matrix

combinations) had an increase in both signal and blank intensity. Ethyl acetate was the most versatile solvent and had the highest S/B for the most compounds (16/48) followed by THF (12/48). The glass fiber paper had the highest S/B for the most compounds (22/48) followed by carbon sputtered paper (18/48).

We hypothesize that carbon sputtered and glass fiber papers are optimal most frequently because both have a higher wet strength meaning they keep the paper fibers intact when exposed to high volumes of liquid. High deformation of the paper can result in unstable spray and therefore decreased analyte signal. Untreated cellulose-based paper swells when wet, changing the porous space between the fibers.[110] It is possible that this change could affect the way that the drug partitions between the solvent and the substrate in addition to its effects on Taylor cone formation. Additionally, coating the paper substrate appeared to result in decreased blank signal. The physical coating may sequester byproducts of the laser cutting process, decreasing their extraction into the spray solvent and subsequent transfer into the instrument. Also, the use of hydrophobic coatings has been shown to improve analyte recovery. This improvement could occur due to weaker substrate-analyte interactions as well as lower absorption of the sample matrix into the paper fibers.

Optimizing the substrate-solvent combination resulted in overall S/B increase across all compound classes. **Figure 3.3** shows the factor change of the S/B for the optimized substrate-solvent conditions versus the starting solvent conditions on untreated paper. Most of the analyte/matrix combinations showed dramatic improvements of more than a factor of 10, with 6 showing more than a 100X increase in S/B ratio. These data indicate that selection of a suitable substrate and solvent when creating a new method can dramatically detection limits. The spray solvent appeared to be less impactful compared to the substrate. Not all analyte classes benefited from optimizing the solvents. The CWA and neat opiate samples, in particular, exhibited no S/B improvement by changing the solvent. Another isolated case of this was seen with valganciclovir, an antiviral drug. For these compounds, the original solvent condition was deemed optimal. Additionally, some of the compounds, namely the CWA, antifungals, and opiates, showed small improvements by changing the substrate and solvent suggesting that more work would need to be done if lower detection limits must be reached.

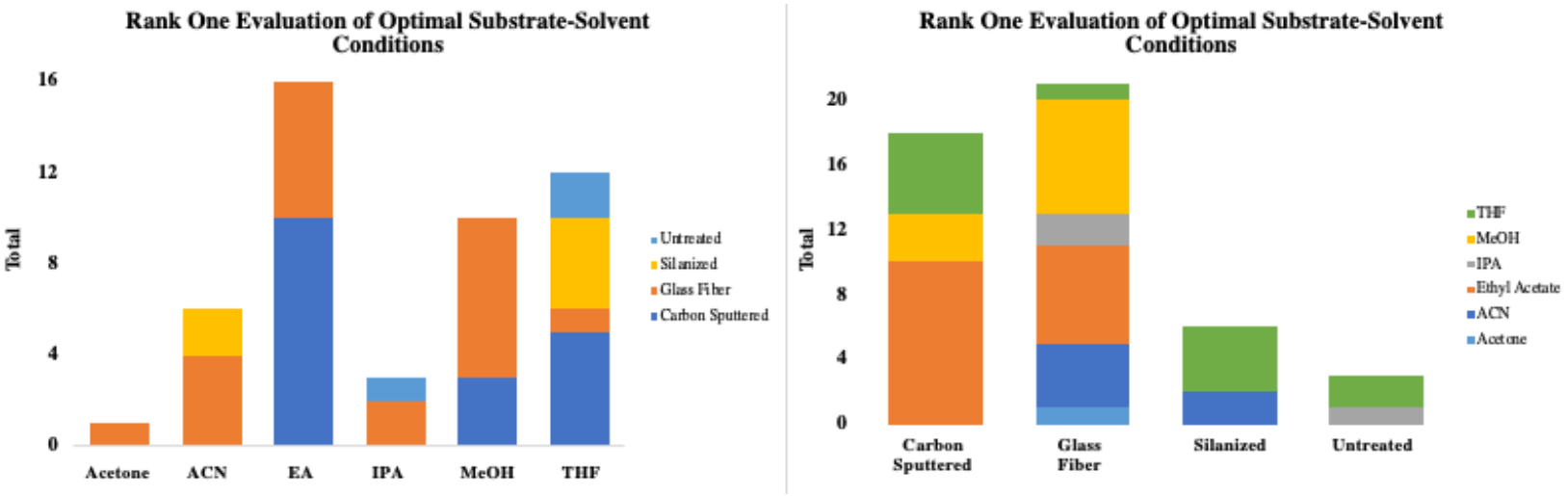

Figure 3.2 Rank one evaluation depicting optimal solvent (left) and substrate (right) type for both neat and plasma samples.

Different trends were observed for the two sample matrixes studied here. Most of the neat analytes (7/18) showed optimal S/B with carbon sputtered paper. There was no clear trend with respect to aprotic versus polar protic spray solvents. Plasma samples, on the other hand, showed significantly different trends. Over half of the analytes in plasma were optimal with the glass fiber spray substrate, and the majority (24/30) were best detected using an aprotic solvent. This is of note since many paper spray assays employ polar protic solvents, namely methanol. Although a significant number of analytes were optimal with methanol, these tended to be in neat samples. Methanol tended to be less favorable in plasma, perhaps due to the much higher salt solubility in methanol compared to the other solvents.

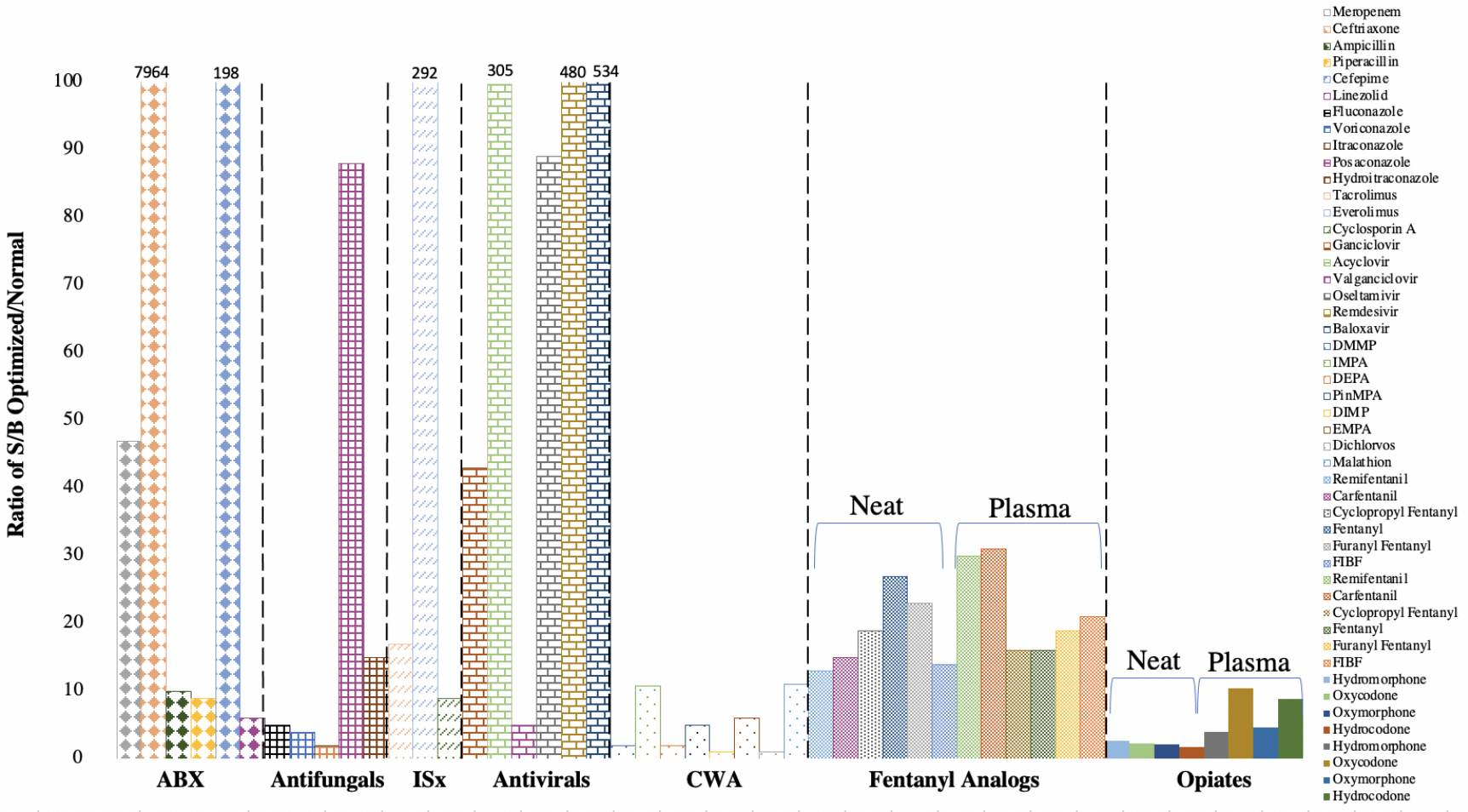

Figure 3.3 Factor change of average S/B showing optimized vs standard paper spray conditions for all samples. Values were calculated by dividing the S/B of the optimized condition by the starting paper spray condition.

3.4.2 Evaluation of Signal Stability

While optimization improved S/B, the signal stability decreased in some cases. Ion signal stability was assessed by plotting the ratio of the quantifying ion to the most intense confirming ion. Scan events were binned every five seconds over the entire range that the voltage was applied (RT 0.1 minutes – 1.1 minutes). Individual moving range control charts were used to assess process stability over the course of each run (**Figure 3.4**). The top chart is a plot of each data point to monitor deviations of individual data points from the mean (green line). The bottom chart plots the moving range as the absolute value of the difference between successive data points. The green line shows the average of the moving range ($\overline{\text{MR}}$). The upper and lower control limits were calculated as +/-three sigma limits. **Figure 3.4** shows IMR charts for everolimus, fentanyl, linezolid, and voriconazole comparing the optimal condition with the starting condition. Here, the optimized conditions produced more variable ion signal scan-to-scan compared to the starting condition. These experiments utilized the same conditions for both the starting and optimized conditions. Some of the experimental parameters, including solvent volume, spray voltage, and distance from the MS inlet, are likely to be substrate/solvent dependent; further optimization of these variables can be expected to improve signal stability.

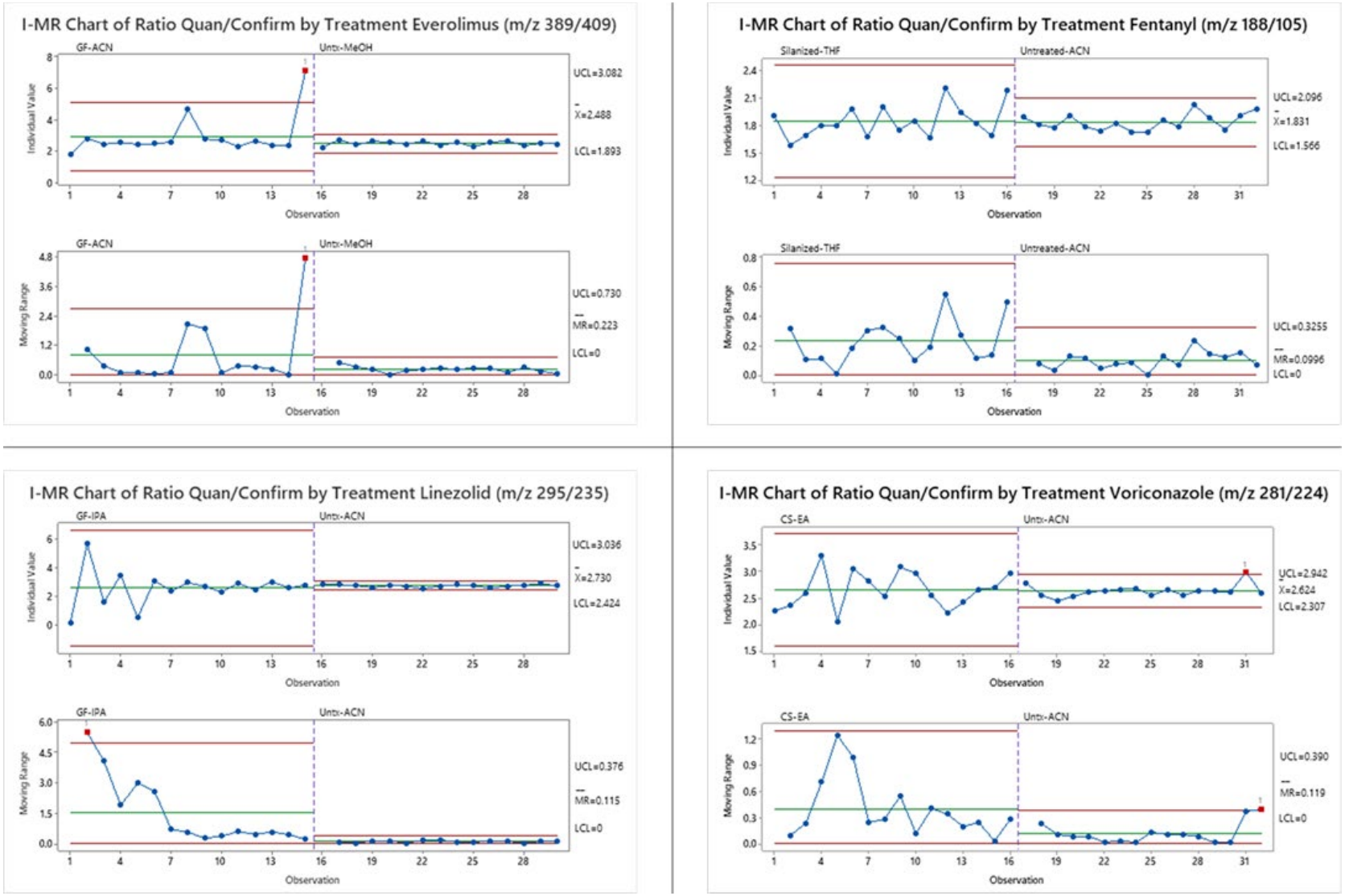

Figure 3.4 Individual Moving Range (IMR) control charts plotting the ratio of the quantifying ion to the most abundant confirming ion over the course of the entire run for everolimus, fentanyl, linezolid, and voriconazole.

3.4.3 Evaluation of Sample Repeatability

Sample repeatability refers to the variation in analyte peak area from sample to sample. While related, signal stability and sample repeatability are distinct. If all other variables are constant, sample repeatability ($s_{repeatability}$) will tend to scale with the average signal stability (s_{signal}) by the formula s_{signal}/sqrt(n), where n is the number of scans within a sample run. This relationship is complicated by the fact that sample repeatability is impacted by numerous other variables which are affected by the ionization substrate and solvent.

To assess the change in signal repeatability, all analytes within a class were analyzed together using the substrate-solvent combination that produced the highest overall S/B for that class of molecules. Six replicates of both spiked and blank matrix were run to determine the average and standard deviation of the signal-to-blank ratio. Results from this experiment are listed in **Table 3.2**. Data reported includes the mean peak area of the six repeats, standard deviation of the peak areas, average S/B, RSD of the S/B, p values from an F-test two-samples for variance comparing the S/B of optimized versus traditional conditions, and results of a two tailed two sample t-test in the form of a p-value. It should be noted that some of the analytes showed smaller or no improvement because their individualized, optimal combinations were not utilized. Lack of improvement is indicated by the high t-test p-values in **Table 3.2** and was observed for some members of the fentanyl analog, CWA simulants, and opiate classes. As was consistent with the screening study, the confirmation runs showed improved S/B ranging from 1x - 1274x in cases where improvement was seen. Over 30% of all analytes had S/B improvement by a factor of 10 or more even though the confirmation run did not use ideal conditions in many cases. The highest S/B value was for Cyclosporin A, which showed an overall S/B of 38,083, an improvement of over 1000X compared to the standard condition. Although many analytes exhibited large improvements in S/B, the RSDs tended to be higher after optimizing conditions for S/B. In some cases, the overall variation was 5x worse in the optimized conditions compared to the traditional paper spray conditions, and the variation in the optimized conditions was at least double the traditional conditions in 50% of all cases. This is reflected in the F-test of equal variance. Here, 73% of the time (35/48) the optimal conditions showed statistically different results ($\alpha = 0.05$) in the F-test compared to the traditional conditions, indicating increased variation. Despite this increased variability, the two-sample T-test did show statistically significant increases in mean S/B for over half (25/48) of the analytes.

This higher variation in analyte signal could decrease quantitative performance of the optimized approach. The intended use of the assay and the required figures of merit should be considered, specifically whether high variation in analyte signal is acceptable for the purpose of the assay. Compromises in analyte signal intensity may be required to improve reproducibility. One example is adding a more polar co-solvent (methanol, water, acetonitrile) when using low polarity aprotic solvents. Previous work indicated that the co-solvent helps to stabilize the spray, especially when a hydrophobic substrate is used.[96] Additionally, internal standardization will also mitigate the impact of higher variability in absolute signal intensity. Internal standardization, particularly with stable isotope-labeled analogs, will significantly improve repeatability since the ratio between the analyte and internal standard is measured rather than the raw area counts. Finally, as indicated above, further optimization of solvent volume, spray voltage, and tip-to-inlet distance should be undertaken to decrease variability.

Table 3.2 Compilation of mean peak areas with standard deviation for AUC, average S/B, and RSDs for the confirmation experiments. P-values provided were for an F-test of equal variance and a two-sample T-test of means to compare the S/B of the optimized versus the original conditions. Data indicated overall improvements in S/B from a range of 1x-1274x across analyte classes.

CLASS	ANALYTE	TREAT-MENT	MEAN	STDEV	AVERAGE S/B	RSD (%)	F TEST	T TEST
IMMUNOSUP-PRESSANTS PLASMA	Cyclosporin A	GF-ACN	5.E+07	2.E+07	38083	32	0.007	0.751
	Cyclosporin A	Untx-MeOH	1.E+06	6.E+05	30	40		
	Everolimus	GF-ACN	2.E+07	7.E+06	9077	48	0.000	0.161
	Everolimus	Untx-MeOH	5.E+07	7.E+06	68	13		
	Tacrolimus	GF-ACN	8.E+07	4.E+07	8132	50	0.507	0.507
	Tacrolimus	Untx-MeOH	2.E+08	2.E+07	101	10		

Table 3. 2 continued

ANTIBIOTICS PLASMS	Ampicillin	GF-IPA	1.E+08	3.E+07	4203	22	0.000	0.038
	Ampicillin	Untx-ACN	2.E+07	3.E+06	315	18		
	Cefepime	GF-IPA	2.E+06	3.E+05	1134	15	0.000	0.125
	Cefepime	Untx-ACN	6.E+04	1.E+04	35	20		
	Ceftriaxone	GF-IPA	2.E+06	1.E+06	603	52	0.000	0.049
	Ceftriaxone	Untx-ACN	3.E+04	2.E+04	49	71		
	Linezolid	GF-IPA	3.E+09	9.E+08	2631	34	0.000	0.184
	Linezolid	Untx-ACN	2.E+08	3.E+07	241	14		
	Meropenem	GF-IPA	3.E+06	1.E+06	90	38	0.000	0.021
	Meropenem	Untx-ACN	5.E+05	1.E+05	2	20		
	Piperacillin	GF-IPA	4.E+07	1.E+07	1049	24	0.000	0.027
	Piperacillin	Untx-ACN	2.E+06	4.E+05	47	19		
ANTI-FUNGALS PLASMA	Fluconazole	CS-THF	2.E+07	3.E+06	559	12	0.003	0.002
	Fluconazole	Untx-ACN	6.E+07	1.E+07	185	25		
	Hydroxyitra-conazole	CS-THF	2.E+05	1.E+05	132	58	0.000	0.210
	Hydroxyitra-conazole	Untx-ACN	7.E+05	1.E+05	42	21		
	Itraconazole	CS-THF	8.E+05	3.E+05	717	33	0.000	0.114
	Itraconazole	Untx-ACN	2.E+06	5.E+05	212	23		
	Posaconazole	CS-THF	2.E+05	7.E+04	84	35	0.000	0.497
	Posaconazole	Untx-ACN	8.E+05	2.E+05	92	24		
	Voriconazole	CS-THF	1.E+08	4.E+07	14829	32	0.000	0.004
	Voriconazole	Untx-ACN	3.E+07	1.E+07	1309	29		
ANTIVIRALS PLASMA	Acyclovir	GF-IPA	5.E+06	5.E+05	45	9	0.000	0.000
	Acyclovir	Untx-MeOH	8.E+05	1.E+05	2	15		
	Baloxavir	GF-IPA	8.E+08	1.E+08	20179	13	0.000	0.006
	Baloxavir	Untx-MeOH	6.E+06	3.E+06	210	57		
	Foscarnet	GF-IPA	4.E+06	3.E+06	2	88	0.000	0.047
	Foscarnet	Untx-MeOH	2.E+05	1.E+05	0	58		
	Ganciclovir	GF-IPA	5.E+07	9.E+06	469	19	0.000	0.000
	Ganciclovir	Untx-MeOH	2.E+05	7.E+04	7	35		

Table 3. 2 continued

	Oseltamivir	GF-IPA	3.E+08	3.E+07	2897	9	0.212	0.000
	Oseltamivir	Untx-MeOH	4.E+07	9.E+06	681	21		
	Remdesivir	GF-IPA	7.E+07	1.E+07	1373	16	0.001	0.004
	Remdesivir	Untx-MeOH	2.E+06	8.E+05	198	51		
	Ribavirin	GF-IPA	2.E+06	4.E+05	1	19	0.001	0.010
	Ribavirin	Untx-MeOH	1.E+06	1.E+05	0	9		
	Valgan-ciclovir	GF-IPA	3.E+07	5.E+06	1013	16	0.333	0.058
	Valgan-ciclovir	Untx-MeOH	5.E+06	6.E+05	341	13		
	Cyclopropyl Fentanyl	CS-MeOH	3.E+07	6.E+04	519	48	0.085	0.497
	Cyclopropyl Fentanyl	Untx-ACN	4.E+07	3.E+04	1417	19		
	Fentanyl	CS-MeOH	4.E+07	1.E+05	384	46	0.001	0.395
	Fentanyl	Untx-ACN	3.E+07	1.E+05	301	24		
	FIBF	CS-MeOH	4.E+07	9.E+04	404	47	0.462	0.078
FENTANYL ANALOGS NEAT	FIBF	Untx-ACN	6.E+07	3.E+04	1910	21		
	Furanyl Fentanyl	CS-MeOH	3.E+07	6.E+04	514	51	0.148	0.578
	Furanyl Fentanyl	Untx-ACN	4.E+07	3.E+04	1132	20		
	Remifentanil	CS-MeOH	4.E+06	4.E+04	94	57	0.000	0.172
	Remifentanil	Untx-ACN	1.E+06	4.E+04	29	43		
	Carfentanil	CS-MeOH	6.E+06	4.E+04	179	46	0.176	0.727
	Carfentanil	Untx-ACN	9.E+06	4.E+04	243	22		
	Cyclopropyl Fentanyl	Sil-THF	2.E+07	2.E+04	1057	76	0.000	0.138
	Cyclopropyl Fentanyl	Untx-ACN	1.E+07	1.E+05	115	33		
	Fentanyl	Sil-THF	3.E+07	3.E+04	811	73	0.000	0.186
FENTANYL ANALOGS PLASMA	Fentanyl	Untx-ACN	2.E+07	2.E+05	102	37		
	FIBF	Sil-THF	2.E+07	3.E+04	707	75	0.000	0.249
	FIBF	Untx-ACN	2.E+07	2.E+05	97	35		
	Furanyl Fentanyl	Sil-THF	2.E+07	2.E+04	1055	75	0.000	0.111
	Furanyl Fentanyl	Untx-ACN	1.E+07	1.E+05	103	28		

Table 3. 2 continued

CWA	Remifentanil	Sil-THF	4.E+06	1.E+04	390	73	0.000	0.173
	Remifentanil	Untx-ACN	2.E+06	2.E+04	142	40		
	Carfentanil	Sil-THF	3.E+06	1.E+04	275	78	0.000	0.172
	Carfentanil	Untx-ACN	2.E+06	2.E+04	88	37		
	DMMP	CS-MeOH	1.E+09	1.E+08	28	10	0.123	0.000
	DMMP	Untx-MeOH	8.E+08	2.E+08	72	22		
	DEPA	CS-MeOH	1.E+09	9.E+07	646	7	0.015	0.006
	DEPA	Untx-MeOH	6.E+08	2.E+08	321	35		
	Dichlorvos	CS-MeOH	2.E+08	1.E+07	28	8	0.256	0.296
	Dichlorvos	Untx-MeOH	9.E+07	2.E+07	37	22		
	DIMP	CS-MeOH	5.E+08	6.E+07	144	14	0.070	0.018
	DIMP	Untx-MeOH	3.E+08	7.E+07	89	25		
	Malathion	CS-MeOH	3.E+08	6.E+07	1877	17	0.003	0.005
	Malathion	Untx-MeOH	2.E+08	5.E+07	447	28		
	IMPA	GF-MeOH	4.E+07	1.E+07	983	27	0.002	0.035
	IMPA	Untx-MeOH	2.E+07	2.E+07	7	103		
	PinMPA	GF-MeOH	6.E+07	3.E+07	2377	45	0.001	0.032
	PinMPA	Untx-MeOH	4.E+07	3.E+07	39	67		
	EMPA	GF-MeOH	4.E+07	1.E+07	392	31	0.000	0.008
	EMPA	Untx-MeOH	2.E+07	2.E+07	9	94		
OPIATES NEAT	Hydro-morphone	GF-ACN	2.E+07	8.E+06	142	41	0.083	0.974
	Hydro-morphone	Untx-ACN	4.E+07	4.E+06	139	11		
	Oxycodone	GF-ACN	1.E+08	3.E+07	360	33	0.000	0.865
	Oxycodone	Untx-ACN	2.E+08	2.E+07	337	10		
	Oxymor-phone	GF-ACN	3.E+07	1.E+07	110	39	0.094	0.166
	Oxymor-phone	Untx-ACN	5.E+07	5.E+06	63	10		

Table 3. 2 continued

OPIATES PLASMA	Hydrocodone	GF-ACN	2.E+07	9.E+06	164	38	0.082	0.772
	Hydrocodone	Untx-ACN	5.E+07	5.E+06	182	11		
	Hydro-morphone	CS-EA	2.E+06	9.E+05	180	38	0.000	0.021
	Hydro-morphone	Untx-ACN	4.E+06	1.E+06	31	27		
	Oxycodone	CS-EA	2.E+07	7.E+06	653	40	0.000	0.019
	Oxycodone	Untx-ACN	3.E+07	6.E+06	112	24		
	Oxymor-phone	CS-EA	3.E+06	1.E+06	85	44	0.000	0.004
	Oxymor-phone	Untx-ACN	7.E+06	2.E+06	14	24		
	Hydrocodone	CS-EA	6.E+06	2.E+06	118	33	0.005	0.007
	Hydrocodone	Untx-ACN	5.E+06	1.E+06	50	25		

3.5 Conclusions

This study was designed to characterize the interaction between solvent, substrate, analyte, and sample media. Data indicates that each individual analyte has an optimal solvent-substrate combination, which can change depending on the type of media the analyte is in. Compounds with similar chemical properties tend to perform optimally under similar conditions. Although no single, optimal substrate-solvent combination was found across all analyte classes, multiplexing is still possible if suitable substrates and solvents for each drug class are determined. Carbon sputtered and glass fiber paper types tended to work optimally for hydrophobic and hydrophilic analytes respectively. The recent development of alternative substrate types for paper spray will widen the range of applications for this technique, providing it with a more real-world usability. Additionally, this study demonstrates that optimizing substrate-solvent combinations significantly improves detection limits for hydrophilic compounds, which has been challenging in the past. More work should be done to investigate how alternative paper modifications can help with the recovery and ionization of various analytes.

CHAPTER 4. SIMULTANEOUS QUANTITATION OF FIVE TRIAZOLE ANTIFUNGAL AGENTS BY PAPER SPRAY MASS SPECTROMETRY

4.1 Abstract

Invasive fungal disease is a life-threatening condition that can be challenging to treat due to pathogen resistance, drug toxicity, and therapeutic failure secondary to suboptimal drug concentrations. Frequent therapeutic drug monitoring (TDM) is required for some anti- fungal agents to overcome these issues. Unfortunately, TDM at the institutional level is difficult, and samples are often sent to a commercial reference laboratory for analysis. To address this gap, the first paper spray-mass spectrometry assay for the simultaneous quantitation of five triazoles was developed. Calibration curves for fluconazole, posaconazole, itraconazole, hydroxyitraconazole, and voriconazole were created utilizing plasma-based calibrants and four stable isotopic internal standards. No sample preparation was needed. Plasma samples were spotted on a paper substrate in pre-manufactured plastic cartridges, and the dried plasma spots were analyzed directly utilizing paper spray-mass spectrometry (paper spray MS/MS). All experiments were performed on a Thermo Scientific TSQ Vantage triple quadrupole mass spectrometer. The calibration curves for the five anti-fungal agents showed good linearity (R^2 = 0.98–1.00). The measured assay ranges (lower limit of quantification [LLOQ]–upper limit of quantitation [ULOQ]) for fluconazole, posaconazole, itraconazole, hydroxyitraconazole, and voriconazole were 0.5–50 μg/mL, 0.1–10 μg/mL, 0.1–10 μg/mL, 0.1–10 μg/mL, and 0.1–10 μg/mL, respectively. The inter- and intra-day accuracy and precision were less than 25% over the respective ranges. We developed the first rapid paper spray- MS/MS assay for simultaneous quantitation of five triazole anti-fungal agents in plasma. The method may be a powerful tool for near-point-of-care TDM aimed at improving patient care by reducing the turnaround time and for use in clinical research.

4.2 Introduction

Fungal disease is a significant clinical and economic burden in the healthcare system, and invasive fungal disease is a leading cause of morbidity and mortality in critically ill and immunocompromised patient.[111-114] Fortunately, the development of anti-fungal agents has dramatically improved clinical outcomes.[115, 116] Despite these advancements, clinicians and

pharmacists struggle with dosing of anti-fungal agents due to altered host pharmacokinetics, drug resistance, and risk of therapeutic failure at suboptimal concentrations.[112, 117-119] Adverse effects are frequently observed, including hepatotoxicity and neurological effects.[117, 118, 120] These issues, as well as unique anti-fungal pharmacokinetics and pharmacodynamics, have pushed the need for therapeutic drug monitoring (TDM) of certain agents.[115, 117, 118]

There are three main classes of systemic anti-fungal agents in clinical use: polyenes, triazoles, and echinocandins. Triazoles are particularly attractive to clinicians as they have broad anti-fungal activity and can often be taken orally.[116, 120-123] Most mold-active triazoles (itraconazole, voriconazole, and posaconazole) require frequent TDM for efficacy and safety.[117, 118, 120-122, 124, 125]

Many assays utilizing high-performance liquid chromatography-mass spectrometry (HPLC-MS) for the quantification of triazoles have been reported in the literature[126-130], and several centralized reference laboratories offer their own methods for clinical use. MS-based approaches are attractive due to their high sensitivity and specificity, lack of interference, multiplex capability, high throughput, and low reagent cost.[131, 132] Nevertheless, logistics, technical expertise, and sample preparation (solid-phase extraction, liquid-liquid extraction, or protein precipitation) often hinder implementation at the institutional level, and patient samples must be shipped to reference laboratories, which leads to long turnaround times and high costs.[131, 133] Delays in result reporting can have a negative impact on patient care and clinical outcomes; therefore, new methods that can be utilized near the point of care are needed.[117, 118]

Paper spray, an ambient ionization technique, is an ideal method for therapeutic monitoring as it allows for rapid analysis of complex biological samples without sample preparation or chromatography.[37, 40, 51, 54] A small sample volume (5–15 μL) is deposited directly onto a porous, triangular paper substrate and allowed to dry. Analysis is performed directly from the dried spot via application of a spray solvent and a high voltage while the sharp tip of the paper is in close proximity to the inlet to the MS[134], where the ions enter the mass spectrometer for detection. A sample can typically be analyzed in 60–90 s.[54] Paper spray-MS/MS methods for fast qualitative and quantitative analysis of both small and large molecules from a variety of biological and environmental matrices have been reported, and it has shown potential for TDM.[53, 61, 87, 135, 136] Paper spray-MS has several advantages over LC-MS/MS methods, including easy sample preparation, lower solvent consumption, less expertise, and faster turnaround times.[40, 53, 61, 87, 135]

In this paper, we present the first validated paper spray-MS/MS method for the simultaneous quantification of five anti-fungal drugs in plasma samples. Remnant patient clinical samples collected from the Indiana University Health Pathology Laboratory (Indianapolis, IN, USA) were analyzed by paper spray-MS/MS. The results obtained by paper spray-MS/MS were compared to measured levels obtained by a reference laboratory via LC-MS/MS (Mayo Clinic Laboratories, Rochester, MN, USA).

4.3 Methods

4.3.1 Chemicals and Reagents

Analytical-grade methanol, water, acetonitrile, acetone, and ammonium acetate were purchased from Fisher Scientific (Pittsburg, PA, USA). Acetic acid, itraconazole, posaconazole, fluconazole, voriconazole, itraconazole-D_4, fluconazole-$^{13}C_3$, and voriconazole-D_3 were purchased from Sigma Aldrich (St. Louis, MO, USA). Hydroxyitraconazole and hydroxyitraconazole-D_5 were purchased from Fitzgerald Industries International (Acton, MA, USA) and Toronto Research Chemicals Incorporated (Ontario, Canada). The external quality control (QC) was purchased from UTAK Laboratories (Valencia, CA, USA). Pre-made plastic cartridges were purchased from Prosolia, Inc. (Indianapolis, IN, USA). Whatman grade 31ET chromatography paper was purchased from Fisher Scientific (Lenexa, KS, USA).

4.3.2 Sample preparation

Stock solutions were prepared in *N*,*N*-dimethylformamide (DMF) at the following concentrations: fluconazole (6.0 mg/mL), voriconazole (1.0 mg/mL), hydroxyitraconazole (1.0 mg/mL), posaconazole (2.0 mg/mL), and itraconazole (2.0 mg/mL). Five spiking solutions (SS1–5), each containing all five analytes, were then prepared in 95:5 methanol/water with 0.01% acetic acid. The concentrations for itraconazole, hydroxyitraconazole, posaconazole, and voriconazole were 200.0 μg/mL (SS1), 60.0 μg/mL (SS2), 20.0 μg/mL (SS3), 6.0 μg/mL (SS4), and 2.0 μg/mL (SS5). Fluconazole concentrations were 1000.0 μg/mL (SS1), 300.0 μg/mL (SS2), 100.0 μg/mL (SS3), 30.0 μg/mL (SS4), and 10.0 μg/mL (SS5). Stock and spiking solutions were stored at −20 °C. Plasma calibrants were prepared by spiking a 100 μL aliquot of plasma with 5 μL of the corresponding spiking solution (SS1–SS5) to make final plasma concentrations of 10.0 μg/mL, 3.0 μg/mL, 1.0 μg/mL, 0.3 μg/mL, and 0.1 μg/mL of itraconazole, hydroxyitraconazole,

posaconazole, and voriconazole. Fluconazole final plasma concentrations were 50.0 μg/mL, 15.0 μg/mL, 5.0 μg/mL, 1.5 μg/mL, and 0.5 μg/mL.

Internal QCs were prepared in a manner similar to the calibrants. Internal QCs at four different concentrations (lower limit of quantification [LLOQ], low, medium, and high) were utilized in this experiment. Four spiking solutions (QCS1–4) were prepared in 95:5 methanol/water with 0.01% acetic acid at the following concentrations: 200.0 μg/mL (QCS1), 20.0 μg/mL (QCS2), 6.0 μg/mL (QCS3), and 2.0 μg/mL (QCS4) for itraconazole, hydroxyitraconazole, posaconazole, and voriconazole, respectively. Fluconazole concentrations were 1000.0 μg/mL (QCS1), 100.0 μg/mL (QCS2), 30.0 μg/mL (QCS3), and 10.0 μg/mL (QCS4). QC samples were prepared by spiking a 100 μL aliquot of plasma with 5 μL of the corresponding spiking solution (QCS1–4) to make final concentrations in plasma of 10.0 μg/mL, 1.0 μg/mL, 0.3 μg/mL, and 0.1 μg/mL of itraconazole, hydroxyitraconazole, posaconazole, and voriconazole, respectively. Final plasma concentrations for fluconazole were 50.0 μg/mL, 5.0 μg/mL, 1.5 μg/mL, and 0.5 μg/mL. The external QCs were prepared according to the manufacturer's instructions. Concentrations for fluconazole, itraconazole, hydroxyitraconazole, voriconazole, and posaconazole in the external QC were reported to be: 18.0 μg/mL, 4.94 μg/mL, 2.87 μg/mL, 3.47 μg/mL, and 5.09 μg/mL, respectively.

The internal standard solution was prepared in 50:50 methanol/50 mM ammonium acetate. The final concentrations of the stable isotopically labeled analogs in the internal standard solution were: voriconazole-D_3 (1.0 μg/mL), itraconazole-D_4 (4.0 μg/mL), hydroxyitraconazole-D_5 (2.0 μg/mL), and fluconazole-$^{13}C_3$ (10.0 μg/mL). A 10 μL aliquot of the internal standard solution was added to all plasma samples with the exception of the double blank plasma samples. Each plasma sample was vortexed for 10 s to thoroughly mix. Eight microliters of each sample was then spotted onto the paper substrate contained within the paper spray cartridge. Cartridges were covered to protect samples from ambient light and were allowed to dry for 1 h at room temperature prior to analysis. Of note, the internal standard solution was found to be stable for 4 days when stored at −20°C.

Remnant patient clinical samples were gathered from the Indiana University Health Pathology Laboratory where they were stored at −20°C until retrieval. The clinical samples were de-identified and anonymized, transported on dry ice, and stored at −80°C until use. Patient plasma

aliquots (100 μL) were spiked with 10 μL of internal standard solution and spotted on the paper spray cartridges as described earlier for calibrants and QCs.

4.3.3 Paper spray-mass spectrometry assay development

Paper spray was performed utilizing plastic cartridges containing Whatman grade 31ET chromatography paper. An automated paper spray source, the Velox 360 (Prosolia, Inc., Indianapolis, IN, USA), was coupled to a Thermo Fisher Scientific TSQ Vantage triple quadrupole mass spectrometer (San Jose, CA, USA). The spray solvent utilized was 85:10:5 acetonitrile/acetone/water with 0.01% acetic acid. Optimized MS parameters were as follows: 300°C capillary temperature, 4200 V spray voltage, positive ion mode, and no sheath or auxiliary gas. The instrument was operated in a selected reaction monitoring (SRM) mode with a dwell time of 0.1 s. SRM transitions and optimized instrument parameters for the five triazoles and the stable isotopic internal standards are shown in **Table 4.1**. The auto- mated Velox 360 source parameters were: cartridge dispense: pump B; number of pump B dispenses: 9; dispense volume: 90 µL; pump B dispense delay: 0 s.

4.3.4 Method validation

Each analytical run consisted of calibrants, internal QCs, an external QC, remnant patient clinical samples, blanks with internal standard, and double blanks without internal standard. Calibration curves were run in duplicate, one at the beginning and one at the end of each experimental run. The number of external and internal QCs for each analytical run was ≥5% of remnant clinical samples as recommended by the Food and Drug Administration (FDA) guidelines [34]. Two or more replicates of each QC (four internal QCs, one external QC) were performed per analytical run. More than 67% of all QCs and 50% of QCs at each concentration level had to meet the acceptance criterion of a difference of ≤25% of the known nominal concentration for the analytical run to be considered valid. Plasma blanks with internal standard and plasma double blanks were used to assess the carryover and blank signal. Remnant patient clinical samples were run in singlet during the validation, and calculated values were compared to values determined by a validated LC-MS/MS-based method (Mayo Clinic Laboratories, Rochester, MN, USA). A total of 110 clinical samples were run: 66 voriconazole, 24 itraconazole/hydroxyitraconazole, and 20

posaconazole samples. Fluconazole patient clinical samples were unavailable at the time of validation.

Table 4.1 The analytes investigated, molecular formulas, parent ions, quantifying and confirming ions, S lens, and CE parameters. Bold items indicate the quantifier for each analyte.

Compound Name	Chemical Formula	Parent m/z	Fragment m/z*	S lens	CE (eV)
Voriconazole	$C_{16}H_{14}F_3N_5O$	350	**281**	83	17
			263		20
			224		18
Voriconazole-D_3	$C_{16}H_{11}D_3F_3N_5O$	353	**284**	84	16
			266		27
			224		19
Fluconazole	$C_{13}H_{12}F_2N_6O$	307	**220**	82	18
			238		16
			169		23
Fluconazole-$^{13}C_3$	$C_{10}[13]C_3\ H_{12}F_2N_6O$	310	**223**	82	18
			241		16
			172		24
Itraconazole	$C_{35}H_{38}Cl_2N_8O_4$	705	**392**	169	35
			348		39
			335		40
Itraconazole-D_4	$C_{35}H_{34}D_4Cl_2N_8O_4$	709	**396**	162	35
			352		39
			339		43
Hydroxyitraconazole	$C_{35}H_{38}Cl_2N_8O_5$	721	**408**	179	45
			392		39
			173		57
Hydroxyitraconazole-D_5	$C_{35}H_{33}D_5Cl_2N_8O_5$	726	**413**	211	37
			397		33
			255		41
Posaconazole	$C_{37}H_{42}F_2N_8O_4$	701	**344**	174	44
			370		41
			614		32

4.3.5 Assessment of long-term stability and interference

Remnant clinical sample stability

Due to the lengthy handling process of the clinical samples, degradation was studied in clinical samples over the course of 14 days, which is well within the typical turnaround time for clinical laboratories. Ten samples for each drug were stored under three temperature conditions (−20°C, 4°C, and 22°C) and were analyzed in duplicate after 0, 7, and 14 days. The samples were analyzed using the validated method and checked for degradation. For samples to be considered passing, differences in nominal concentration could not exceed 20%. Additionally, spiking solutions for the calibrants and QCs were evaluated for linearity, accuracy, and precision at the beginning of each day.

Assessment of endogenous interference

Hemolysis was assessed in accordance with established protocols.[137] Briefly, fresh drug-free whole blood was shaken vigorously and stored at −20°C for 30 min. Hemolyzed blood was spiked into blank plasma to create two test groups consisting of 0.5% (0.5 μL hemolyzed blood in 100 μL of blank plasma) and 2% (2 μL hemolyzed blood in 100 μL of blank plasma) hemolyzed plasma. A test group with 0% hemolysis was utilized as a control. Low-concentration QCs utilizing plasma from the three test groups were prepared, and five replicates were analyzed as described earlier. To be considered negligible, the difference in nominal concentration between hemolyzed and non-hemolyzed samples had to be ≤25% for all analytes.

Drug-free icteric and lipidemic plasma samples were collected from the Indiana University Health Pathology Laboratory and stored at −20°C until use. QCs at the high and low levels were prepared in five separate lipidemic samples and three separate icteric samples. QCs prepared in normal plasma were used as the control. Five replicates of each sample were analyzed as described earlier. To be considered negligible, lipidemic and icteric samples had to meet precision and accuracy acceptance criteria of ≤25% for all analytes.

4.3.6 Data and statistical analysis

Data analysis was performed using Tracefinder 3.3 (Thermo Fisher Scientific Inc., San Jose, CA, USA). The calibration curves were calculated using $1/x^2$ weighted linear least squares.[138]

All statistics were performed using Minitab (Minitab Inc., State College, PA, USA) or Excel (Microsoft Corp., Redmond, WA, USA).

To further assess the accuracy and systematic bias of the paper spray-MS/MS assay, a comparison of the two methods was performed using the Passing-Bablok regression[139], which calculates a regression equation ($y = a + bx$) and the 95% confidence intervals (CIs) for the constant (a) and proportional bias (b). A Kolmogorov-Smirnov CUSUM test was performed to confirm the linearity of these values as assumed by the Passing-Bablok regression. A p-value of <0.05 indicates a statistically significant deviation from linearity. Bland-Altman plots were utilized to further assess agreement and bias between measured results of the two methods.[139]

4.3.7 IRB approval

The study was reviewed and approved by the Indiana University – Purdue University Indianapolis Institutional Review Board.

4.4 Results

4.4.1 Method validation

Validation was performed using FDA guidelines as a basic framework.[140] The method was validated in terms of linearity, limit of detection (LOD), LLOQ, accuracy (%bias), precision (%CV), matrix effects, carryover, stability, and endogenous interference. **Figure 4.1** shows an overlay of the calibration curves collected over 7 different days for each analyte. The calibration curves had average coefficients of determination (R2) of ≥ 0.99 with the exception of posaconazole (≥ 0.98). Posaconazole did not have a stable isotopically labeled analog as its internal standard; deuterated hydroxyitraconazole was used as the internal standard instead. **Table 4.2** shows the observed variation in the calibration curve slopes, which was $<5\%$ in all cases. The average calculated LODs and measured LLOQs are shown in **Table 4.2**. **Table 4.3** shows the average intra- and inter-day accuracy (%bias) and precision (%CV) for all analytes. These values were below the established acceptance criteria of $\leq 25\%$ for both accuracy and precision values.

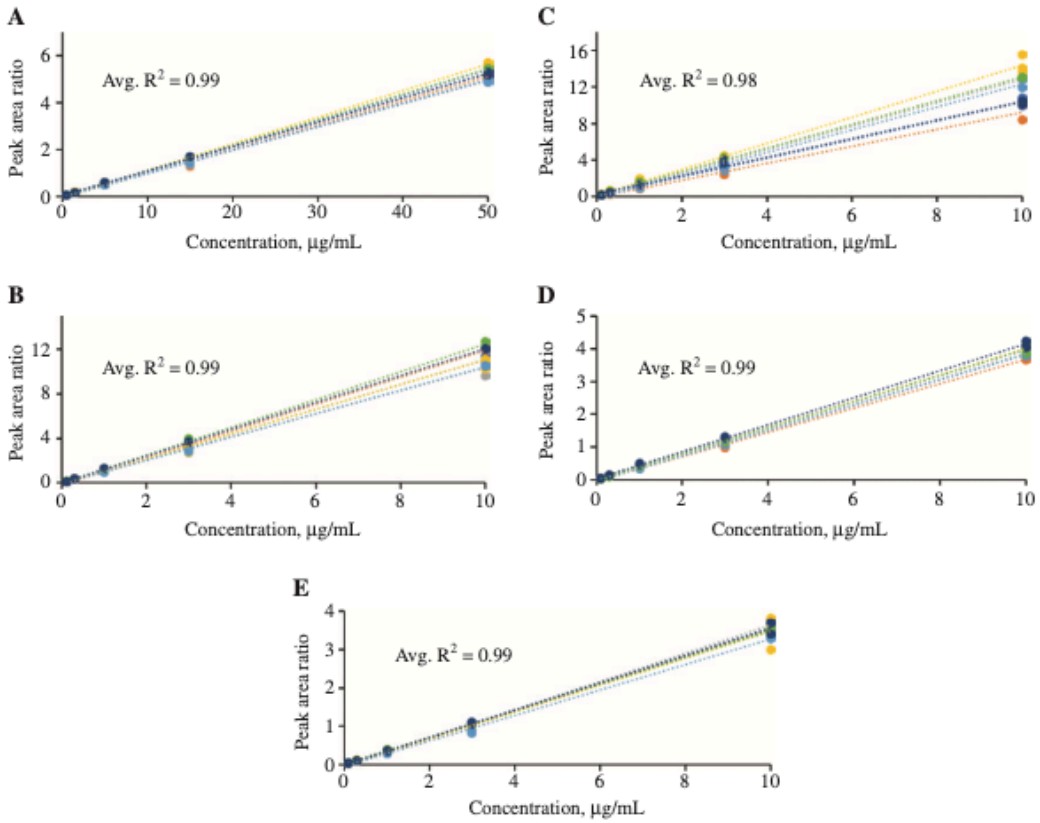

Figure 4.1 Overlays of calibration curves for the five triazoles: fluconazole (A), voriconazole (B), posaconazole (C), itraconazole (D), and hydroxyitraconazole (E). Data were collected over 7 different days (one calibration curve/day). Linearity ranged from R^2 = 0.94–0.99.

Table 4.2 The average coefficient of determination (R^2), average relative error of the slope (%), average LOD (µg/mL), and measured LLOQ values (µg/mL) for the five triazoles. Data were collected over seven runs on 7 separate days. The standard deviation of the calculated LOD is also shown. [a]LOD = 3*(standard error of the intercept/slope). [b]LLOQ = concentration at which the signal-noise ratio was consistently ≥10. LOD, limit of detection; LLOQ, lower limit of quantification.

Target	Average R^2	Average Relative Error of Slope (%)	Average LOD* (µg/mL)	Measured LLOQ‡ (µg/mL)
Fluconazole	0.99	2	0.06 +/- 0.02	0.5
Itraconazole	0.99	2	0.01 +/- 0.00	0.1
Posaconazole	0.98	5	0.03 +/- 0.01	0.1
Voriconazole	0.99	2	0.02 +/- 0.01	0.1
Hydroxyitraconazole	0.99	3	0.02 + 0.01	0.1

Table 4.3 Accuracy (%bias) and precision (%CV) were calculated across seven experimental days. The intra-day % bias and %CV values are the average value obtained within a run across all seven days. The inter-day %bias and %CV were calculated for every replicate across all seven days. *%Bias = (Grand mean of calculated concentration-nominal concentration/nominal concentration)*100 ǂ%CV = (Standard deviation/mean)*100.

Intra-day accuracy* and precisionǂ										
	QC LLOQ		QC Low		QC Medium		QC High		QC External	
Analyte	Bias (%)	CV (%)	Bias (%)	CV (%)	Bias (%)	CV (%)	Bias (%)	CV (%)	Bias (%)	CV (%)
Fluconazole	1	5	8	7	-1	4	1	4	-2	2
Hydroxyitraconazole	11	13	8	7	3	6	7	6	8	7
Itraconazole	3	7	5	7	-1	3	-3	4	-10	2
Posaconazole	1	12	2	15	-4	10	-6	10	-11	8
Voriconazole	-16	2	3	2	-8	6	-6	6	-1	4
Inter-day accuracy* and precisionǂ										
	QC LLOQ		QC Low		QC Medium		QC High		QC External	
Analyte:	Bias (%)	CV (%)	Bias (%)	CV (%)	Bias (%)	CV (%)	Bias (%)	CV (%)	Bias (%)	CV (%)
Fluconazole	-2	10	8	10	-1	5	1	6	-2	4
Hydroxyitraconazole	10	16	8	10	3	8	8	9	11	-1
Itraconazole	1	13	5	11	-1	5	-2	6	-10	6
Posaconazole	-2	17	0	18	3	10	-5	15	-12	13
Voriconazole	-9	13	1	19	-7	7	-5	10	-2	7

Stock and spiking solutions were evaluated for stability over the course of 3 months. No degradation was found for the stock solutions dissolved in DMF. Degradation was observed at 10 weeks in the neat spiking solutions stored at −20°C (data not shown). In addition, no significant degradation was found when analyzing remnant clinical patient samples kept at three different temperatures (−20°C, 4°C, and 22°C) over the course of 2 weeks. Of note, the internal standard signal was found to decrease over time when the dried plasma spots were exposed to constant ambient light. **Figure 4.2** shows itraconazole-D_4 signal (**Figure 4. 2A**) when the plasma spots were exposed to light over the course of 16 h. Significant signal decrease occurred over the course of

this experiment. This decrease in signal response was largely eliminated by covering the samples (**Figure 4. 2B**). This same trend was seen for the other three internal standards (data not shown), and similarly, the issue was resolved when shielding the spotted samples from ambient light.

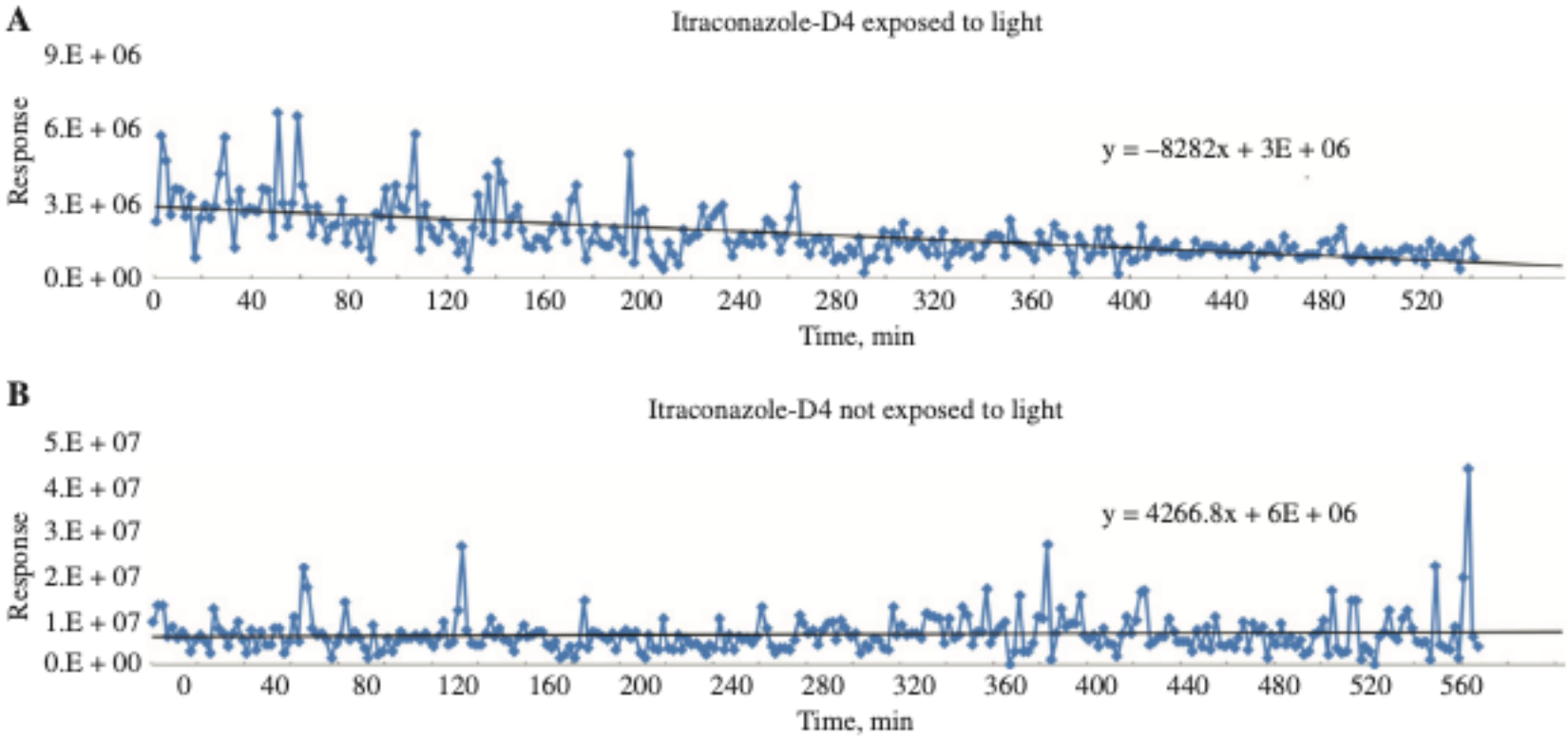

Figure 4.2 Signal response of the stable isotopic internal standard, itraconazole-D4, in plasma samples stored under ambient light and plasma samples stored in a dark environment. There was a decrease in the internal standard signal response over the course of 16 h (A) when exposed to light. This problem was corrected by shielding the samples from ambient light (B).

Endogenous interference from two common metabolites, posaconazole N-β-D-glucuronide and voriconazole- N-oxide, was evaluated. Interference from posaconazole glucuronide on the posaconazole SRM channel was found to be 3%. Voriconazole-n-oxide was also evaluated, and the interference was negligible. In addition, the potential effects of hemolysis, icterus, and lipidemia were evaluated. All lipidemic and hemolyzed samples passed within the established acceptance criterion of ≤25%. All icteric samples passed within limits with the exception of posaconazole high QC samples, which indicates there could be a potential interference from bilirubin at high posaconazole concentrations.

Matrix effects were assessed using a method developed by Matuszewski et al., in which calibration curves were prepared in seven separate individual donor lots of plasma.[141] Matrix effects were then assessed by determining the variation of the calibration slopes. The %CV of the slopes were 3% for fluconazole, 4% for itraconazole and voriconazole, and 10% for posaconazole. In addition, no carryover was noted during the course of the validation.

4.4.2 Reference laboratory cross-validation

Anti-fungal concentrations in remnant clinical samples were measured via the validated paper spray-MS/ MS method and compared to the values obtained via LC-MS/MS. The normality of the differences between the two methods was tested using a Kolmogorov-Smirnov CUSUM test, and all data were considered linear ($p = \geq 0.5450$). A Passing-Bablok regression analysis was performed to assess correlation between the paper spray-MS/MS concentrations and the LC-MS/MS values (**Figure 4.3**). Regression equations and 95% CIs for the slope and intercept of each analyte (dashed lines) are displayed on each plot. High R^2 values (0.90–0.98) were obtained for all analytes, which indicated good linearity and correlation between the two methods. The individual data points were randomly distributed around the best fit regression line indicating no obvious trends in the data. When evaluating the 95% CIs around the regression line in relation to the line of equality (y = x line, where slope = 1 and intercept = 0), the regression lines for voriconazole and posaconazole results were not significantly different from equality. For both itraconazole and hydroxyitraconazole, the slope of 1 was outside the 95% CI, indicating a proportional negative bias of paper spray-MS/MS.

Bland-Altman plots depicting the relative difference between the two methods vs. mean concentration are displayed in Figure 3. The mean bias of paper spray-MS was −5% (1.96*SD: −30% to +21%) for voriconazole, −21% (1.96*SD: −40% to −1.2%) for itraconazole, −6% (1.96*SD: −28% to +16%) for hydroxyitraconazole, and −12% (1.96*SD: −37% to +13%) for posaconazole.

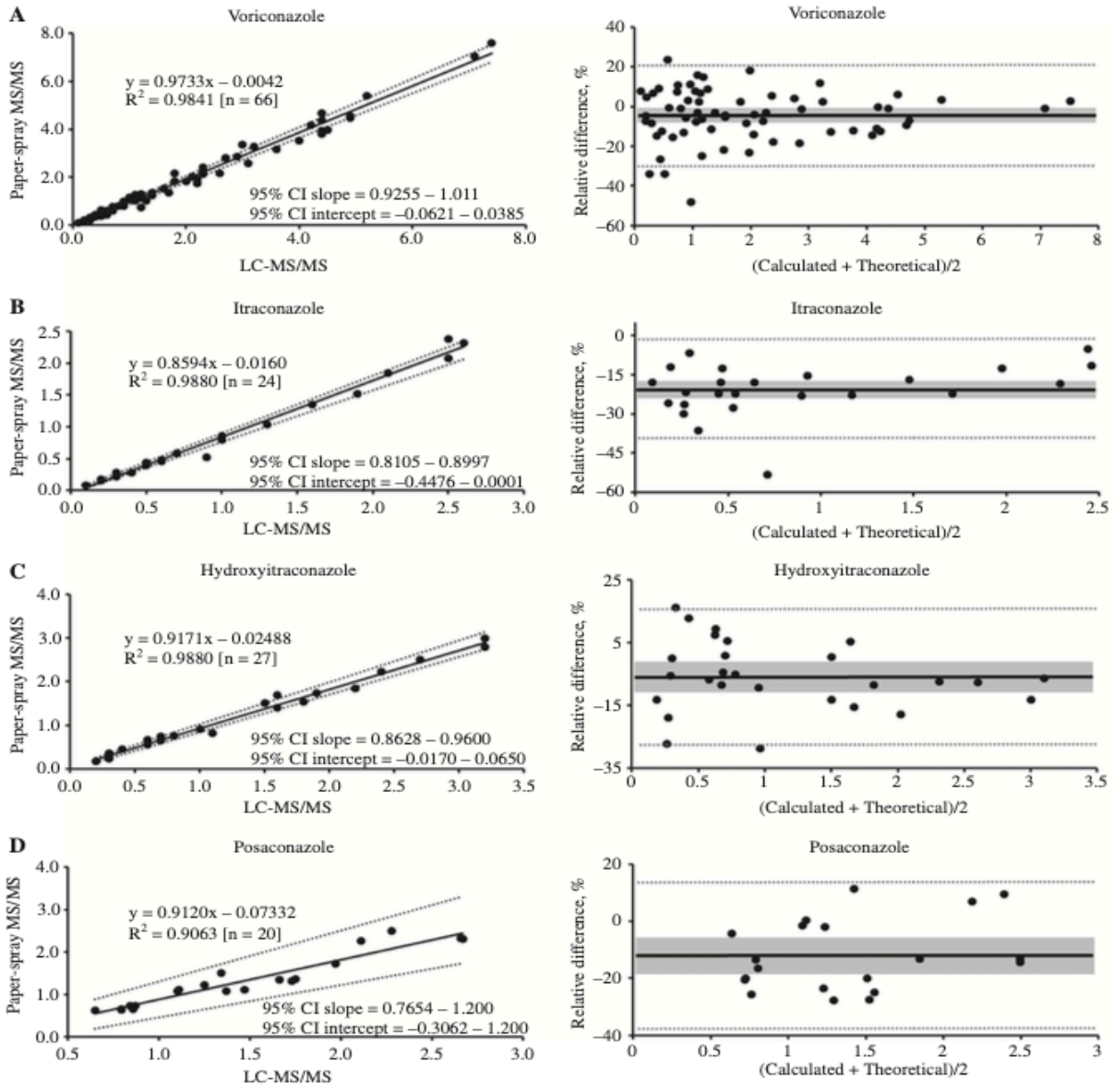

Figure 4.3 Comparison between paper spray-MS/MS and LC-MS/MS. Passing-Bablok regressions (left) comparing paper spray-MS/MS to the reference laboratory LC-MS/MS method were performed. Dotted lines represent the upper and lower CIs. Overall, the data showed good linearity (R^2 = 0.90–0.98). Bland-Altman plots (right) depicting the %relative differences between the paper spray-MS/MS and LC-MS/MS reference value are shown. The solid line indicates the mean of the %relative difference of the two methods. The shaded region depicts the 95% CI for that mean. The dotted lines represent the limits of agreement of ±1.96*SD.

4.5 Discussion

The first paper spray-MS/MS method for the rapid simultaneous quantitation of five anti-fungal triazoles was developed and cross-validated with clinical samples. Overall, the calibration curves showed good linearity (R^2 = 0.94 – 1.00) for all analytes across the measured ranges. The measured LLOQs were well below the therapeutic levels of these drugs, and the upper limits of quantitation (ULOQs) were well above the minimum inhibitory concentrations of affected fungal pathogens.[117, 142-145] Additionally, the paper spray-MS/MS assay ranges were similar to ranges reported by commercial reference laboratories, such as Mayo Clinic Laboratories and ARUP laboratories.

Typically, the acceptance criteria is 15–20% for validated methods depending on the concentration of the QCs.[140] On average, the overall precision (%CV) and accuracy (%bias) were ≤20%, highlighting the quantitative capabilities of this method. The external QC further reinforced the accuracy of the method as they were prepared by a commercial external source; neither the %CV nor the %bias for the external QC material exceeded 15%. An acceptance criteria of ≤25% was chosen for posaconazole to accommodate the greater variation arising from the lack of an isotopically labeled analog for this analyte. A commercially available, stable isotopically labeled analog of posaconazole (posaconazole-D_4) was evaluated. However, posaconazole-D_4 has the same nominal mass as itraconazole, and interference on the itraconazole SRM channels arising from posaconazole-D_4 was observed.

Matrix effects are often evaluated by comparing analyte response in the neat solution to analyte response in biological samples. This approach is not particularly informative for this assay due to the use of internal standardization and matrix-matched calibrants. Instead, matrix effects were evaluated by determining the variability of calibration slopes generated in multiple different plasma donors. This approach addresses the most relevant question about the effect of matrix on analytical measurements[141]: Can a calibration curve generated in a single lot of biofluid be used to determine analyte concentrations in different lots? The variation in slopes was ≤4% for all analytes except posaconazole, which had a higher variation (10%) due to the lack of an isotopically labeled internal standard. This variation arising from the matrix was deemed insignificant.

Remnant clinical samples were analyzed by the paper spray-MS/MS method and a validated external reference laboratory LC-MS/MS assay to further assess correlation and agreement between the two methods. The Kolmogorov- Smirnov CUSUM test of normality indicated that the

relationship was linear ($p = \geq 0.5450$). Correlation was further assessed via the Passing-Bablok regression, and it demonstrated good linearity throughout the measured range (**Figure 4.3**). However, the regression analysis showed there was a statistically significant underestimation for itraconazole and hydroxyitraconazole by the paper spray-MS/MS method. The Bland-Altman plots also showed a statistically significant systematic underestimation for all analytes (**Figure 4.3**). Across all of the analytes, ~95% of the data points did lie within the limits of agreement (±1.96*SD), indicating the relative differences were normally distributed.[146] While the bias could have arisen due to the method itself, many other factors could have also caused these discrepancies. There were systematic differences in sample age, handling, transport, and storage conditions, as well as different calibration materials used for the two assays. Inter-laboratory variation has been widely reported in the literature for many analytes, including triazoles. At present, we identified only one study assessing the agreement between triazole MS-based quantitative assays utilized by different laboratories.[147] In that study, voriconazole measurements made by two different HPLC-MS methods at different laboratories had an average difference of 4%, which is comparable to what we obtained for paper spray-MS/MS. Several studies assessing agreement between quantitative immunoassays and MS- or chromatographic-based methods have been conducted, and wide variations have been reported.[148-151] Furthermore, there have been reports of internal standard choice affecting triazole quantitative results.[150, 152]

From a clinical standpoint, the underestimation obtained here would not alter patient management. For example, the therapeutic trough range for voriconazole is 1.0 – 5.5 μg/mL[117, 124], and a trough of <1.0 μg/mL would prompt the clinician to increase the dose for efficacy. In the voriconazole clinical specimens with drug levels <1.0 μg/mL as measured by LC-MS/MS, the relative difference between the two methods ranged from −34% to +24%. This equates to absolute differences of −0.17 to +0.13 μg/mL, which is negligible. In terms of safety, voriconazole toxicity (i.e. neurotoxicity, self-limited photopsia, hepatotoxicity) is typically seen at >5.5 μg/mL.[117, 153] It is unlikely that toxicity would be exacerbated due to drug-level underestimation as the relative differences between the two methods' results were much smaller at concentrations of >4 μg/mL (−15% to +6%).

A similar argument can be made for itraconazole and posaconazole, which have therapeutic trough goals of >1.0 μg/mL and >0.7 μg/mL (>1.0 μg/mL for severe disease), respectively. In itraconazole clinical specimens <1.0 μg/mL by LC-MS/MS, the relative difference between the

two methods ranged from −53% to −6% (absolute difference: −0.38 to −0.02 μg/mL), which indicates a negative bias for paper spray-MS/MS. For posaconazole clinical specimens <1.0 μg/mL by LC-MS/MS, the negative bias was not as prominent with relative differences between the two methods ranging from −26% to −4%, or absolute differences of −0.2 to −0.04 μg/mL. As with voriconazole, the physician would be prompted to increase the dose of the triazole if levels did not meet therapeutic goals. For itraconazole, toxicity at high concentrations is less of a concern as absorption is problematic, and dosage is often limited by clinical side effects (i.e. gastrointestinal intolerance, fluid retention) rather than a maximum "toxic" plasma concentration. For posaconazole, absorption can also be difficult, and there is insufficient data to establish a maximum plasma concentration as there is no relationship between adverse effects and plasma concentrations. Therefore, while the negative bias for itraconazole and posaconazole are statistically significant, this issue is unlikely to be clinically significant.

Another important issue facing paper spray is interference, which could cause an over-estimation of the target compound due to the lack of separation. Endogenous interferences can be identified by analysis of drug-free plasma from several donors. Other sources of interference are labile metabolites of the parent drugs that can fragment in-source to yield the parent drug. This type of interference was reported previously for posaconazole glucuronides.[154] Our analysis of the posaconazole glucuronide standard revealed an interference of 3%, which was deemed insignificant considering the plasma concentrations of the glucuronide metabolites are 3 – 4 times lower than that of posaconazole itself.[155] The extent of interference will vary with different MS models; interference from glucuronide metabolites should therefore be re-evaluated for each type of mass spectrometer.

In conclusion, the developed paper spray-MS/MS method agreed reasonably well when compared to the "gold"-standard LC-MS/MS method. This study showed that rapid quantitation of triazoles using paper spray-MS/ MS is feasible and may prove to be a powerful tool for clinical care and research. Further studies utilizing clinical specimens are needed to determine the cause of systematic underestimation of triazole quantitative results obtained with in-house paper spray-MS/MS compared to send-out HPLC-MS/MS results. However, this issue is unlikely to have any significant clinical effect.

CHAPTER 5. CHEMICAL ASSAY FOR THE DETECTION OF VERTEBRAE FECAL METABOLITES IN ADULT BLOW FLIES (DIPTERA: CALLIPHORIDAE)

5.1 Abstract

Filth flies are commonly implicated in pathogen transmission routes due to their affinity for vertebrate waste and their synanthropic associations. However, solidifying the link between flies and infected feces in the wild can be difficult, as interpretations made solely from microbial culturing or sequencing methods may represent an incomplete picture of pathogen acquisition. We present an analytical assay using high performance liquid chromatography tandem mass spectrometry (HPLC MS/MS) to detect vertebrate fecal metabolites (urobilinoids) in adult blow fly guts. Proof-of-concept experiments consisted of controlled feeding in which flies were grouped into three treatments (unfed, exposure to beef liver tissue, and exposure to canine feces; N = 20/treatment) using the black blow fly *Phormia regina* Meigen (Diptera: Calliphoridae). It was revealed that only feces-related samples exhibited peaks with an m/z of 591 and MS/MS spectra consistent with urobilinoids. These peaks were not seen for beef liver tissue, flies exposed to beef liver tissue, or unfed flies. Samples taken directly from beef liver tissue and from feces of several animals were also tested. To test this assay in wild flies, 216 flies were additionally analyzed to determine whether they had ingested vertebrate feces. About 13% of the wild flies exhibited these same peaks, providing a baseline measure of blow flies collected in urban and residential areas consuming feces from the environment. Overall, this assay can be used for *P. regina* collected in an applied setting and its integration with microbial culturing and sequencing methods will help to improve its use.

5.2 Introduction

Filth flies have long been implicated in pathogen transmission routes due to their association with unsanitary conditions.[156] The tendency for numerous families of adult filth flies to associate with feces from humans[157-159] and animals[160-162] represents the basis for mechanical transmission theories in which viral and microbial pathogens are assumed to be acquired by the flies directly from infected feces.[163, 164] Visitation to feces may be opportunistic (i.e., the fly may haphazardly alight on animal waste) or it may rep- resent a required nutrient resource for the fly. For example,

female blow flies (Diptera: Calliphoridae) can achieve partial or complete follicle development by feeding on carnivore (e.g., dog and cat) or herbivore (e.g., cow, pig, and sheep) feces.[165-167] Furthermore, proteins from feces are also important for male blow fly reproductive organ development and in increasing the probability of successful insemination.[166] It has been shown that adult *Phormia regina* Meigen (Diptera: Calliphoridae) acquire more *Escherichia coli* O157:H7 cells from manure compared with the house fly*, Musca domestica* Linnaeus (Diptera: Muscidae) and distribute these bacteria to food products. Additionally, viral pathogens may be acquired and transmitted in the same manner. For example, the blow fly *Calliphora nigribarbis* Vollenhoven (Diptera: Calliphoridae) was suspected to have played a major role in the spread of H5N1 bird flu in Japan as the H5 influenza A virus gene detected and isolated from the guts of flies captured near infected poultry facilities was identical to the strain found in infected chickens (*Gallus gallus domesticaus* Linnaeus, Galliformes: Phasianidae) and crows (*Corvus macrorhynchos* Wagler, Passeriformes: Corvidae.[168] However, the acquisition route could not be resolved, as flies may have picked up viral DNA from infected feces, carcasses, living tissue, or even contaminated feed. In tropical areas such as Manila, flies such as *Chrysomya megacephala* Fabricius (Diptera: Calliphoridae) and *M. domestica* even have the potential to disseminate disease-causing parasites as both species have been found to harbor eggs of parasitic worms on the outside of their bodies, presumably acquired from waste.[169] However, in many real-world applications, it is almost impossible to distinguish between potential acquisition modes in a fly-pathogen association, as it may occur as the result of: 1) visitation to feces, resulting in ingestion of pathogens or attachment of pathogens to the outer surface of the fly (i.e., mouth- parts, legs[170]; 2) possible acquisition of the pathogen from another contaminated source (e.g., garbage, carrion, and offal[171] and/or 3) an intrinsic association independent of fecal visitation by the adults (e.g., carryover of bacteria from immature stages of *M. domestica* to adulthood, reviewed in the study by Nayduch and Burrus 2017.[172]

Pathogenic bacteria associated with filth flies are typically extracted for analysis via microbiological culturing methods[173], molecular methods [168, 174, 175], or by using an integrated approach of culturing and DNA sequencing.[176, 177] Controlled laboratory experiments in which flies are experimentally exposed to vertebrate feces and analyzed for pathogens have given more support to the mechanical transmission theory. Such studies have shown that house flies and blow flies can acquire *E. coli* O157:H7 and *Salmonella enterica* from cow manure and successfully

transfer these bacteria to spinach leaves.[177, 178] Female house flies are also capable of acquiring more bacterial colony-forming units than males soon after exposure to manure.[173] However, in applied settings in which wild- caught flies are of primary interest, without physically observing flies ingesting or touching infected waste and linking those flies to targeted pathogens also found in the feces, there is no qualitative method for confirming that the source of the pathogen originated from feces.

The purpose of this project was to qualitatively identify vertebrate fecal biomarkers that can be detected in the alimentary canals of blow flies. Screening of these biomarkers in wild flies can then be used to test hypotheses that pathogen acquisition originates from feces. In the clinical/medical field, metabolomic studies have investigated biomarkers associated with human feces to assist in disease detection and to elucidate metabolite pathways.[179, 180] Numerous fecal compounds have been investigated for profiling human and animal metabolites, including steroids[181, 182], various bile acids[183-185], and sterols.[186] Other metabolites of interest include bilirubin and its derivatives, urobilin and stercobilin, as well as the oxidized form of urobilin, urobilinogen, as these metabolites are associated with vertebrate urine and feces.[187] These urobilinoids are formed from the breakdown of bilirubin by gut microflora[188-190] and represent a complex mixture of similar chemical structures which include the colorless urobilinogens, the yellow urobilins, and the brown stercobilins. Urobilin especially has been used as a target compound in environmental wastewater contamination studies using high performance liquid chromatography– electrospray mass spectrometry (HPLC-ES-MS).[191] This compound has also been detected in human fecal samples using ultra performance liquid chromatography quadrupole time-of-flight mass spectrometry[180], and pressurized liquid extraction turbulent flow chromatography tandem mass spectrometry (MS/MS).[192, 193] Given the suite of fecal biomarkers characterized by modern analytical techniques in metabolomics, we chose to investigate these compounds using modified liquid chromatography mass spectrometry methods. In wild-caught flies, evidence that pathogens have been acquired from animal feces would consist of 1) a confirmation that the fly in question is infected with viral or microbial pathogens, and 2) a confirmation that the fly has recently contacted or ingested animal feces. Here, we describe a method that addresses the latter consideration: we implement HPLC MS/MS to detect compounds associated with vertebrate feces in the alimentary canal of the black blow fly, *P. regina*. This fly represents one of the most common blow flies in North America, it has importance in human and

veterinary medicine as a secondary myiasis producer[194], and it has forensic utility as a primary colonizer of corpses.[195]

5.3 Methods

5.3.1 Feeding Experiment

In order to determine whether fecal metabolites could be detected from flies, controlled feeding experiments were implemented in which flies were exposed to vertebrate feces, beef liver, or a control (i.e., flies were unfed). A laboratory colony (G_3; originally generated from wild-caught *P. regina* collected from Military Park, Indianapolis, IN, USA, housed in 29.85 × 29.85 × 29.85 cm insect rearing cages [BugDorm, MegaView Science Co., Ltd., Taichung, Taiwan]) was maintained at ambient conditions (~22°C, 50% RH) in the 'fly room' at IUPUI, Indianapolis, IN, USA and given water and table sugar *ad libitum.* For the feeding experiment, ~100 colony-reared pupae were placed inside of a bleach-cleaned 21 × 12 cm mosquito breeder (BioQuip, Rancho Dominguez, CA) filled with ~2.5 cm pine shavings to ensure no access to any vertebrate tissue. Upon eclosion, experimental adult flies were transferred to bleach- cleaned rearing cages with non-sterilized water and sugar for 4 d.

Sixty adults were randomly assigned to one of the three treatments: dog feces (*Canis lupus familiaris* Linnaeus, Carnivora: Canidae), bovine (*Bos Taurus* Linnaeus, Artiodactyla: Bovidae) liver, or negative control (i.e., unfed). Flies were individually exposed to their respective resources to eliminate competition and give each fly ample opportunity to 'taste' the resource. To do this, first a damp, folded Kimwipe (Kimberley-Clark, Dallas, TX) was placed in a 29.57 mL plastic condiment cup (Diamond Multi-Purpose Mini Cups, Jarden Home Brands, Fishers, IN) and ~1 g of dog feces or beef liver was placed on top (negative control flies were only exposed to the damp Kimwipe). The purpose of the Kimwipe was to prevent desiccation of the resource. Once flies were anesthetized via refrigeration, they were quickly placed inside a feeding cup and sealed with a breathable lid (N = 10 males, 10 females/treatment; N = 60 total flies). Feeding cups were placed inside of a Percival I-36VL incubator (Percival Scientific Inc., Perry, IA) at 28°C and 65% RH for 4 h and then freeze killed at −80°C.

Several additional controls were also analyzed to confirm the presence of urobilinoids in fecal samples derived from animals occupying different trophic positions. Confirmatory samples of dog (*Canis lupus familiaris* Linnaeus, Carnivora: Canidae), lion (*Panthera leo* Linnaeus,

Carnivora: Felidae), Grant's Zebra (*Equus quagga boehmi* Matschie, Perissodactyla: Equidae), and Guinea Baboon (*Papio papio* Desmarest, Primates: Cercopithecidae) feces ($N = 5$ per animal) were analyzed to verify whether urobilinoids would be present in a sample regardless of the host diet. All exotic animal fecal samples were collected with permission from the Indianapolis Zoo, Indianapolis, IN, USA in the spring and fall of 2016. Exotic animal fecal samples were collected from overnight holding areas in the zoo after animals had been moved to their day-time enclosures, but before the areas were cleaned by staff. Maximum age of fecal samples was ~10 h. These samples were collected with a sterilized tongue depressor and placed in sterile 50 ml falcon tubes, which were immediately stored at −20°C. All dog fecal samples were collected in the same manner shortly after defecation and then stored at −20°C until needed. Beef liver tissue ($N = 5$) was also tested as a negative control in order to confirm that urobilinoids would only be present in feces-related samples. All previously frozen fecal material and beef liver tissue were thawed at room temperature for ~1 h prior to the beginning the experiment.

5.3.2 Wild Blow Fly Collections

P. regina were sampled from six geographic locations in Central Indiana (**Table 5.1**) from March to June 2016. Each sampling site was composed of a forested park set within, adjacent to, or nearby an urban area. Collections were made with an aerial sweep net at a decayed chicken liver bait (aged 1–2 wk at ambient temperature), which was protected from flies alighting on the bait, over a period of 20 min at each site. Flies were killed in 70% ethanol immediately after this time period and stored at −20°C until needed for laboratory analyses. For the current study, $N = 216$ wild-caught flies underwent dissection and DNA extraction as described below.

Table 5.1 Proportion of Phormia regina that tested positive for urobilinoid signals collected in Central Indiana from March 2016 to June 2016. Positive urobilinoid signals were seen in 13% of the flies tested (i.e., 29 out of 216). Values are given as proportions of positive flies from all flies tested per geographic site. Exact location of each park is given by geographic coordinates in degrees, minutes, and seconds (dms).

PARK	CITY, STATE	LATITUDE	LONGITUDE	PROPORTION POSITIVE FLIES
MILITARY PARK	Indianapolis, IN	39°46′13.99″	−86°10′06.99″	5/60
BROAD RIPPLE PARK	Indianapolis, IN	39°52′17.99″	−86°07′49.00″	5/36
SKILES-TEST NATURE PARK	Indianapolis, IN	39°52′21.00″	−86°29′49.99″	6/32
NORTHWEST PARK	Greenwood, IN	39°37′42.99″	−86°08′36.99″	8/43
UNIVERSITY PARK	Greenwood, IN	39°36′39.99″	−86°30′20.00″	2/24
PROVINCE PARK	Franklin, IN	39°28′37.99″	−86°06′39.99″	3/21

5.3.3 Gut Dissections and DNA Extractions

The mid- and hind-guts of each fly was dissected using flame sterilized forceps for standard organic DNA extractions (DNA is being used for a parallel study in which vertebrate DNA within the gut contents is being sequenced, unpublished data). The typically discarded phenol:chloroform:isoamyl (PCI) alcohol layer from these extractions was then used for chemical analysis. In greater detail, the guts of individual flies were placed inside a sterile 1.5 mL microcentrifuge tube. Digestion was performed by adding 200 µL ChargeSwitch lysis buffer (Invitrogen, Carlsbad, CA) and 10 µL of 20 mg/ml proteinase K (Invitrogen) to each sample and incubated for 4 h at 60°C. 100 µL of PCI alcohol (25:24:1) (Thermo Fisher, Waltham, MA) was added to the lysate and centrifuged at 5,000 rpm for 5 min, separating the extraction into an organic 'waste' layer and an aqueous DNA layer. The aqueous layer was transferred into a new tube to continue the DNA extraction procedure, whereas the organic layer was refrigerated until use in chemical analysis.

5.3.4 Preliminary Presumptive Fecal Test

The Edelman's presumptive test for urobilinoids in feces, which is commonly used in forensic laboratories, detects urobilinogen following a chemical reaction with zinc chloride, mercuric chloride, and isoamyl alcohol.[196] This test was found to be unsuitable for the current application, as the mid- and hind-guts of control flies (i.e., not exposed to any fecal or tissue sources) exhibited back- ground fluorescence (data not shown).

5.3.5 Qualitative LC MS/MS Analyses

A 50 µL aliquot of the PCI layer from the DNA extraction was evaporated under a stream of nitrogen at ambient temperature, resuspended in 50 µL of a 1:1 methanol:water solution, and vortexed for at least 10 min. The samples were separated using an Agilent 1100 HPLC system (Agilent Technologies, Santa Clara, CA) using reversed phase chromatography on a 100 × 2.1 mm C18 column at a flow rate of 200 µL/min and identified using a LTQ XL Linear Ion Trap Quadrupole (Thermo Fisher) mass spectrometer. The solvents were 0.1% formic acid in water (solvent A) and 0.1% formic acid in 70:30 acetonitrile:methanol (solvent B) over 15 min. The separation began with an initial 1 min hold at 30% B followed by a 9-min linear gradient to 95% B followed by a 4 min at 400 µL/ min re-equilibration of the initial mobile phase composition. Mass spectra data were acquired in the positive ion mode. Mass spectral scans consisted of a full MS followed by directed MS/MS scans at m/z 591, 593, 595, and 597 to screen for various tetrapyrrole urobilinoids. Urobilinogen standards (Thermo Fisher and Santa Cruz Biotechnology, Inc., Dallas, TX) were also tested, each consisting of a mixture of isomers with molecular weights ranging from 590.7 to 598.8 g/mol.

5.3.6 Statistical Analyses

Experimental and wild flies were compared statistically. The nonparametric Kruskal–Wallis rank sum[197] test was implemented (as peak area data were not normally distributed and could not be transformed), followed by post-hoc paired comparisons using Dunn's test.[198] All statistics were performed in R (R Core Team 2017)[199] using the packages stats (native) and dunn.test.[200]

5.4 Results

Direct extraction of feces and gut extractions from feces-fed flies showed several peaks with an *m*/*z* of 591 that had MS/MS spectra consistent with tetrapyrrole urobilinoids. Known urobilinoids with an *m*/*z* of 591 include d-urobilinogen and *i*-urobilin. Two partially resolved HPLC peaks with retention times of 6.3 and 6.6 min were obtained (**Figure 5.1A**). Both peaks had indistinguishable MS/MS spectra containing *m*/*z* 343 and 466 in similar ratios (**Figure 5.1C**), both of which were similar to the MS/MS spectrum reported for *i*-urobilin by Quinn et al.[201] Feces-fed fly controls also contained a third prominent peak with *m*/*z* 591 eluting at ~8.2 min, which gave only one prominent fragment ion at *m*/*z* 466 (**Figure 5.1B** and **D**). This fragment ion is also

suggestive of a urobilinoid, as the neutral loss of 125 mass units is consistent with the loss of a pyrrole unit. We analyzed commercial urobilinoid standards, and peaks with identical retention times and tandem mass spectra were obtained. The commercial standards were complex mixtures of numerous similar isomers, however, so we could not make exact molecular identifications of the urobilinoids detected in the feces-fed flies. Quinn et al. (2012)[201] reported on the MS/MS spectra of urobilin and stercobilin, but these spectra were obtained from direct infusion of a standard composed of a mixture of isomers as well.

We screened for urobilinoids with *m*/*z* 593, 595, and 597 as well. Stercobilin, with *m*/*z* 595, eluted at 6.76 min and yielded two primary fragment ions at *m*/*z* 595 → 470 and 345. This peak was identified as stercobilin by comparison with an MS/MS spectra reported in the literature.[201] Though stercobilin is the primary brown pigment in feces, it did not prove to be a reliable marker for feces consumption. Although stercobilin was strongly detected in zebra and baboon feces extracts, it was absent or very low in lion and canine feces extracts (data not shown). This urobilinoid was detected in only a small fraction of feces-fed control flies, and, when present, the intensity was significantly lower than the three *m*/*z* 591 urobilinoids. Because of this, stercobilin was eliminated as a targeted compound in this assay. The well-known urobilinoids *i*-urobilinogen (*m*/*z* 593) and *i*-stercobilinogen (*m*/*z* 597) were also not detected in feces-fed control flies.

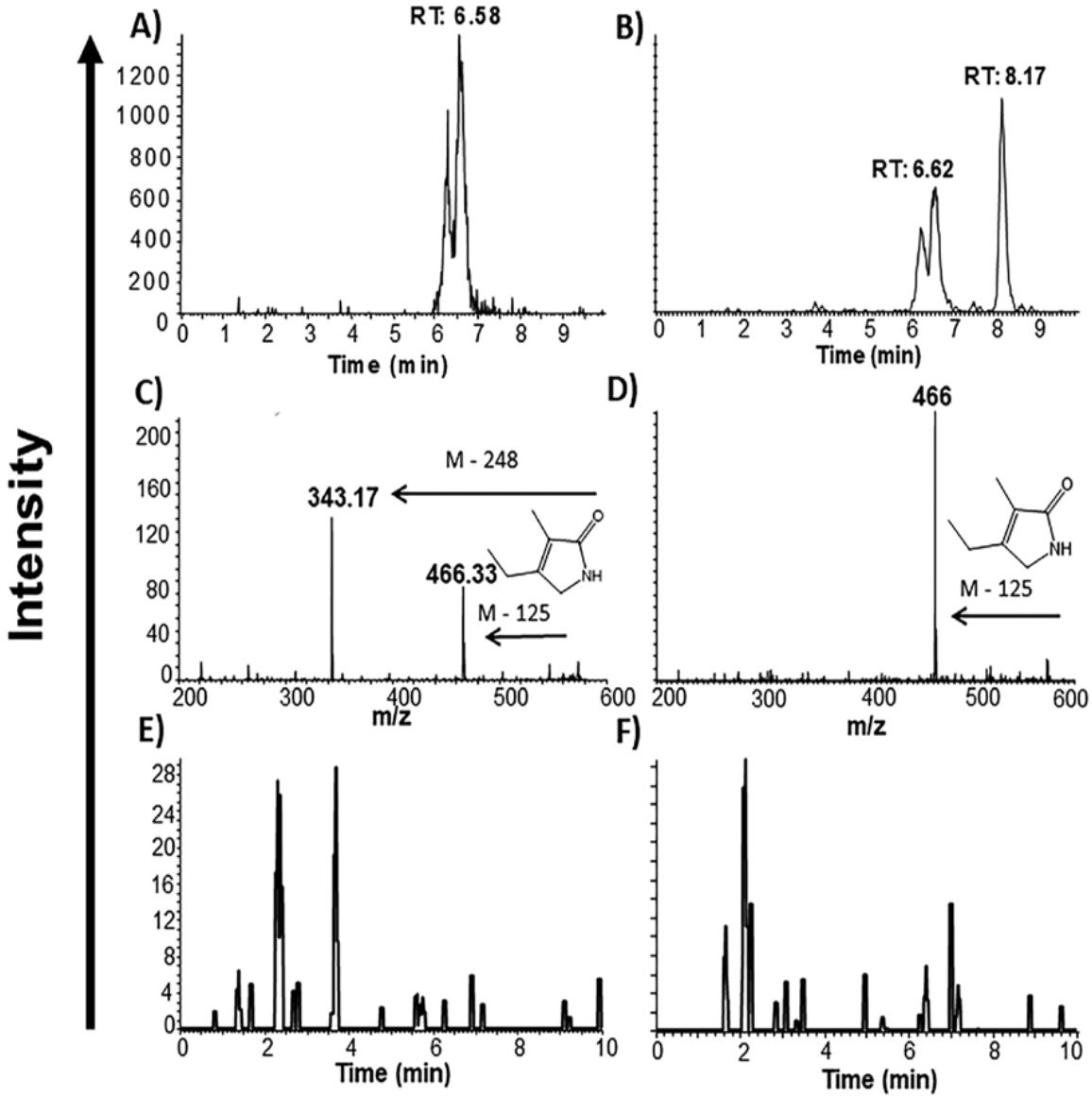

Figure 5.1 Extracted ion MS/MS chromatograms (XIC) and MS/MS spectra for fly samples (absolute intensities). (A) Extracted ion MS/MS chromatogram for m/z 591 → 343 for a feces-fed fly. (B) Extracted ion MS/MS chromatogram for m/z 591 → 466 for a feces-fed fly. (C) MS/MS spectrum of m/z 591 at 6.5 min. 'M' indicates the mass of the primary molecule (591), with 248 and 125 representing neutral loss fragments, e.g., 'M – 248' indicates the loss of the 248 molecule to give the 343.17 daughter ion. (D) MS/MS spectrum of m/z 591 at 8.2 min. 'M' indicates the mass of the primary molecule (591), with 125 representing the neutral loss fragment, i.e., 'M – 125' indicates the loss of the 125 molecule to give the 466 daughter ion. Representative XIC for m/z 591 → 343 (E) and m/z 591 → 466 (F) for a liver-fed flies (i.e., no peaks are present at 6 or 8 min).

Data for positive controls (i.e., vertebrate feces) varied considerably among and between species (dog, lion, zebra, and baboon); however, all were positive for one or more of the *m*/*z* 591 urobilinoids described above (**Figure 5.2**). Zebra samples contained the 8.2 min peak, but not the peaks at 6.3–6.6 min, whereas lion samples displayed a strong peak at 6.6 min but relatively low-intensity peaks for the other two urobilinoids peaks at 6.3 and 8.2 min. However, none of the relevant urobilinoid peaks were present in the beef liver tissue extractions (**Figure 5.2**). All feces-related samples contained peaks indicative of urobilinoids that were not present in the other samples tested.

Although peak areas were highly variable across feeding experiment flies and wild flies, all feces-fed flies exhibited readily detectable signals for the *m*/*z* 591 urobilinoids. None of the unfed or liver-fed flies showed any peaks indicating the presence of urobilinoid compounds (**Figures 5.1** and **5.2**). The Kruskal–Wallis test revealed significant effects of treatments at 6 min ($\chi^2 = 72.8$, df = 3, $P < 0.0001$) and 8 min ($\chi^2 = 78.3$, df = 3, $P < 0.0001$), and post-hoc tests revealed significant differences between flies testing positive for urobilinoids and those which tested negative for these compounds (**Table 5.2**). Comparing the peak areas for wild flies versus experimental flies, there were no statistical differences at 6 min ($P = 0.5290$), but a significant difference was observed between the two sets at the 8 min peak ($P = 0.0205$). The urobilinoid signal is greater in feces-fed flies versus wild flies. Though speculative, this difference is likely due to the recent feeding event for experimental flies versus an unknown time since feeding for the wild flies. Wild blow fly data showed that 13% ($N = 29$ of 216) of the *P. regina* collected and tested from urban parks in Indiana, USA were positive for urobilinoids (**Figure 5.2** and **Table 5.1**). Peak area values (6.3–6.6 and 8.2 min) of wild flies clustered with all feces control samples (**Figure 5.2**). The mean proportion of flies with positive urobilinoid signals at 6.3– 6.6 and 8.2 min peaks varied slightly by site (mean = 0.14 ± 0.05).

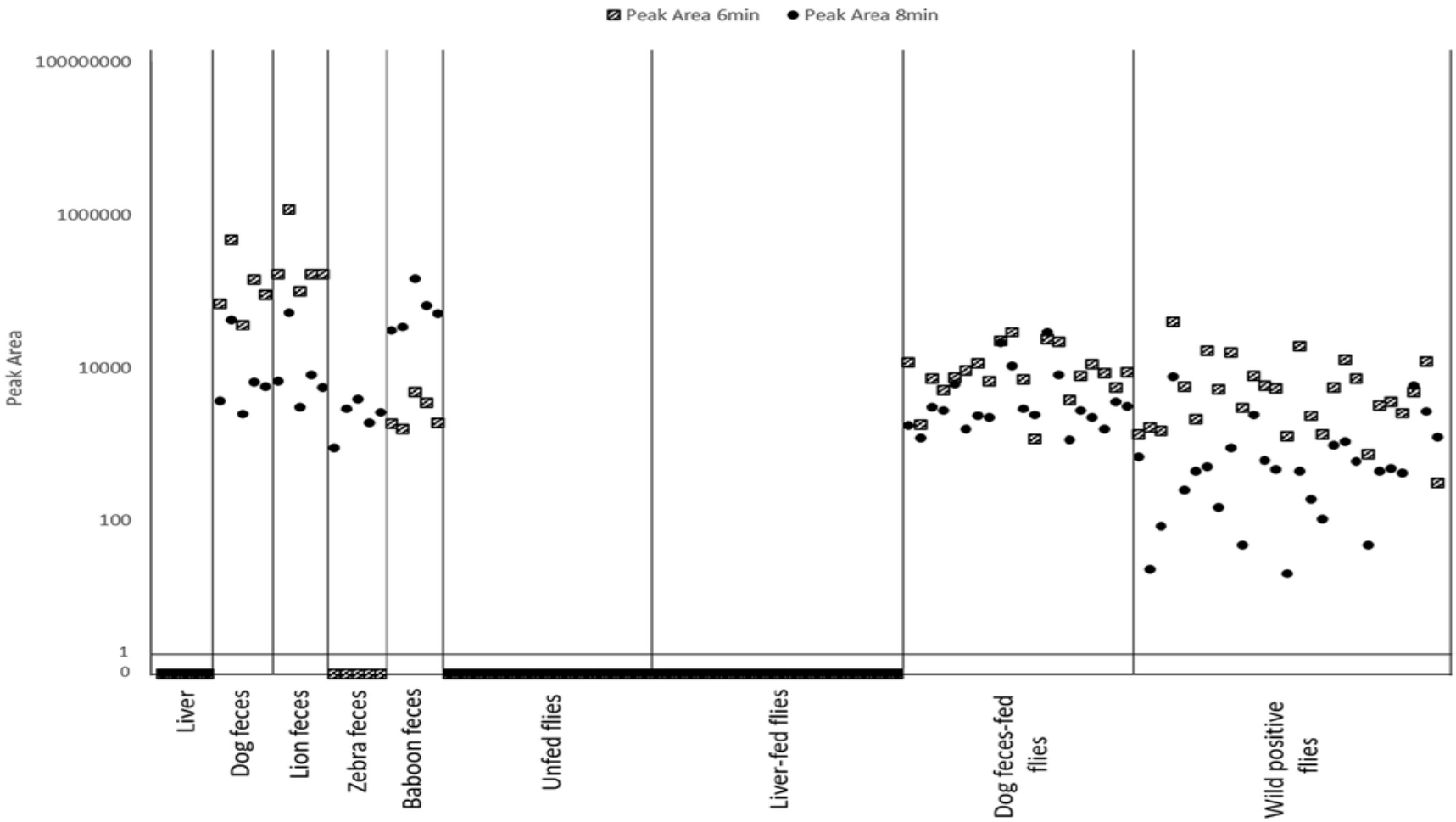

Figure 5.2 Scatterplot comparison of LC MS/MS 6.3 – 6.6 and 8.2 min peak area data for all tissue and fecal controls, as well as all experimental and wild flies (logarithmic scale). Controls consisted of beef liver tissue, dog, lion, zebra, and baboon feces (N = 5 per control). Experimental feeding treatments for flies included unfed, beef liver-fed, and dog feces-fed individuals (N = 20 per treatment). Wild flies (N = 29) were collected from March to June 2016 in urban parks in Central Indiana, and samples with positive signals are shown here. Black circles = peak area data at 6 min, striped squares = peak area data at 8 min.

Table 5.2 Results for Dunn's test for nonparametric multiple com- parisons between experimental (N = 20/treatment) and wild-caught (N = 29) flies for peak areas at 6 and 8 min. Experimental treatments included unfed flies, beef liver-fed flies, and feces-fed flies. *Statistically significant comparison at $P < 0.05$.

Paired Comparison	Peak Area (6 min)		Peak Area (8 min)	
	z-statistic	P	z-statistic	P
Feces-fed-Liver-fed	6.4562	<0.0001*	7.1809	<0.0001*
Feces-fed-Unfed	6.4562	<0.0001*	7.1809	<0.0001*
Feces-fed-Wild	1.3521	0.5290	2.7043	0.0205*
Liver-fed-Unfed	0.0000	1.0000	0.0000	1.0000
Liver-fed-Wild	−5.5681	<0.0001*	−4.9928	<0.0001*
Unfed-Wild	−5.5681	<0.0001*	−4.9928	<0.0001*

5.5 Discussion

Surprisingly, few studies have investigated the diet of wild or experimental insects using LC/MS methods, with the exception of detecting sugars in the guts of sand flies (Diptera: Psychodidae)[202, 203] and mosquitos (Diptera: Culicidae).[204] Larval, though not adult, blow fly diet has been previously investigated using gas chromatography/MS and LC–MS/MS for the purpose of detecting legal and illicit drugs present in corpse tissues consumed by maggots.[205-207] Our research represents an important first step in qualitatively assessing the diet of an adult filth fly of medical, veterinary, and forensic importance using LC/MS methods. Furthermore, this method was utilized without the aid of microbiological culturing or molecular DNA sequencing, which is common in studies which aim to detect and isolate pathogens/pathogen genes from filth flies. However, the integration of all three methods (microbial culturing and sequencing with urobilinoid analysis) would likely produce an even more precise method for confirming the presence and source of feces ingested by a filth fly, as well as the pathogens associated with the resource.

This study shows that a mixture of the urobilinoids consisting of d-urobilinogen and i-urobilin were definitively and consistently transferred to the guts of *P. regina* from ingested feces. Though flies in this study were only exposed to one type of feces (dog), a strong urobilinoid signal observed for all fecal samples (and their absence in tissue samples) indicate that similar results would likely be seen in flies that had ingested feces from various vertebrate species. In addition to experimental verification, this assay also confirmed that wild, randomly sampled blow flies from urban areas consume vertebrate feces. This is not unexpected as several of the collection sites were adjacent to dog parks and residential areas. Sources impacting the variability in signal intensity in positive flies likely include the amount of feces ingested by flies and the amount of gut contents

subjected to DNA extraction. The liquid–liquid extraction and analytical measurement also contributed to the observed variation. Fluctuations in signal intensity within and between animal fecal samples were expected as the relative amounts of the urobilinoids likely varies depending on the gut microflora[208], or exposure of the samples to air and light, which has been shown to induce a conversion from urobilinogen to urobilin.[209] Furthermore, the amount of urobilinoids present in wild-caught fly guts would likely be significantly affected by variables such as the amount and type of feces consumed, the time between feeding and collection, and environmental conditions such as temperature, which may affect the speed of fly metabolism. These uncontrollable variables would complicate interpretation of quantitative data. The variability of stercobilin specifically may have arisen from differences listed above, as well as liver functioning of the host animal, which could vary by individual. As such, the observed variability made this compound problematic for our purposes.

The assay described here can aid in testing transmission hypotheses. Specifically, it can confirm that wild flies collected in applied settings (e.g., during routine inspection inside and around farms, during a disease outbreak, and as part of ecological surveys) have ingested animal feces. This method can be applied to several different situations in which determining fecal consumption of flies could be critical, including when the putative, but not confirmed, source of a pathogenic transmission is a filth insect. Though the method presented here is not intended to pinpoint a geographic location of the pathogen source, a general knowledge of the recorded dispersal abilities of the species in question would likely benefit those utilizing this method in an applied setting. Additionally, the detection of urobilinoids could prove useful in conservation studies in which filth flies may be used as 'environmental drones' to gain ecological information about vertebrate species (targeted or nonspecific) in virtually any ecosystem that is conducive for filth flies. The method proposed here could be used to improve such studies by differentiating between fecal and tissue resources, which could be critical in conservation studies which are centered on finding evidence that the species of interest is alive. Utilizing the method provided here in conjunction with vertebrate DNA sequencing tools could lead to a more informed understanding of spatiotemporal distributions of endangered and threatened animals, as well as overall vertebrate diversity of an ecosystem.

5.6 Conclusion

Our experimental data show that HPLC MS/MS provides an accurate qualitative test for detection of fecal urobilinoids in *P. regina*. Though the intensities of these signals were variable across individuals, chemical signatures associated with feces were evident and strong compared with unfed flies and flies fed liver tissue with no false positives or negatives observed (i.e., urobilinoids were only detected in flies exposed to animal feces), thus supporting the validity of this method in detecting the presence of fecal material and providing a strong indication that blow flies feed on animal feces.

The qualitative test presented here may be of great utility to several disciplines, however, there are limitations that should be addressed. Factors that could impact the urobilinoid signal intensity of fly guts include the amount of feces consumed by a fly, as well as the number of meals each fly may take within a given period of time. Currently, the duration of detectable urobilinoid signals in fly guts is unknown (i.e., we cannot determine when a wild fly may have ingested feces in the environment). This is largely due to the variability in peak signals that were observed among individuals in the controlled feeding experiment. Regardless, the sole purpose of this study was simply to illustrate that urobilinoids are only detected in flies exposed to feces, and that these compounds are not associated with flies otherwise. Experimental results provide support that the signals seen from our wild flies were real, indicating that they were, in fact, feeding on feces in the environment. In the future, this method should be implemented and validated using multiple species of filth flies and other coprophagous insects. This method will be most impactful when combined with microbial culturing and DNA sequencing methods, as well as vertebrate DNA sequencing methods, to precisely identify the source of pathogens mechanically acquired by filth insects from vertebrate feces.

REFERENCES

1. Hoffmann, E. d.; Stroobant, V., *Mass Spectrometry Principles and Applications*. 3 ed.; John Wiley & Sons: Chichester, West Sussex, England, 2012.
2. Gross, J. H., *Mass Spectrometry*. 3 ed.; Springer Nature: Heidelberg, Germany, 2017.
3. Greaves, J.; Roboz, J., *Mass Spectrometry for the Novice*. CRC Press: Boca Raton, FL, 2014.
4. Watson, J. T.; Sparkman, O. D., *Introduction to Mass Spectrometry: Instrumentation, Applications, and Strategies for Data interpretation*. 4 ed.; John Wiley & Sons, Ltd: Chichester, West Sussex, England, 2008.
5. Willoughby, R.; Sheehan, E.; Mitrovich, S., *A Global View of LC/MS: How to solve your most challenging analytical problems*. 2 ed.; Global View Publishing: Pittsburg, PA, 2002.
6. Electrospray Ionization (ESI) Mass Spectrometry. 2020.
7. Medhe, S., Mass Spectrometry: Detectors Review. *Chemical and Biomolecular Engineering* **2018,** *3* (4), 51-58.
8. Koppenaal, D. W.; Barinaga, C. J.; Denton, M. B.; Sperline, R. P.; Hieftje, G. M.; Schilling, G. D.; Andrade, F. J.; Barnes, J. H. t., MS detectors. *Anal. Chem.* **2005,** *77* (21), 418A-427A.
9. Li, Y.; Cao, Y.; Guo, Y., Recent Advances in Atmospheric Ionization Mass Spectrometry: Developments and Applications. *Chinese Journal of Chemistry* **2019,** *38* (1), 25-38.
10. Monge, M. E.; Fernández, F. M., An Introduction to Ambient Ionization Mass Spectrometry. In *Ambient Ionization Mass Spectrometry*, The Royal Society of Chemistry: 2014; pp 1-22.
11. Hsu, C. C.; Dorrestein, P. C., Visualizing life with ambient mass spectrometry. *Curr Opin Biotechnol* **2015,** *31*, 24-34.
12. Rankin-Turner, S.; Heaney, L. M., Applications of ambient ionization mass spectrometry in 2020: An annual review. *Analytical Science Advances* **2021,** *2* (3-4), 193-212.
13. McKenna, J.; Jett, R.; Shanks, K.; Manicke, N. E., Toxicological Drug Screening using Paper Spray High-Resolution Tandem Mass Spectrometry (HR-MS/MS). *J Anal Toxicol* **2018,** *42* (5), 300-310.
14. Li, N.; Nie, H.; Jiang, L.; Ruan, G.; Du, F.; Liu, H., Recent advances of ambient ionization mass spectrometry imaging in clinical research. *J Sep Sci* **2020,** *43* (15), 3146-3163.
15. Xiao, Y.; Deng, J.; Yao, Y.; Fang, L.; Yang, Y.; Luan, T., Recent advances of ambient mass spectrometry imaging for biological tissues: A review. *Anal Chim Acta* **2020,** *1117*, 74-88.

16. Zhang, W.; Wang, X.; Xia, Y.; Ouyang, Z., Ambient Ionization and Miniature Mass Spectrometry Systems for Disease Diagnosis and Therapeutic Monitoring. *Theranostics* **2017,** *7* (12), 2968-2981.

17. Li, L. H.; Hsieh, H. Y.; Hsu, C. C., Clinical Application of Ambient Ionization Mass Spectrometry. *Mass Spectrom (Tokyo)* **2017,** *6* (Spec Iss), S0060.

18. Liu, H.; Gao, W.; Tian, Y.; Liu, A.; Wang, Z.; Cai, Y.; Zhao, Z., Rapidly detecting tetrabromobisphenol A in soils and sediments by paper spray ionization mass spectrometry combined with isotopic internal standard. *Talanta* **2019,** *191*, 272-276.

19. Reeber, S. L.; Gadi, S.; Huang, S.-B.; Glish, G. L., Direct analysis of herbicides by paper spray ionization mass spectrometry. *Analytical Methods* **2015,** *7* (23), 9808-9816.

20. McKenna, J.; Dhummakupt, E. S.; Connell, T.; Demond, P. S.; Miller, D. B.; Michael Nilles, J.; Manicke, N. E.; Glaros, T., Detection of chemical warfare agent simulants and hydrolysis products in biological samples by paper spray mass spectrometry. *Analyst* **2017,** *142* (9), 1442-1451.

21. Laskin, J.; Lanekoff, I., Ambient Mass Spectrometry Imaging Using Direct Liquid Extraction Techniques. *Anal. Chem.* **2016,** *88* (1), 52-73.

22. Perez, C. J.; Bagga, A. K.; Prova, S. S.; Yousefi Taemeh, M.; Ifa, D. R., Review and perspectives on the applications of mass spectrometry imaging under ambient conditions. *Rapid Commun Mass Spectrom* **2019,** *33 Suppl 3* (S3), 27-53.

23. Swiner, D. J.; Jackson, S.; Burris, B. J.; Badu-Tawiah, A. K., Applications of Mass Spectrometry for Clinical Diagnostics: The Influence of Turnaround Time. *Anal. Chem.* **2020,** *92* (1), 183-202.

24. Jackson, A. U.; Shum, T.; Sokol, E.; Dill, A.; Cooks, R. G., Enhanced detection of olefins using ambient ionization mass spectrometry: Ag+ adducts of biologically relevant alkenes. *Anal Bioanal Chem* **2011,** *399* (1), 367-76.

25. Duncan, K. D.; Fang, R.; Yuan, J.; Chu, R. K.; Dey, S. K.; Burnum-Johnson, K. E.; Lanekoff, I., Quantitative Mass Spectrometry Imaging of Prostaglandins as Silver Ion Adducts with Nanospray Desorption Electrospray Ionization. *Anal. Chem.* **2018,** *90* (12), 7246-7252.

26. Li, Y.; Guo, X.; Tian, Y.; Zhang, T.; Luo, Z.; Liu, X.; Qian, C.; Dai, J.; Duan, Y., *Methylation in combination with temperature programming enables rapid identification of polysaccharides by ambient micro-fabrication glow discharge plasma (MFGDP) desorption ionization mass spectrometry*. 2020/08/17 ed.; 2020; Vol. 218, p 121156.

27. Jakka Ravindran, S.; Kumar, R.; Srimany, A.; Philip, L.; Pradeep, T., *Early Detection of Biofouling on Water Purification Membranes by Ambient Ionization Mass Spectrometry Imaging*. 2017/12/07 ed.; American Chemical Society: 2018; Vol. 90, p 988-997.

28. Jarmusch, A. K.; Pirro, V.; Kerian, K. S.; Cooks, R. G., Detection of strep throat causing bacterium directly from medical swabs by touch spray-mass spectrometry. *Analyst* **2014,** *139* (19), 4785-9.

29. Hamid, A. M.; Jarmusch, A. K.; Pirro, V.; Pincus, D. H.; Clay, B. G.; Gervasi, G.; Cooks, R. G., Rapid discrimination of bacteria by paper spray mass spectrometry. *Anal. Chem.* **2014,** *86* (15), 7500-7.

30. Ferreira, C. R.; Yannell, K. E.; Jarmusch, A. K.; Pirro, V.; Ouyang, Z.; Cooks, R. G., Ambient Ionization Mass Spectrometry for Point-of-Care Diagnostics and Other Clinical Measurements. *Clin Chem* **2016,** *62* (1), 99-110.

31. Banerjee, S., Empowering Clinical Diagnostics with Mass Spectrometry. *ACS Omega* **2020,** *5* (5), 2041-2048.

32. Feider, C. L.; Krieger, A.; DeHoog, R. J.; Eberlin, L. S., Ambient Ionization Mass Spectrometry: Recent Developments and Applications. *Anal. Chem.* **2019,** *91* (7), 4266-4290.

33. Zaitsu, K., Introduction to ambient ionization mass spectrometry. In *Ambient Ionization Mass Spectrometry in Life Sciences*, Zaitsu, K., Ed. Elsevier: 2020; pp 1-32.

34. Monge, M. E.; Harris, G. A.; Dwivedi, P.; Fernandez, F. M., Mass spectrometry: recent advances in direct open air surface sampling/ionization. *Chem Rev* **2013,** *113* (4), 2269-308.

35. Venter, A. R.; Douglass, K. A.; Shelley, J. T.; Hasman, G., Jr.; Honarvar, E., Mechanisms of real-time, proximal sample processing during ambient ionization mass spectrometry. *Anal. Chem.* **2014,** *86* (1), 233-49.

36. Klampfl, C. W.; Himmelsbach, M., Direct ionization methods in mass spectrometry: An overview. *Anal Chim Acta* **2015,** *890*, 44-59.

37. Wang, H.; Liu, J.; Cooks, R. G.; Ouyang, Z., Paper spray for direct analysis of complex mixtures using mass spectrometry. *Angew Chem Int Ed Engl* **2010,** *49* (5), 877-80.

38. Ouyang, Z. New sampling and ionization methods for MS-Based Chemical Analysis and Bionmedical Diagnosis. https://engineering.purdue.edu/BioMS/ionization.htm#PaperSpray (accessed May).

39. Chiang, S.; Zhang, W.; Ouyang, Z., Paper spray ionization mass spectrometry: recent advances and clinical applications. *Expert Rev Proteomics* **2018,** *15* (10), 781-789.

40. Yang, Q.; Wang, H.; Maas, J. D.; Chappell, W. J.; Manicke, N. E.; Cooks, R. G.; Ouyang, Z., Paper spray ionization devices for direct, biomedical analysis using mass spectrometry. *Int J Mass Spectrom* **2012,** *312*, 201-207.

41. Ronald, D. M.; Thomas W. Nolan, P. D.; Lloyd, P. P., *Quality Improvement Through Planned Experimentation, Third Edition*. 3rd ed. ed.; McGraw-Hill Education: New York, 2012.

42. Montgomery, D. C., *Design and analysis of experiments*. 8th ed. ed.; John Wiley & Sons Inc: Place of publication not identified, 2013.

43. Hicks, C. R., *Fundamental concepts in the design of experiments*. Holt, Rinehart and Winston: New York, 1993.

44. Montgomery, D. C., *Introduction to statistical quality control*. Wiley: Hoboken, NJ, 2013.

45. Box, G. E. P., *Statistics for experimenters: an introduction to design, data analysis, and model building*. New York : Wiley: New York, 1978.

46. Rencher, A. C.; Christensen, W. F., *Methods of multivariate analysis*. 2012.

47. Takats, Z.; Wiseman, J. M.; Gologan, B.; Cooks, R. G., Mass spectrometry sampling under ambient conditions with desorption electrospray ionization. *Science* **2004,** *306* (5695), 471-3.

48. Cody, R. B.; Laramee, J. A.; Durst, H. D., Versatile new ion source for the analysis of materials in open air under ambient conditions. *Anal. Chem.* **2005,** *77* (8), 2297-302.

49. Cooks, R. G.; Ouyang, Z.; Takats, Z.; Wiseman, J. M., Detection Technologies. Ambient mass spectrometry. *Science* **2006,** *311* (5767), 1566-70.

50. Huang, M. Z.; Yuan, C. H.; Cheng, S. C.; Cho, Y. T.; Shiea, J., Ambient Ionization Mass Spectrometry. In *Annual Review of Analytical Chemistry, Vol 3*, Yeung, E. S.; Zare, R. N., Eds. Annual Reviews: Palo Alto, 2010; Vol. 3, pp 43-65.

51. Liu, J.; Wang, H.; Manicke, N. E.; Lin, J. M.; Cooks, R. G.; Ouyang, Z., Development, characterization, and application of paper spray ionization. *Anal. Chem.* **2010,** *82* (6), 2463-71.

52. Evard, H.; Kruve, A.; Lõhmus, R.; Leito, I., Paper spray ionization mass spectrometry: Study of a method for fast-screening analysis of pesticides in fruits and vegetables. *J. Food Compos. Anal.* **2015,** *41*, 221-225.

53. Espy, R. D.; Manicke, N. E.; Ouyang, Z.; Cooks, R. G., Rapid analysis of whole blood by paper spray mass spectrometry for point-of-care therapeutic drug monitoring. *Analyst* **2012,** *137* (10), 2344-9.

54. Manicke, N. E.; Bills, B. J.; Zhang, C., Analysis of biofluids by paper spray MS: advances and challenges. *Bioanalysis* **2016,** *8* (6), 589-606.

55. Wang, H.; Manicke, N. E.; Yang, Q.; Zheng, L.; Shi, R.; Cooks, R. G.; Ouyang, Z., Direct analysis of biological tissue by paper spray mass spectrometry. *Anal. Chem.* **2011,** *83* (4), 1197-201.

56. Kissinger, P. T., Thinking about dried blood spots for pharmacokinetic assays and therapeutic drug monitoring. *Bioanalysis* **2011,** *3* (20), 2263-6.

57. Maurer, H. H., Mass Spectrometry for Research and Application in Therapeutic Drug Monitoring or Clinical and Forensic Toxicology. *Ther Drug Monit* **2018,** *40* (4), 389-393.

58. Spooner, N.; Lad, R.; Barfield, M., Dried blood spots as a sample collection technique for the determination of pharmacokinetics in clinical studies: considerations for the validation of a quantitative bioanalytical method. *Anal. Chem.* **2009,** *81* (4), 1557-63.

59. Michely, J. A.; Meyer, M. R.; Maurer, H. H., Paper Spray Ionization Coupled to High Resolution Tandem Mass Spectrometry for Comprehensive Urine Drug Testing in Comparison to Liquid Chromatography-Coupled Techniques after Urine Precipitation or Dried Urine Spot Workup. *Anal. Chem.* **2017,** *89* (21), 11779-11786.

60. Shi, R. Z.; El Gierari el, T. M.; Faix, J. D.; Manicke, N. E., Rapid Measurement of Cyclosporine and Sirolimus in Whole Blood by Paper Spray-Tandem Mass Spectrometry. *Clin Chem* **2016,** *62* (1), 295-7.

61. Shi, R. Z.; El Gierari el, T. M.; Manicke, N. E.; Faix, J. D., Rapid measurement of tacrolimus in whole blood by paper spray-tandem mass spectrometry (PS-MS/MS). *Clin Chim Acta* **2015,** *441*, 99-104.

62. Yannell, K. E.; Kesely, K. R.; Chien, H. D.; Kissinger, C. B.; Cooks, R. G., Comparison of paper spray mass spectrometry analysis of dried blood spots from devices used for in-field collection of clinical samples. *Anal Bioanal Chem* **2017,** *409* (1), 121-131.

63. Damon, D. E.; Davis, K. M.; Moreira, C. R.; Capone, P.; Cruttenden, R.; Badu-Tawiah, A. K., Direct Biofluid Analysis Using Hydrophobic Paper Spray Mass Spectrometry. *Anal. Chem.* **2016,** *88* (3), 1878-84.

64. Zhang, C.; Glaros, T.; Manicke, N. E., Targeted Protein Detection Using an All-in-One Mass Spectrometry Cartridge. *J Am Chem Soc* **2017,** *139* (32), 10996-10999.

65. Wichert, W. R. A.; Dhummakupt, E. S.; Zhang, C.; Mach, P. M.; Bernhards, R. C.; Glaros, T.; Manicke, N. E., Detection of Protein Toxin Simulants from Contaminated Surfaces by Paper Spray Mass Spectrometry. *J Am Soc Mass Spectrom* **2019,** *30* (8), 1406-1415.

66. Long, G. L.; Winefordner, J. D., Limit of Detection A Closer Look at the IUPAC Definition. *Analytical Chemistry* **2012,** *55* (07), 712A-724A.

67. Bills, B. J.; Kinkade, J.; Ren, G.; Manicke, N. E., The impacts of paper properties on matrix effects during paper spray mass spectrometry analysis of prescription drugs, fentanyl and synthetic cannabinoids. *Forensic Chemistry* **2018,** *11*, 15-22.

68. Vega, C.; Spence, C.; Zhang, C.; Bills, B.; Manicke, N. E., Ionization Suppression and Recovery in Direct Biofluid Analysis using Paper Spray Mass Spectrometry. *Journal of the American Society for Mass Spectrometry* **2016,** *27* (4), 726-734.

69. Wang, T.; Zheng, Y.; Wang, X.; Austin, D. E.; Zhang, Z., Sub-ppt Mass Spectrometric Detection of Therapeutic Drugs in Complex Biological Matrixes Using Polystyrene-Microsphere-Coated Paper Spray. *Anal. Chem.* **2017,** *89* (15), 7988-7995.

70. El-Najjar, N.; Hosl, J.; Holzmann, T.; Jantsch, J.; Gessner, A., UPLC-MS/MS method for therapeutic drug monitoring of 10 antibiotics used in intensive care units. *Drug Test Anal* **2018,** *10* (3), 584-591.

71. Takats, Z.; Wiseman, J. M.; Cooks, R. G., Ambient mass spectrometry using desorption electrospray ionization (DESI): instrumentation, mechanisms and applications in forensics, chemistry, and biology. *J Mass Spectrom* **2005,** *40* (10), 1261-75.

72. Tillner, J.; Wu, V.; Jones, E. A.; Pringle, S. D.; Karancsi, T.; Dannhorn, A.; Veselkov, K.; McKenzie, J. S.; Takats, Z., Faster, More Reproducible DESI-MS for Biological Tissue Imaging. *J Am Soc Mass Spectrom* **2017,** *28* (10), 2090-2098.

73. Na, N.; Zhao, M.; Zhang, S.; Yang, C.; Zhang, X., Development of a dielectric barrier discharge ion source for ambient mass spectrometry. *J Am Soc Mass Spectrom* **2007,** *18* (10), 1859-62.

74. Harper, J. D.; Charipar, N. A.; Mulligan, C. C.; Zhang, X.; Cooks, R. G.; Ouyang, Z., Low-temperature plasma probe for ambient desorption ionization. *Anal. Chem.* **2008,** *80* (23), 9097-104.

75. Chen, H.; Venter, A.; Cooks, R. G., Extractive electrospray ionization for direct analysis of undiluted urine, milk and other complex mixtures without sample preparation. *Chem Commun (Camb)* **2006,** (19), 2042-4.

76. Wu, C.; Siems, W. F.; Hill, H. H., Jr., Secondary electrospray ionization ion mobility spectrometry/mass spectrometry of illicit drugs. *Anal. Chem.* **2000,** *72* (2), 396-403.

77. Haddad, R.; Sparrapan, R.; Eberlin, M. N., Desorption sonic spray ionization for (high) voltage-free ambient mass spectrometry. *Rapid Commun Mass Spectrom* **2006,** *20* (19), 2901-5.

78. McEwen, C. N.; McKay, R. G.; Larsen, B. S., Analysis of solids, liquids, and biological tissues using solids probe introduction at atmospheric pressure on commercial LC/MS instruments. *Anal. Chem.* **2005,** *77* (23), 7826-31.

79. McVey, P. A.; Alexander, L. E.; Fu, X.; Xie, B.; Galayda, K. J.; Nikolau, B. J.; Houk, R. S., Light-Dependent Changes in the Spatial Localization of Metabolites in Solenostemon scutellarioides (Coleus Henna) Visualized by Matrix-Free Atmospheric Pressure Electrospray Laser Desorption Ionization Mass Spectrometry Imaging. *Front Plant Sci* **2018,** *9*, 1348.

80. Shiea, J.; Huang, M. Z.; Hsu, H. J.; Lee, C. Y.; Yuan, C. H.; Beech, I.; Sunner, J., Electrospray-assisted laser desorption/ionization mass spectrometry for direct ambient analysis of solids. *Rapid Commun Mass Spectrom* **2005,** *19* (24), 3701-4.

81. Wei, J.; Buriak, J. M.; Siuzdak, G., Desorption-ionization mass spectrometry on porous silicon. *Nature* **1999,** *399* (6733), 243-246.

82. Skaggs, C. L.; Ren, G. J.; Elgierari, E. T. M.; Sturmer, L. R.; Shi, R. Z.; Manicke, N. E.; Kirkpatrick, L. M., Simultaneous quantitation of five triazole anti-fungal agents by paper spray-mass spectrometry. *Clin Chem Lab Med* **2020,** *58* (5), 836-846.

83. Jeong, E. S.; Kim, K. H.; Cha, E.; Kwon, O. S.; Cha, S.; Lee, J., Direct and rapid quantitation of ephedrines in human urine by paper spray ionization/high resolution mass spectrometry. *J Chromatogr B Analyt Technol Biomed Life Sci* **2016,** *1028*, 237-241.

84. Yang, Y.; Wu, J.; Deng, J.; Yuan, K.; Chen, X.; Liu, N.; Wang, X.; Luan, T., Rapid and on-site analysis of amphetamine-type illicit drugs in whole blood and raw urine by slug-flow microextraction coupled with paper spray mass spectrometry. *Anal Chim Acta* **2018,** *1032*, 75-82.

85. Mendes, T. P. P.; Pereira, I.; de Lima, L. A. S.; Morais, C. L. M.; Neves, A.; Martin, F. L.; Lima, K. M. G.; Vaz, B. G., Paper Spray Ionization Mass Spectrometry as a Potential Tool for Early Diagnosis of Cervical Cancer. *J Am Soc Mass Spectrom* **2020**.

86. Ren, Y.; Wang, H.; Liu, J.; Zhang, Z.; McLuckey, M. N.; Ouyang, Z., Analysis of Biological Samples Using Paper Spray Mass Spectrometry: An Investigation of Impacts by the Substrates, Solvents and Elution Methods. *Chromatographia* **2013,** *76* (19-20), 1339-1346.

87. Manicke, N. E.; Abu-Rabie, P.; Spooner, N.; Ouyang, Z.; Cooks, R. G., Quantitative analysis of therapeutic drugs in dried blood spot samples by paper spray mass spectrometry: an avenue to therapeutic drug monitoring. *J Am Soc Mass Spectrom* **2011,** *22* (9), 1501-7.

88. Su, Y.; Wang, H.; Liu, J.; Wei, P.; Cooks, R. G.; Ouyang, Z., Quantitative paper spray mass spectrometry analysis of drugs of abuse. *Analyst* **2013,** *138* (16), 4443-7.

89. Oradu, S. A.; Cooks, R. G., Multistep mass spectrometry methodology for direct characterization of polar lipids in green microalgae using paper spray ionization. *Anal. Chem.* **2012,** *84* (24), 10576-85.

90. Tsai, C.-W.; Tipple, C. A.; Yost, R. A., Application of paper spray ionization for explosives analysis. *Rapid communications in mass spectrometry : RCM* **2017,** *31* (19), 1565-1572.

91. Mach, P. M.; Dhummakupt, E. S.; Carmany, D. O.; McBride, E. M.; Busch, M. W.; Demond, P. S.; Rizzo, G. M.; Hollinshead, D. E.; Glaros, T., On-substrate derivatization for detection of highly volatile G-series chemical warfare agents via paper spray mass spectrometry. *Rapid Communications in Mass Spectrometry* **2018,** *32* (23), 1979-1983.

92. Domingos, E.; de Carvalho, T. C.; Pereira, I.; Vasconcelos, G. A.; Thompson, C. J.; Augusti, R.; Rodrigues, R. R. T.; Tose, L. V.; Santos, H.; Araujo, J. R.; Vaz, B. G.; Romão, W., Paper spray ionization mass spectrometry applied to forensic chemistry – drugs of abuse, inks and questioned documents. *Analytical Methods* **2017,** *9* (30), 4400-4409.

93. Wang, Q.; Bhattarai, M.; Zhao, P.; Alnsour, T.; Held, M.; Faik, A.; Chen, H., Fast and Sensitive Detection of Oligosaccharides Using Desalting Paper Spray Mass Spectrometry (DPS-MS). *Journal of the American Society for Mass Spectrometry* **2020,** *31* (10), 2226-2235.

94. Owings, C. G.; Skaggs, C.; Sheriff, W.; Manicke, N.; Picard, C. J., Chemical Assay for the Detection of Vertebrate Fecal Metabolites in Adult Blow Flies (Diptera: Calliphoridae). *Environ Entomol* **2018,** *47* (3), 586-593.

95. Skaggs, C.; Kirkpatrick, L.; Wichert, W. R. A.; Skaggs, N.; Manicke, N. E., A statistical approach to optimizing paper spray mass spectrometry parameters. *Rapid Commun Mass Spectrom* **2020,** *34* (7), e8601.

96. Li, A.; Wang, H.; Ouyang, Z.; Cooks, R. G., Paper spray ionization of polar analytes using non-polar solvents. *Chemical Communications* **2011,** *47* (10), 2811-2813.

97. Espy, R. D.; Muliadi, A. R.; Ouyang, Z.; Cooks, R. G., Spray mechanism in paper spray ionization. *International Journal of Mass Spectrometry* **2012,** *325-327*, 167-171.

98. Wleklinski, M.; Li, Y.; Bag, S.; Sarkar, D.; Narayanan, R.; Pradeep, T.; Cooks, R. G., Zero Volt Paper Spray Ionization and Its Mechanism. *Anal. Chem.* **2015,** *87* (13), 6786-93.

99. Zhang, Z.; Xu, W.; Manicke, N. E.; Cooks, R. G.; Ouyang, Z., Silica coated paper substrate for paper-spray analysis of therapeutic drugs in dried blood spots. *Anal. Chem.* **2012,** *84* (2), 931-8.

100. Liu, J.; He, Y.; Chen, S.; Ma, M.; Yao, S.; Chen, B., New urea-modified paper substrate for enhanced analytical performance of negative ion mode paper spray mass spectrometry. *Talanta* **2017,** *166*, 306-314.

101. Han, F.; Yang, Y.; Ouyang, J.; Na, N., Direct analysis of in-gel proteins by carbon nanotubes-modified paper spray ambient mass spectrometry. *Analyst* **2015,** *140* (3), 710-715.

102. Dhummakupt, E. S.; Carmany, D. O.; Mach, P. M.; Tovar, T. M.; Ploskonka, A. M.; Demond, P. S.; DeCoste, J. B.; Glaros, T., Metal–Organic Framework Modified Glass Substrate for Analysis of Highly Volatile Chemical Warfare Agents by Paper Spray Mass Spectrometry. *ACS Applied Materials & Interfaces* **2018,** *10* (9), 8359-8365.

103. Zheng, Y.; Zhang, X.; Yang, H.; Liu, X.; Zhang, X.; Wang, Q.; Zhang, Z., Facile preparation of paper substrates coated with different materials and their applications in paper spray mass spectrometry. *Analytical Methods* **2015,** *7* (13), 5381-5386.

104. Bambauer, T. P.; Maurer, H. H.; Weber, A. A.; Hannig, M.; Pütz, N.; Koch, M.; Manier, S. K.; Schneider, M.; Meyer, M. R., Evaluation of novel organosilane modifications of paper spray mass spectrometry substrates for analyzing polar compounds. *Talanta* **2019,** *204*, 677-684.

105. Dulay, M. T.; Zare, R. N., Polymer-spray mass spectrometric detection and quantitation of hydrophilic compounds and some narcotics. *Rapid Commun Mass Spectrom* **2017,** *31* (19), 1651-1658.

106. Colletes, T. C.; Garcia, P. T.; Campanha, R. B.; Abdelnur, P. V.; Romao, W.; Coltro, W. K.; Vaz, B. G., A new insert sample approach to paper spray mass spectrometry: a paper substrate with paraffin barriers. *Analyst* **2016,** *141* (5), 1707-13.

107. Borges, M. M. C.; Santos, H.; Vasconcelos, G. A.; Nascimento, T. A.; Dutra, F. V. A.; Pires, B. C.; Allochio Filho, J. F.; Aquije, G. M. F. V.; Borges, W. S.; Lacerda, V.; Vaz, B. G.; Arroyo-Mora, L. E.; Romão, W.; Borges, K. B., The use of conductive polymers as a substrate for paper spray ionization mass spectrometry. *Analytical Methods* **2019,** *11* (27), 3388-3400.

108. Dhummakupt, E. S.; Mach, P. M.; Carmany, D.; Demond, P. S.; Moran, T. S.; Connell, T.; Wylie, H. S.; Manicke, N. E.; Nilles, J. M.; Glaros, T., Direct Analysis of Aerosolized Chemical Warfare Simulants Captured on a Modified Glass-Based Substrate by "Paper-Spray" Ionization. *Anal. Chem.* **2017,** *89* (20), 10866-10872.

109. Kim, S.; Chen, J.; Cheng, T.; Gindulyte, A.; He, J.; He, S.; Li, Q.; Shoemaker, B. A.; Thiessen, P. A.; Yu, B.; Zaslavsky, L.; Zhang, J.; Bolton, E. E., PubChem in 2021: new data content and improved web interfaces. *Nucleic Acids Res* **2021,** *49* (D1), D1388-D1395.

110. Alava, M.; Niskanen, K., The physics of paper. *Reports on Progress in Physics* **2006,** *69* (3), 669-723.

111. Pana, Z. D.; Roilides, E.; Warris, A.; Groll, A. H.; Zaoutis, T., Epidemiology of Invasive Fungal Disease in Children. *J Pediatric Infect Dis Soc* **2017,** *6* (Suppl), S3-S11.

112. Menzin, J.; Meyers, J. L.; Friedman, M.; Perfect, J. R.; Langston, A. A.; Danna, R. P.; Papadopoulos, G., Mortality, length of hospitalization, and costs associated with invasive fungal infections in high-risk patients. *Am J Health Syst Pharm* **2009,** *66* (19), 1711-7.

113. Clark, T. A.; Hajjeh, R. A., Recent trends in the epidemiology of invasive mycoses. *Curr Opin Infect Dis* **2002,** *15* (6), 569-74.

114. Drgona, L.; Khachatryan, A.; Stephens, J.; Charbonneau, C.; Kantecki, M.; Haider, S.; Barnes, R., Clinical and economic burden of invasive fungal diseases in Europe: focus on pre-emptive and empirical treatment of Aspergillus and Candida species. *Eur J Clin Microbiol Infect Dis* **2014,** *33* (1), 7-21.

115. Scorzoni, L.; de Paula, E. S. A. C.; Marcos, C. M.; Assato, P. A.; de Melo, W. C.; de Oliveira, H. C.; Costa-Orlandi, C. B.; Mendes-Giannini, M. J.; Fusco-Almeida, A. M., Antifungal Therapy: New Advances in the Understanding and Treatment of Mycosis. *Front Microbiol* **2017,** *8*, 36.

116. Denning, D. W.; Hope, W. W., Therapy for fungal diseases: opportunities and priorities. *Trends Microbiol* **2010,** *18* (5), 195-204.

117. Andes, D.; Pascual, A.; Marchetti, O., Antifungal therapeutic drug monitoring: established and emerging indications. *Antimicrob. Agents Chemother.* **2009,** *53* (1), 24-34.

118. Ashbee, H. R.; Barnes, R. A.; Johnson, E. M.; Richardson, M. D.; Gorton, R.; Hope, W. W., Therapeutic drug monitoring (TDM) of antifungal agents: guidelines from the British Society for Medical Mycology. *J. Antimicrob. Chemother.* **2014,** *69* (5), 1162-1176.

119. Pfaller, M. A., Antifungal drug resistance: mechanisms, epidemiology, and consequences for treatment. *Am J Med* **2012,** *125* (Suppl), S3-13.

120. Boast, A.; Curtis, N.; Cranswick, N.; Gwee, A., Voriconazole dosing and therapeutic drug monitoring in children: experience from a paediatric tertiary care centre. *J Antimicrob Chemother* **2016,** *71* (7), 2031-6.

121. Park, W. B.; Kim, N. H.; Kim, K. H.; Lee, S. H.; Nam, W. S.; Yoon, S. H.; Song, K. H.; Choe, P. G.; Kim, N. J.; Jang, I. J.; Oh, M. D.; Yu, K. S., The effect of therapeutic drug monitoring on safety and efficacy of voriconazole in invasive fungal infections: a randomized controlled trial. *Clin Infect Dis* **2012,** *55* (8), 1080-7.

122. Pascual, A.; Calandra, T.; Bolay, S.; Buclin, T.; Bille, J.; Marchetti, O., Voriconazole therapeutic drug monitoring in patients with invasive mycosis improves efficacy and safety outcomes. *Clin. Infect. Dis.* **2008,** *46* (2), 201-211.

123. Mellinghoff, S. C.; Panse, J.; Alakel, N.; Behre, G.; Buchheidt, D.; Christopeit, M.; Hasenkamp, J.; Kiehl, M.; Koldehoff, M.; Krause, S. W.; Lehners, N.; von Lilienfeld-Toal, M.; Lohnert, A. Y.; Maschmeyer, G.; Teschner, D.; Ullmann, A. J.; Penack, O.; Ruhnke, M.; Mayer, K.; Ostermann, H.; Wolf, H. H.; Cornely, O. A., Primary prophylaxis of invasive fungal infections in patients with haematological malignancies: 2017 update of the recommendations of the Infectious Diseases Working Party (AGIHO) of the German Society for Haematology and Medical Oncology (DGHO). *Ann Hematol* **2018,** *97* (2), 197-207.

124. Smith, J.; Safdar, N.; Knasinski, V.; Simmons, W.; Bhavnani, S. M.; Ambrose, P. G.; Andes, D., Voriconazole therapeutic drug monitoring. *Antimicrob. Agents Chemother.* **2006,** *50* (4), 1570-1572.

125. Denning, D. W.; Tucker, R. M.; Hanson, L. H.; Hamilton, J. R.; Stevens, D. A., Itraconazole therapy for cryptococcal meningitis and cryptococcosis. *Arch Intern Med* **1989,** *149* (10), 2301-8.

126. Decosterd, L. A.; Rochat, B.; Pesse, B.; Mercier, T.; Tissot, F.; Widmer, N.; Bille, J.; Calandra, T.; Zanolari, B.; Marchetti, O., Multiplex ultra-performance liquid chromatography-tandem mass spectrometry method for simultaneous quantification in human plasma of fluconazole, itraconazole, hydroxyitraconazole, posaconazole, voriconazole, voriconazole-N-oxide, anidulafungin, and caspofungin. *Antimicrob. Agents Chemother.* **2010,** *54* (12), 5303-5315.

127. Rochat, B.; Pascual, A.; Pesse, B.; Lamoth, F.; Sanglard, D.; Decosterd, L. A.; Bille, J.; Marchetti, O. J. A. a.; chemotherapy, Ultra-performance liquid chromatography mass spectrometry and sensitive bioassay methods for quantification of posaconazole plasma concentrations after oral dosing. *Antimicrob Agents Chemother* **2010,** *54* (12), 5074-5081.

128. Farowski, F.; Cornely, O. A.; Vehreschild, J. J.; Hartmann, P.; Bauer, T.; Steinbach, A.; Ruping, M. J.; Muller, C., Quantitation of azoles and echinocandins in compartments of peripheral blood by liquid chromatography-tandem mass spectrometry. *Antimicrob Agents Chemother* **2010,** *54* (5), 1815-9.

129. Kousoulos, C.; Tsatsou, G.; Apostolou, C.; Dotsikas, Y.; Loukas, Y. L., Development of a high-throughput method for the determination of itraconazole and its hydroxy metabolite in human plasma, employing automated liquid–liquid extraction based on 96-well format plates and LC/MS/MS. *Anal Bioanal Chem* **2006,** *384* (1), 199-207.

130. Muller, C.; Gehlen, D.; Blaich, C.; Prozeller, D.; Liss, B.; Streichert, T.; Wiesen, M. H. J., Reliable and Easy-To-Use Liquid Chromatography-Tandem Mass Spectrometry Method for Simultaneous Analysis of Fluconazole, Isavuconazole, Itraconazole, Hydroxy-Itraconazole, Posaconazole, and Voriconazole in Human Plasma and Serum. *Ther Drug Monit* **2017,** *39* (5), 505-513.

131. Jannetto, P. J.; Fitzgerald, R. L., Effective Use of Mass Spectrometry in the Clinical Laboratory. *Clin Chem* **2016,** *62* (1), 92-8.

132. Nair, H.; Clarke, W.; editors, *Mass spectrometry for the clinical laboratory*. 1st ed.; Elsevier Ltd: Academic Press: Amsterdam; Boston, 2017.

133. Clarke, W.; Rhea, J. M.; Molinaro, R., Challenges in implementing clinical liquid chromatography-tandem mass spectrometry methods- seeing the light at the end of the tunnel. *J Mass Spectrom* **2013,** *48* (7), 755-67.

134. Espy, R. D.; Muliadi, A. R.; Ouyang, Z.; Cooks, R. G., Spray mechanism in paper spray ionization. *Int J Mass Spectrom.* **2012,** *325*, 167-171.

135. Shi, R. Z.; El Gierari el, T. M.; Faix, J. D.; Manicke, N. E., Rapid measurement of cyclosporine and sirolimus in whole blood by paper spray-tandem mass spectrometry. *Clin Chem* **2016,** *62* (1), 295-297.

136. Yang, Q.; Manicke, N. E.; Wang, H.; Petucci, C.; Cooks, R. G.; Ouyang, Z., Direct and quantitative analysis of underivatized acylcarnitines in serum and whole blood using paper spray mass spectrometry. *Anal Bioanal Chem* **2012,** *404* (5), 1389-97.

137. Meng, M.; Carter, S.; Bennet, P., LC-MS bioanalysis of drugs in hemolyzed and lipemic samples. In *Handbook of LC-MS bioanalysis: best practices, experimental protocols, and regulations*, Li, W.; Zhang, J.; Tse, F., Eds. John Wiley & Sons, Inc. : Hoboken, New Jersey, 2013; pp 369-379.

138. Almeida, A. M.; Castel-Branco, M. M.; Falcão, A. C., Linear regression for calibration lines revisited: weighting schemes for bioanalytical methods. *J Chromatogr B Analyt Technol Biomed Life Sci* **2002,** *774*, 215-222.

139. Giavarina, D., Understanding Bland Altman analysis. *Biochem Med (Zagreb)* **2015,** *25* (2), 141-51.

140. FDA *Bioanalytical method validation guidance for industry*; Food and Drug Administration, White Oaks, Maryland: 2018.

141. Matuszewski, B. K., Standard line slopes as a measure of a relative matrix effect in quantitative HPLC-MS bioanalysis. *J Chromatogr B Analyt Technol Biomed Life Sci* **2006,** *830* (2), 293-300.

142. Hussaini, T.; Ruping, M. J.; Farowski, F.; Vehreschild, J. J.; Cornely, O. A., Therapeutic drug monitoring of voriconazole and posaconazole. *Pharmacotherapy* **2011,** *31* (2), 214-25.

143. Yi, W. M.; Schoeppler, K. E.; Jaeger, J.; Mueller, S. W.; MacLaren, R.; Fish, D. N.; Kiser, T. H., Voriconazole and posaconazole therapeutic drug monitoring: a retrospective study. *Ann Clin Microbiol Antimicrob* **2017,** *16* (1), 60.

144. CLSI *Performance standards for antifungal testing of yeasts. CLSI document M60*; Clinical and Laboratory Standards Institute, Wayne, PA: 2017.

145. CLSI *Performance standards for antifungal susceptibility testing of filamentous fungi. CLSI document M61*; Clinical and Laboratory Standards Institute, Wayne, PA: 2017.

146. Bland, J.; Altman, D., Statistical methods for assessing agreement between two methods of clinical measurement. *Lancet* **1986,** *327* (8476), 307-310.

147. Mak, J.; Sujishi, K. K.; French, D., Development and validation of a liquid chromatography–tandem mass spectrometry (LC–MS/MS) assay to quantify serum voriconazole. *J Chromatogr B Analyt Technol Biomed Life Sci* **2015,** *986-987*, 94-99.

148. Hostetler, J. S.; Heykants, J.; Clemons, K. V.; Woestenborghs, R.; Hanson, L. H.; Stevens, D. A., Discrepancies in bioassay and chromatography determinations explained by metabolism of itraconazole to hydroxyitraconazole: studies of interpatient variations in concentrations. *Antimicrob Agents Chemother* **1993,** *37* (10), 2224-7.

149. Perea, S.; Pennick, G. J.; Modak, A.; Fothergill, A. W.; Sutton, D. A.; Sheehan, D. J.; Rinaldi, M. G., Comparison of high-performance liquid chromatographic and microbiological methods for determination of voriconazole levels in plasma. *Antimicrob Agents Chemother* **2000,** *44* (5), 1209-13.

150. Warnock, D. W.; Turner, A.; Burke, J., Comparison of high performance liquid chromatographic and microbiological methods for determination of itraconazole. *J Antimicrob Chemother* **1988,** *21* (1), 93-100.

151. Bruggemann, R. J.; Touw, D. J.; Aarnoutse, R. E.; Verweij, P. E.; Burger, D. M., International interlaboratory proficiency testing program for measurement of azole antifungal plasma concentrations. *Antimicrob Agents Chemother* **2009,** *53* (1), 303-5.

152. Law, D.; Moore, C. B.; Denning, D. W., Bioassay for serum itraconazole concentrations using hydroxyitraconazole standards. *Antimicrob Agents Chemother* **1994,** *38* (7), 1561-6.

153. Miyakis, S.; van Hal, S. J.; Ray, J.; Marriott, D., Voriconazole concentrations and outcome of invasive fungal infections. *Clin Microbiol Infect* **2010,** *16* (7), 927-33.

154. Krueger, R.; Vogeser, M.; Burghardt, S.; Vogelsberger, R.; Lackner, K. J., Impact of glucuronide interferences on therapeutic drug monitoring of posaconazole by tandem mass spectrometry. *Clin. Chem. Lab. Med.* **2010,** *48* (12), 1723-1731.

155. Krieter, P.; Flannery, B.; Musick, T.; Gohdes, M.; Martinho, M.; Courtney, R., Disposition of posaconazole following single-dose oral administration in healthy subjects. *Antimicrob Agents Chemother* **2004,** *48* (9), 3543-51.

156. Greenberg, B., *Flies and disease. Volume I. Ecology, classification and biotic associations*. 1971; p x +856 pp.

157. Steyskal, G. C., The Relative Abundance of Flies (Diptera) collected at Human Feces. *Zeitschrift fur Angewandte Zoologie* **1957,** *44* (1), 79-83.

158. Bohart, G. E.; Gressitt, J. L., *Filth-inhabiting Flies of Guam*. Honolulu: 1951; p vii+ 152 pp.

159. Liu, S.-Y.; Chen, H.-H.; Lien, J.-C., A Brief Study of the Bionomics of Fly Breeding in Keelung City, Taiwan. *Journal of the Formosan Medical Association* **1957,** *56* (Nos. 9/10), 417-25.

160. Axtell, R.; Arends, J., Ecology and management of arthropod pests of poultry. *Annual review of entomology* **1990,** *35* (1), 101-126.

161. Conn, D. B.; Weaver, J.; Tamang, L.; Graczyk, T. K., Synanthropic flies as vectors of Cryptosporidium and Giardia among livestock and wildlife in a multispecies agricultural complex. *Vector-Borne and Zoonotic Diseases* **2007,** *7*, 643+.

162. Fatchurochim, S.; Geden, C. J.; Axtell, R. C., Filth fly (Diptera) oviposition and larval development in poultry manure of various moisture levels. *Journal of Entomological Science* **1989,** *24* (2), 224-231.

163. Hall, D. G., *Blowflies of North America*. Thomas Say Foundation: London, 1948.

164. Greenberg, B., *Flies and disease. Vol. II. II. Biology and disease transmission*. Princeton University Press, Princeton, New Jersey.: 1973; p x+447 pp.

165. Linhares, A. X.; Avancini, R. P. M., Ovarian development in the blowflies *Chrysomya putoria* and *C. megacephala* on natural diets. *Medical and Veterinary Entomology* **1989,** *3* (3), 293-295.

166. Stoffolano, J. G.; Li, M.-F.; Sutton, J. A.; Yin, C.-M., Faeces feeding by adult Phormia regina (Diptera: Calliphoridae): impact on reproduction. *Medical and Veterinary Entomology* **1995,** *9* (4), 388-392.

167. Stoffolano, J. G.; Bartley, M. M.; Yin, C.-M., Male and female Phormia regina (Diptera: Calliphoridae) trapped at two different baits in the field. *Annals of the Entomological Society of America* **1990,** *83* (3), 603-606.

168. Sawabe, K.; Hoshino, K.; Isawa, H.; Sasaki, T.; Hayashi, T.; Tsuda, Y.; Kurahashi, H.; Tanabayashi, K.; Hotta, A.; Saito, T.; Yamada, A.; Kobayashi, M., Detection and isolation of highly pathogenic H5N1 avian influenza a viruses from blow flies collected in the vicinity of an infected poultry farm in Kyoto, Japan, 2004. *The American Journal of Tropical Medicine and Hygiene* **2006,** *75* (2), 327-332.

169. Monzon, R.; Sanchez, A.; Tadiaman, B.; Najos, O.; Valencia, E.; De Rueda, R.; Ventura, J., A comparison of the role of *Musca domestica* (Linnaeus) and *Chrysomya megacephala* (Fabricius) as mechanical vectors of helminthic parasites in a typical slum area of Metropolitan Manila. *Southeast Asian J Trop Med Public Health* **1991,** *22* (2), 222-228.

170. Barro, N.; Aly, S.; Tidiane, O. C. A.; SababÉNÉDjo, T. A., Carriage of Bacteria by Proboscises, Legs, and Feces of Two Species of Flies in Street Food Vending Sites in Ouagadougou, Burkina Faso. *Journal of Food Protection* **2006,** *69* (8), 2007-2010.

171. Fischer, O.; Mátlová, L.; Dvorská, L.; Švástová, P.; Bartl, J.; Melichárek, I.; Weston, R. T.; Pavlík, I., Diptera as vectors of mycobacterial infections in cattle and pigs. *Medical and Veterinary Entomology* **2001,** *15* (2), 208-211.

172. Nayduch, D.; Burrus, R. G., Flourishing in Filth: House Fly–Microbe Interactions Across Life History. *Annals of the Entomological Society of America* **2017,** *110* (1), 6-18.

173. Thomson, J. L.; Yeater, K. M.; Zurek, L.; Nayduch, D., Abundance and Accumulation of Escherichia coli and Salmonella Typhimurium Procured by Male and Female House Flies (Diptera: Muscidae) Exposed to Cattle Manure. *Annals of the Entomological Society of America* **2017,** *110* (1), 37-44.

174. Scully, E.; Friesen, K.; Wienhold, B.; Durso, L. M., Microbial Communities Associated With Stable Fly (Diptera: Muscidae) Larvae and Their Developmental Substrates. *Annals of the Entomological Society of America* **2017,** *110* (1), 61-72.

175. Brazil, S. M.; Steelman, C. D.; Szalanski, A. L., Detection of Pathogen DNA from Filth Flies (Diptera: Muscidae) Using Filter Paper Spot Cards. *Journal of Agricultural and Urban Entomology* **2007,** *24* (1), 13-18.

176. Szalanski, A. L.; Owens, C. B.; McKay, T.; Steelman, C. D., Detection of Campylobacter and Escherichia coli O157:H7 from filth flies by polymerase chain reaction. *Medical & Veterinary Entomology* **2004,** *18* (3), 241-246.

177. Pace, R. C.; Talley, J. L.; Crippen, T. L.; Wayadande, A. C., Filth Fly Transmission of Escherichia coli O157:H7 and Salmonella enterica to Lettuce, Lactuca sativa. *Annals of the Entomological Society of America* **2017,** *110* (1), 83-89.

178. Talley, J. L.; Wayadande, A. C.; Wasala, L. P.; Gerry, A. C.; Fletcher, J.; DeSilva, U.; Gilliland, S. E., Association of Escherichia coli O157:H7 with Filth Flies (Muscidae and Calliphoridae) Captured in Leafy Greens Fields and Experimental Transmission of E. coli O157:H7 to Spinach Leaves by House Flies (Diptera: Muscidae). *Journal of Food Protection* **2009,** *72* (7), 1547-1552.

179. Buzatto, A. Z.; de Sousa, A. C.; Guedes, S. F.; Cieslarová, Z.; Simionato, A. V. C., Metabolomic investigation of human diseases biomarkers by CE and LC coupled to MS. *ELECTROPHORESIS* **2014,** *35* (9), 1285-1307.

180. Cao, H.; Huang, H.; Xu, W.; Chen, D.; Yu, J.; Li, J.; Li, L., Fecal metabolome profiling of liver cirrhosis and hepatocellular carcinoma patients by ultra performance liquid chromatography–mass spectrometry. *Analytica Chimica Acta* **2011,** *691* (1), 68-75.

181. Eneroth, P.; Hellström, K.; Ryhage, R., Identification and quantification of neutral fecal steroids by gas–liquid chromatography and mass spectrometry: studies of human excretion during two dietary regimens. *Journal of Lipid Research* **1964,** *5* (2), 245-262.

182. Ziegler, T. E.; Wittwer, D. J., Fecal steroid research in the field and laboratory: improved methods for storage, transport, processing, and analysis. *American Journal of Primatology* **2005,** *67* (1), 159-174.

183. Eneroth, P.; Gordon, B.; Ryhage, R.; Sjövall, J., Identification of mono-and dihydroxy bile acids in human feces by gas-liquid chromatography and mass spectrometry. *Journal of lipid research* **1966,** *7* (4), 511-523.

184. Perwaiz, S.; Tuchweber, B.; Mignault, D.; Gilat, T.; Yousef, I. M., Determination of bile acids in biological fluids by liquid chromatography-electrospray tandem mass spectrometry. *Journal of Lipid Research* **2001,** *42* (1), 114-119.

185. Grundy, S. M.; Ahrens, E.; Miettinen, T. A., Quantitative isolation and gas–liquid chromatographic analysis of total fecal bile acids. *Journal of Lipid Research* **1965,** *6* (3), 397-410.

186. Isobe, K. O.; Tarao, M.; Zakaria, M. P.; Chiem, N. H.; Minh, L. Y.; Takada, H., Quantitative Application of Fecal Sterols Using Gas Chromatography−Mass Spectrometry To Investigate Fecal Pollution in Tropical Waters: Western Malaysia and Mekong Delta, Vietnam. *Environmental Science & Technology* **2002,** *36* (21), 4497-4507.

187. McMaster, P. D.; Elman, R., STUDIES ON UROBILIN PHYSIOLOGY AND PATHOLOGY II. *The Journal of Experimental Medicine* **1925,** *41* (4), 513.

188. Fahmy, K.; Gray, C. H.; Nicholson, D. C., The reduction of bile pigments by faecal and intestinal bacteria. *Biochimica et Biophysica Acta (BBA) - General Subjects* **1972,** *264* (1), 85-97.

189. Moscowitz, A.; Weimer, M.; Lightner, D. A.; Petryka, Z. J.; Davis, E.; Watson, C. J., The in vitro conversion of bile pigments to the urobilinoids by a rat clostridia species as compared with the human fecal flora: III. Natural d-urobilin, synthetic i-urobilin, and synthetic i-urobilinogen. *Biochemical Medicine* **1970,** *4* (2), 149-164.

190. Pullman, B.; Perault, A.-M., On the metabolic breakdown of hemoglobin and the electronic structure of the bile pigments. *Proceedings of the National Academy of Sciences* **1959,** *45* (10), 1476-1480.

191. Jones-Lepp, T., Chemical markers of human waste contamination: analysis of urobilin and pharmaceuticals in source waters. *Journal of Environmental Monitoring* **2006,** *8* (4), 472-478.

192. Song, Y.; Song, Q.; Li, J.; Zheng, J.; Li, C.; Zhang, Y.; Zhang, L.; Jiang, Y.; Tu, P., An integrated platform for directly widely-targeted quantitative analysis of feces part I: Platform configuration and method validation. *Journal of Chromatography A* **2016,** *1454*, 58-66.

193. Song, Y.; Song, Q.; Li, J.; Zheng, J.; Li, C.; Zhang, Y.; Zhang, L.; Jiang, Y.; Tu, P., An integrated platform for directly widely-targeted quantitative analysis of feces part II: An application for steroids, eicosanoids, and porphyrins profiling. *Journal of Chromatography A* **2016,** *1460*, 74-83.

194. James, M. T., *The flies that cause myiasis in man*. US Department of Agriculture: 1947.

195. Byrd, J. H.; Allen, J. C., The development of the black blow fly, Phormia regina (Meigen). *Forensic Science International* **2001,** *120* (1), 79-88.

196. Li, R., *Forensic biology*. CRC Press: 2015.

197. Kruskal, W. H.; Wallis, W. A., Use of ranks in one-criterion variance analysis. *J Am Stat Assoc* **1952,** *47* (260), 583-621.

198. Dunn, O. J., Multiple comparisons using rank sums. *Technometrics* **1964,** *6* (3), 241-252.

199. R Core Team *R: A language and environment for statistical computing*, R Foundation for Statistical Computing: Vienna, Austria, 2017.

200. Dinno, A. *dunn.test: Dunn's test of multiple comparisons using rank sums*, R package version 1.3.4: 2017.

201. Quinn, K. D.; Nguyen, N. Q.; Wach, M. M.; Wood, T. D., Tandem mass spectrometry of bilin tetrapyrroles by electrospray ionization and collision-induced dissociation. *Rapid Commun Mass Spectrom* **2012,** *26* (16), 1767-75.

202. Moore, J. S.; Kelly, T. B.; Killick-Kendrick, R.; Killick-Kendrick, M.; Wallbanks, K. R.; Molyneux, D. H., Honeydew sugars in wild-caught Phlebotomus ariasi detected by high performance liquid chromatography (HPLC) and gas chromatography (GC). *Medical and Veterinary Entomology* **1987,** *1* (4), 427-434.

203. MacVicker, J. A.; Moore, J.; Molyneux, D.; Maroli, M., Honeydew sugars in wild-caught Italian phlebotomine sandflies (Diptera: Psychodidae) as detected by high performance liquid chromatography. *Bulletin of Entomological Research* **1990,** *80* (3), 339-344.

204. Burkett, D. A.; Kline, D. L.; Carlson, D. A., Sugar meal composition of five north central Florida mosquito species (Diptera: Culicidae) as determined by gas chromatography. *Journal of medical entomology* **1999,** *36* (4), 462-467.

205. Pien, K.; Laloup, M.; Pipeleers-Marichal, M.; Grootaert, P.; De Boeck, G.; Samyn, N.; Boonen, T.; Vits, K.; Wood, M., Toxicological data and growth characteristics of single post-feeding larvae and puparia of Calliphora vicina (Diptera: Calliphoridae) obtained from a controlled nordiazepam study. *International Journal of Legal Medicine* **2004,** *118* (4), 190-193.

206. Bushby, S. K.; Thomas, N.; Priemel, P. A.; Coulter, C. V.; Rades, T.; Kieser, J. A., Determination of methylphenidate in Calliphorid larvae by liquid–liquid extraction and liquid chromatography mass spectrometry – Forensic entomotoxicology using an in vivo rat brain model. *Journal of Pharmaceutical and Biomedical Analysis* **2012,** *70*, 456-461.

207. Campobasso, C. P.; Gherardi, M.; Caligara, M.; Sironi, L.; Introna, F., Drug analysis in blowfly larvae and in human tissues: a comparative study. *International Journal of Legal Medicine* **2004,** *118* (4), 210-214.

208. Vitek, L.; Majer, F.; Muchova, L.; Zelenka, J.; Jiraskova, A.; Branny, P.; Malina, J.; Ubik, K., Identification of bilirubin reduction products formed by *Clostridium perfringens* isolated from human neonatal fecal flora. *J Chromatogr B Analyt Technol Biomed Life Sci* **2006,** *833* (2), 149-57.

209. Wilbur, R. L., Urobilin: Its Clinical Significance. *Archives of Internal Medicine* **1914,** *XIII* (2), 235-286.

PUBLICATIONS

1. Jett, R.; Skaggs, C.; Manicke, N. E., Drug screening method development for paper spray coupled to a triple quadrupole mass spectrometer. *Analytical Methods* **2017,** *9* (34), 5037-5043.
2. Owings, C. G.; Skaggs, C.; Sheriff, W.; Manicke, N.; Picard, C. J., Chemical Assay for the Detection of Vertebrate Fecal Metabolites in Adult Blow Flies (Diptera: Calliphoridae). *Environmental Entomology* **2018,** *47* (3), 586-593.
3. Owings, C. G.; Banerjee, A.; Asher, T. M. D.; Gilhooly, W. P.; Tuceryan, A.; Huffine, M.; Skaggs, C. L.; Adebowale, I. M.; Manicke, N. E.; Picard, C. J., Female Blow Flies As Vertebrate Resource Indicators. *Scientific Reports* **2019,** *9* (1), 10594.
4. Skaggs, C.; Kirkpatrick, L.; Wichert, W. R. A.; Skaggs, N.; Manicke, N. E., A statistical approach to optimizing paper spray mass spectrometry parameters. *Rapid Communications in Mass Spectrometry* **2020,** *34* (7), e8601.
5. Christine, L. S.; Greta, J. R.; El Taher, M. E.; Lillian, R. S.; Run, Z. S.; Nicholas, E. M.; Lindsey, M. K., Simultaneous quantitation of five triazole anti-fungal agents by paper spray-mass spectrometry. *Clinical Chemistry and Laboratory Medicine (CCLM)* **2020,** *58* (5), 836-846.

VITA

Education

2016-2021 Indiana University-Purdue University Indianapolis Indianapolis, IN

- PhD Candidate Department of Chemistry and Chemical Biology
- GPA 3.525

2012–2015 Marian University Indianapolis, IN

- Bachelor of Science in Chemistry and Biology with a Concentration in Bio-Organic Chemistry
- Global Studies Minor
- GPA 3.32, graduated of December 2015

2012-2015 (Summers Only) Ivy Tech Community College Kokomo, IN

- General Education classes to fulfill Marian University graduation requirements
- GPA: 3.87

Awards

2016-2021 IUPUI Indianapolis, IN

- IUPUI Dissertation Award Scholar 2021
- Volunteer of the Year Award for the American Chemical Society Global Winner 2020
- Volunteer of the Year Award for the American Chemical Society Indiana Local Section 2020
- Recipient of Ancient Accepted Scottish Rite Abbott Scholarship
- IUPUI School of Science Graduate Student Leadership and Service Award
- IUPUI Elite 50 Award

2012-2015 Marian University Indianapolis, IN

- Recipient of Richard G. Lugar Fellow Global Studies Scholarship
- Recipient of Saint Clare Academic Scholarship
- Recipient of D. J. Angus Scientech Educational Foundation Scholarship
- Recipient of Ancient Accepted Scottish Rite Abbott Scholarship
- Sigma Zeta National Science and Mathematics Honor Society
- Student Athlete: MU Softball

Internships

Jan 2021 – May 2021 Eli Lilly and Company Indianapolis, IN

MIH Research and Development Intern

- Provide lab support to ongoing projects related to trace analysis of genotoxic impurities (GTIs) via LC-MS, GC-MS, and LC-UV
- Provide lab support to projects relating to structural elucidation of peptides

May 2019 – Aug 2019 ThermoFisher Scientific San Jose, CA

Senior BioPharma Intern

- Provide lab support related to database development projects including sample preparation, operation of LC-MS, data processing, and database testing
- Developed a simultaneous assay to quantitate various anti-infectious disease drugs in plasma via LC-HRMS
    - Presented poster presentations on work entitled "Simultaneous Quantitative Analysis of Anti-infectious Disease Drug Classes in Human Plasma by LC-HRMS"
- Performed research developing an LC-HRMS assay for the simultaneous detection of genotoxic impurities in over-the-counter pharmaceuticals

June 2015-Oct 2015 Heritage Research Group Indianapolis, IN

Summer Intern

- Field work for Occupational Environmental Hygiene: Research
- Created reports for field samples that were analyzed with GC-FID
- Worked with Xcalibur to create a database of compounds usable by a LC-MS

Research Mentoring Presentations

2016-Present IUPUI Indianapolis, IN

- Iyunade Adebowale (undergraduate mentee), **Christine Skaggs**, Sarah Dowling, Nick Manicke. 2019. Hydrophobic Coatings on Paper Substrates to Analyze Hydrophilic Compounds Using Paper Spray Mass Spectrometry, IUPUI Capstone Poster Session. Indianapolis, Indiana. (Internal)
- Catherine Skaggs (undergraduate mentee), **Christine Skaggs,** Nicole Skaggs, David Styers-Barnet, Katherine Stickney, and Alicia Cecil. 2019. Screening of Design Parameters to Kill Antibiotic Resistant Bacteria on Vegetables. Midwestern Universities Analytical Chemistry Conference, Indianapolis, Indiana. (Regional)
- Iyunade Adebowale (undergraduate mentee), **Christine Skaggs**, Sarah Dowling, Nick Manicke. 2019. Hydrophobic Coatings on Paper Substrates to Analyze Hydrophilic Compounds Using Paper Spray Mass Spectrometry. Society for Advancement of Chicanos/Hispanics and Native Americans in Science, Honolulu, Hawaii. (National).

- **Christine Skaggs**, Iyun Adebowlae (undergraduate mentee), Charity G. Owings, Nicholas Manicke, Christine J. Picard 2019. LC-MS/MS Detects Urobilinoids from Feces in Fly Guts. IUPUI Research Day, Indianapolis, IN. (Internal)
- **Christine Skaggs**, Austin Kellogg (undergraduate mentee), Charity G. Owings, Nicholas Manicke, Christine J. Picard 2018. LC-MS/MS Detection of Herbicides in Adult Blow Fly Gut Extracts Department of Chemistry and Chemical Biology Research Day, Indianapolis, IN (Internal)
- **Christine Skaggs**, Cory Hagemier (undergraduate mentee), Charity G. Owings, Nicholas Manicke, Christine J. Picard 2018. LC-MS/MS Detects Urobilinoids from Feces in Fly Guts. Department of Chemistry and Chemical Biology Research Day, Indianapolis, IN (Internal)
- **Christine Skaggs** and Nicholas Manicke 2018. Targeted Detection of Fentanyl and Its Analogs in Water Samples. Midwestern Association for Toxicology and Therapeutic Drug Monitoring, Indianapolis, IN (Regional)
- **Christine Skaggs**, Cory Hagemier (undergraduate mentee), Charity G. Owings, Nicholas Manicke, Christine J. Picard 2018. LC-MS/MS Detects Urobilinoids from Feces in Fly Guts. IUPUI Research Day, Indianapolis, IN (Internal)

2016-Present IUPUI Indianapolis, IN

Mentee Names: Shanell Mooney, Gaige Deweese, Jason Kim, Catherine Skaggs, Iyun Adebowale, Austin Kellogg, Cory Hagemier, Winyu Sheriff

Oral Presentations

2016-Present IUPUI Indianapolis, IN

- **Christine Skaggs**, Lindsey Kirkpatrick, Greta Ren, and Nicholas Manicke. 2019. Paper Spray Mass Spectrometry for Screening of Antifungal Drugs from Plasma Samples. Pittcon Annual Meeting, Philadelphia, PA. (National)
- **Christine Skaggs** and Nicholas Manicke. 2019. Paper Spray Mass Spectrometry for the Clinician. Marian University Mass Spectrometry Speaker Series, Indianapolis, IN. (Regional)

Poster Presentations

2016-Present IUPUI Indianapolis, IN

- **Christine Skaggs**, Nicholas Manicke, Neloni Wijerante, and Lindsey Kirkpatrick, 2020. Optimization and Quantitation of Antibiotics in Dried Plasma Spots Utilizing Paper Spray Mass Spectrometry, American Society of Mass Spectrometry Annual Meeting, Houston, TX. (National)
- **Christine L. Skaggs**, Greta J. Ren, El Taher M. Elgierari, Lillian R. Sturmer, Run Z. Shi, Nicholas E. Manicke, and Lindsey M. Kirkpatrick. 2019. Simultaneous Quantitation of Five Triazole Anti-fungal Agents by Paper Spray-Mass Spectrometry. IUPUI Capstone Poster Session, Indianapolis, Indiana. (Internal)

- **Christine L. Skaggs**, Greta J. Ren, El Taher M. Elgierari, Lillian R. Sturmer, Run Z. Shi, Nicholas E. Manicke, and Lindsey M. Kirkpatrick. 2019. Simultaneous Quantitation of Five Triazole Anti-fungal Agents by Paper Spray-Mass Spectrometry. Midwestern Universities Analytical Chemistry Conference, Indianapolis, Indiana. (Regional)
- **Christine Skaggs** and Kate Comstock. 2019. Simultaneous Quantitative Analysis of Anti-infectious Disease Drug Classes in Human Plasma by LC-HRMS. American Association of Pharmaceutical Sciences, San Antonio, Texas. (National)
- **Christine Skaggs**, Lindsey Kirkpatrick, William R. A. Wichert, Nicole Skaggs, Nicholas E. Manicke 2018. Optimization of Design Parameters for the Detection of Ampicillin In Dried Plasma Spots Using Paper Spray Ionization Mass Spectrometry (PSI-MS). Midwestern Universities Analytical Chemistry Conference, Lansing, MI. (Regional)
- **Christine Skaggs**, Lindsey Kirkpatrick, William R. A. Wichert, Nicole Skaggs, Nicholas E. Manicke 2018. Optimization of Design Parameters for the Detection of Ampicillin In Dried Plasma Spots Using Paper Spray Ionization Mass Spectrometry (PSI-MS). Turkey Run Analytical Conference, Marshall, IN. (Regional)
- **Christine Skaggs**, Charity G. Owings, Nicholas Manicke, Christine J. Picard 2018. LC-MS/MS Detects Urobilinoids from Feces in Fly Guts. American Society of Mass Spectrometry Annual Meeting, San Diego, CA. (National)
- **Christine Skaggs** and Nicholas Manicke 2018. Targeted Detection of Fentanyl and Its Analogs in Water Samples. IUPUI Graduate Student Multidisciplinary Poster Session, Indianapolis, IN. (Internal)
- **Christine Skaggs**, Charity G. Owings, Nicholas Manicke, Christine J. Picard 2018. LC-MS/MS Detects Urobilinoids from Feces in Fly Guts. American Chemical Society Annual Meeting, New Orleans, LA. (National)
- **Christine Skaggs**, Charity G. Owings, Nicholas Manicke, Christine J. Picard 2018. LC-MS/MS Detects Urobilinoids from Feces in Fly Guts. Graduate Student Regional Research Conference. Louisville, KY. (Regional)
- **Christine Skaggs** and Nicholas Manicke. 2017. Paper Spray Mass Spectrometry for Screening of Antifungal Drugs from Plasma Samples. Indiana University – Purdue University Indianapolis Fall Poster Symposium. Indianapolis, IN. (Internal)
- **Christine Skaggs** and Nicholas Manicke. 2017. Paper Spray Mass Spectrometry for Screening of Antifungal Drugs from Plasma Samples. Midwestern Universities Analytical Chemistry Conference. Athens, Ohio. (Regional)
- **Christine Skaggs** and Nicholas Manicke. 2017. Paper Spray Mass Spectrometry for Screening of Antifungal Drugs from Plasma Samples. American Society for Mass Spectrometry Annual Meeting, Indianapolis, IN. (National)

2013 – December 2015 Marian University Indianapolis, IN

- Evidence Supports That There Is No Significant Difference In The Way Males and Females Perceive Colors: MU Fall 2013 Poster Symposium
- Planarian Regeneration: MU Spring 2014 Poster Symposium; MEEC Poster Symposium, Dayton, OH
- Methods of Solubility for Riboflavin: MU Fall 2014 Poster Symposium

- In vitro analysis of the antimicrobial efficacy of rose bengal and green light on *Staphylococcus aureus*: MU Spring 2015 Poster Symposium; Sigma Zeta National Conference Poster Symposium
- Experimental Study and Computation of the Quantum-Mechanical Modeling of the Ammonia Inversion Barrier via Intrinsic Reaction Coordinate: MU Fall 2016 Poster Symposium
- Using the Six Sigma Problem Solving Methodology to Optimize the Organic Synthesis of Adipic Acid: MU Fall 2016 Poster Symposium

Professional Affiliations and Certifications

2014-Present American Chemical Society Indianapolis, IN

- Younger Chemists Committee Co-chair, 2021
- Mentorship Committee Chair, 2020, 2021
- Senior Chemists Mentorship Program Chair, 2020, 2021
- Diversity, Equity, Inclusion, and Respect Committee Co-Chair, 2020, 2021
- Secretary, 2019, 2020, 2021
- Think Like a Molecule Poster Symposium Planning Committee, 2019, 2020
- IU Bicentennial Cross-Disciplinary Poster Planning Committee, 2020
- COVID Kits for Kids Event Chair, 2020
- Think Like a Molecule Poster Symposium Judge, 2018

2016-Present American Society of Mass Spectrometry Indianapolis, IN

- Member

2016-2021 IUPUI Indianapolis, IN

- Graduate School Chemistry Society: MOLE
    - ACS Representative, 2019, 2020
    - President, 2017, 2018
    - Co-founder, 2016
    - Member
- School of Science Graduate Student Council Chemistry Representative, 2019
- IUPUI Multidisciplinary Committee Member, 2017

2019 American Association of Pharmaceutical Scientists Arlington, VA

- Member

2015-2020 Villanova University Villanova, PA

- Lean Six Sigma Black Belt

2013-2015 Marian University Indianapolis, IN

- Sigma Zeta National Science and Mathematics Honor Society
- Studied abroad at Harlaxton College in Grantham, England (Summer 2014)
- Studied abroad in Paris, France (Summer 2014)
- Studied abroad in Italy, Spain, and Portugal (Summer 2015)
- Indiana Statehouse Page
- Senator for Nursing Our Faith Academics Club
- President of Marian University Book Club

Outreach Events

2013-Present Indianapolis, IN

- Celebrate Science Indiana, 2013, 2014, 2015, 2017, 2018, 2019, 2020
- Ignite Your Super Power, 2018, 2020
- Conner Prairie Passport to High Tech, 2017, 2020
- Hoosier Science and Engineering Fair, 2019
- You Be the Chemist, 2016, 2017, 2018
- Marian University Science Fair, 2013, 2014, 2015

Community Service

2012-2015 Marian University Indianapolis, IN

- Salvation Army Bell Ringer
- Make-A-Wish Volunteer
- Relay for Life Volunteer
- Marian University STARR Volunteer
- Kokomo High School and Marian University Softball Clinic Volunteer
- Marian University Peyton Manning's Children's Hospital Christmas Tree Lighting Volunteer
- Marian University Knight Nation

Work Experience

Aug 2017 – Present IUPUI Indianapolis, IN

Graduate Research Assistant

- Designed and conducted research using LC-MS and PS-MS
- Presented both oral and poster presentations on research
- Mentored graduate students (6) undergraduate students (8)
- Published novel research findings

Aug 2016 – July 2017 IUPUI Indianapolis, IN

General Chemistry Teaching Assistant

- Responsible for mentoring 60 students a semester on laboratory work
- Provided assistance with grading

Aug 2014–Dec 2015 Marian University Indianapolis, IN

Organic Laboratory Assistant and Teacher's Assistant

- Responsible for lab maintenance and upkeep
- Provided aid with grading and laboratory work

Aug 2014–May 2015 Marian University Indianapolis, IN

Clare Hall Resident Assistant and Resident Assistant Council Member

- Responsible for 34 residences
- Resolved resident issues
- Involved in event planning for the floor and their entire building

Aug 2014–May 2015 Marian University Indianapolis, IN

Campus Activities Board Committee Chair

- Scheduled interactive student activities campus-wide

Summer 2014 Howard Community Hospital Kokomo, IN

Emergency Room and Pediatrics Job Shadowing

- Observed patient and treatment consultations

2013-2014 Marian University Indianapolis, IN

Computer Help Desk Representative Tutor

- Assisted residents with network access issues
- Co-ordinated work orders for network repairs

2013-2014 Marian University Indianapolis, IN

Tutor

- Tutored residents in General Chemistry, Molecular Genetics, and Beginning and Intermediate Spanish courses

2011-Dec 2015 Self-Employed Kokomo, IN

Fastpitch Softball Pitching and Hitting Instructor

Skills

Lab Skills

- LC-MS
- GC-MS
- LC-UV
- Extensive microscope use
- Scanning Electron Microscope (SEM)
- GC-FID
- Sputter Deposition
- Laser Engraving
- Various filtration techniques
- PS-MS
- Maintenance and Instrument Technical Support
- Various separation techniques
- Centrifugation techniques
- IR Spectroscopy
- Mass Spectrometry

Computer Skills

- Microsoft Office Products
- Logger Pro
- Xcalibur
- Minitab
- JMP
- Compound Discoverer
- Tracefinder
- SPSS
- mzVault
- ChemStation
- Chromeleon
- Freestyle